Draft Research Report
Research Project T9233, Task 39
Evaluation of Design Methodologies for Soil Nailed Walls

EVALUATION OF DESIGN METHODOLOGIES FOR SOIL-NAILED WALLS

VOLUME 2
DISTRIBUTION OF AXIAL FORCES IN SOIL NAILS BASED ON INTERPRETATION OF MEASURED STRAINS

by

Todd D. Wentworth
Civil Engineering
University of Washington

Washington State Transportation Center (TRAC)
University of Washington, Box 354802
University District Building
1107 NE 45th Street, Suite 535
Seattle, Washington 98105-4631

Washington State Department of Transportation
Technical Monitor
Tony Allen
Geotechnical Engineer

Prepared for

Washington State Transportation Commission
Department of Transportation
and in cooperation with
U.S. Department of Transportation
Federal Highway Administration

July 1998

TECHNICAL REPORT STANDARD TITLE PAGE

1. REPORT NO.	2. GOVERNMENT ACCESSION NO.	3. RECIPIENT'S CATALOG NO.
WA-RD 371.2		

4. TITLE AND SUBTITLE	5. REPORT DATE
EVALUATION OF DESIGN METHODOLOGIES FOR SOIL-NAILED WALLS, VOLUME 2: DISTRIBUTION OF AXIAL FORCES IN SOIL NAILS BASED ON INTERPRETATION OF MEASURED STRAINS	July 1998
	6. PERFORMING ORGANIZATION CODE
7. AUTHOR(S)	8. PERFORMING ORGANIZATION REPORT NO.
Sunirmal Banerjee, Andrew Finney, Todd Wentworth, Mahalingam Bahiradhan	
9. PERFORMING ORGANIZATION NAME AND ADDRESS	10. WORK UNIT NO.
Washington State Transportation Center (TRAC) University of Washington, JD-10 University District Building; 1107 NE 45th Street, Suite 535 Seattle, Washington 98105-4631	11. CONTRACT OR GRANT NO. Agreement T9233, Task 39
12. SPONSORING AGENCY NAME AND ADDRESS	13. TYPE OF REPORT AND PERIOD COVERED
Washington State Department of Transportation Transportation Building, MS 7370 Olympia, Washington 98504-7370	Draft research report
	14. SPONSORING AGENCY CODE

15. SUPPLEMENTARY NOTES

This study was conducted in cooperation with the U.S. Department of Transportation, Federal Highway Administration.

16. ABSTRACT

Comparative evaluations of seven soil nail wall design computer programs are described and analyzed. The performance evaluations of the available programs (**SNAIL**, **NAIL-SOLVER**, **STARS**, **NAILM**, **GOLDNAIL**, **TALREN**, and **COLDUIM**) was accomplished by conducting a number of example analyses. Ten hypothetical cases and five case studies used in the analyses represented common design scenarios. Also examined were the magnitude and distribution of loads on the nails under normal working conditions. This was accomplished by observing the response of soil nails for a number of walls instrumented with strain gages. From this a general approach for estimating nail loads from strain history data was developed.

17. KEY WORDS	18. DISTRIBUTION STATEMENT
Soil nailing, walls, computer program, design, working loads	No restrictions. This document is available to the public through the National Technical Information Service, Springfield, VA 22616

19. SECURITY CLASSIF. (of this report)	20. SECURITY CLASSIF. (of this page)	21. NO. OF PAGES	22. PRICE
None	None	118	

DISCLAIMER

The contents of this report reflect the views of the authors, who are responsible for the facts and the accuracy of the data presented herein. The contents do not necessarily reflect the official views or policies of the Washington State Transportation Commission, Department of Transportation, or the Federal Highway Administration. This report does not constitute a standard, specification, or regulation.

Table of Contents

List of Figures

List of Tables

Acknowledgments

The author wishes to express sincere appreciation to R. John Byrne of Golder Associates, for his guidance and assistance during the course of the research. I would also like to thank Professors Banerjee and Taylor for their assistance in reviewing this manuscript.

Chapter 1

Introduction

1.1 Introduction

Soil nailing is a relatively new technique of reinforcing in situ soils for stabilization of slopes and excavations. The principle of soil nailing is to increase the shearing resistance of the ground by insertion of closely spaced inclusions which can withstand tensile forces. As shown in Figure 1.1, the goal is to create a reinforced soil zone which acts much like a gravity wall supporting the in situ soil behind it. The wall face is usually protected from erosion and local sloughing by shotcrete or geogrids. The presence of the ground inclusions enable the reinforced soil zone to safely withstand tensile forces and to resist soil movements by bond stress at the soil-inclusion interface.

In many design situations, soil nailing can be more attractive than other retaining systems. Soil nail walls can be constructed more rapidly, do not require over-excavation or fill, involve less expensive materials and equipment (no sheet piles, soldier piles, or tensioning equipment), and can easily accommodate design changes during construction. It is for these advantages that soil nailing has been utilized to support excavated slopes for highways and railroads, and construction excavations for underground facilities. The technique has also been used to stabilize landslides and repair existing retaining structures.

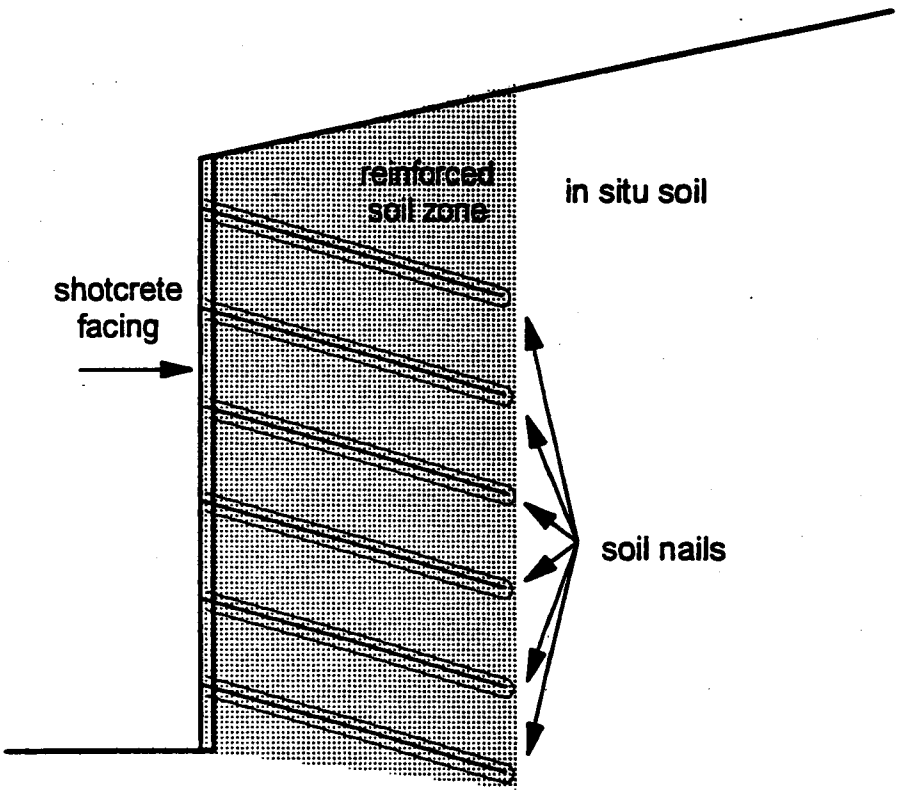

Figure 1.1 Typical soil nail cross-section.

Detailed descriptions of soil nailing have been presented by Chassie(1992), Juran and Elias (1991), Gassler (1990a), and Jewell (1990). This chapter presents a brief discussion of the soil nailing construction method and existing design methods. The purpose of this study, and an outline of the subsequent chapters is also presented herein.

1.2 Soil nailing construction

A brief description of the construction sequence is presented in order to explain the reinforcing action of soil nails. This procedure is displayed in Figure 1.2. Initially an unsupported cut, usually 1 m to 2 m in depth, is excavated. Soil nails are typically installed in a row by drilling boreholes of appropriate length at 10° to 20° inclination below the horizontal, with horizontal spacing of 1 m to 2 m. A steel reinforcing bar (rebar) with centralizers is inserted, and the entire borehole length is filled with concrete grout. While other less common methods and materials for constructing soil nails have been developed, this is the only type considered in this study. After a row of nails has been installed, the cut face is usually protected from erosion and local sloughing by shotcrete or geogrid facing. The nails are connected to the facing by a small steel plate (with the threaded end of the rebar extending through it) and hand tightening a nut on the bar against the plate. The next row of nails is constructed by excavating below the completed portion of the soil nail wall, and repeating the described procedure.

Most of the measured displacements in soil nails occur immediately following excavation. Data from instrumented nails indicate that the majority of nail tensioning occurs during the three excavation steps that follow the nail

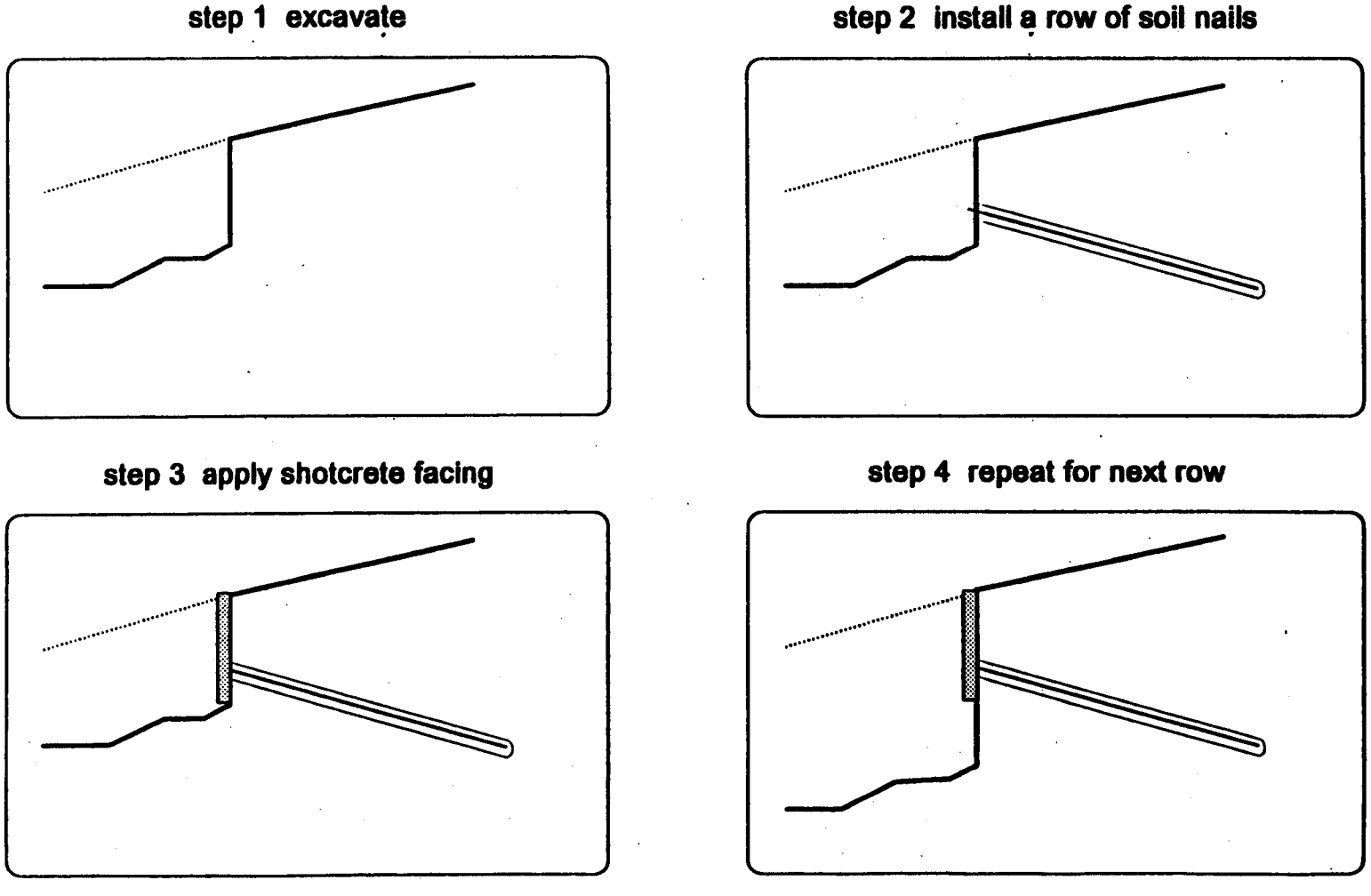

Figure 1.2 Construction sequence for soil nail walls.

installation, i.e. during excavation for the three rows immediately below the instrumented nail (Chassie, 1992).

1.3 Soil nailing design

Design of soil nail walls requires due consideration of the necessary construction constraints and static stability of the earth mass. Common construction constraints include: a) the stand up time of an unsupported cut; b) the nail pullout capacity; c) the geometry of the proposed wall and any nearby structures; and d) the type of available construction equipment. These constraints are important in the sense that they determine the choice of the various design parameters. The vertical spacing of the nails is controlled by the stand-up time. The local stability at each individual nail is governed by the pull-out capacity which in turn is a function of the ultimate soil-grout bond stress. The size and inclination of the boreholes depend on the availability of equipment. The design analysis currently employed are static stability analysis based on the limit equilibrium approach. Several analysis packages written in FORTRAN for the IBM personal computers are available. Some of the existing analysis packages have been evaluated by Finney (1993). Invariably, the analysis returns the factor of safety against overall instability along the most probable failure surface for a given wall design.

One of the important deficiencies of design methods is the prediction of the actual nail loads. The working loads can only be estimated for the following reasons. The reinforcements are passive inclusions, and the construction methods and sequences influence how the soil deforms to mobilize the reinforcements. Then again, the properties, stratigraphy and variability of the in situ soils are not well known. It is difficult to accurately model the soil-structure

interaction phenomena in the pre-failure state. Limit equilibrium analysis only considers the reinforced soil mass on the verge of failure, which is hardly the case for many in-service walls. More over, the insufficient design and construction experience precludes relying on empirical relationships for estimating working nail loads.

Although current design methods have been quite successful, the degree of over-design inherent in the limit equilibrium approach is not known. Also, it is not possible to design soil nail walls to minimize wall deflections. Although, inclinometer data for many constructed soil nail walls have been reported, this information cannot be used effectively in the design if the corresponding nail loads are not known.

1.4 Overview of thesis

The purpose of this study was to examine the distribution and magnitude of the axial nail forces from several instrumented soil nail walls. In order to do this, it was necessary to develop a method of estimating the axial force that had developed in the composite soil nail (concrete grout encapsulated steel reinforcing bar) using data from strain gauges attached to the reinforcing bar. The proposed method predicts how the concrete grout contributes to the axial stiffness of the soil nail from the measured strains at the grout steel interface. The method is independent of the soil properties; therefore, the estimated nail forces can be compared with the predictions based on the classical soil mechanics theories or on empirical observations. The resulting axial force distributions along the soil nails, and the maximum nail loads are presented for several case histories.

Chapter 2 summarizes the previous case histories and the nail load distributions and magnitudes published in the literature. Also included in this Chapter is a summary of the published reports which considered a composite nail stiffness for estimating nail forces. Chapter 3 describes the method which was developed in this study to estimate working nail loads based on the record of their performance. The basis of the adopted procedure is explained in detail in Chapter 3. In Chapter 4, the proposed method is applied to ten instrumented soil nail walls. A short description of the case histories and the corresponding nail forces are presented. Finally, Chapter 5 contains a discussion of the results and conclusions of the study. The algorithm for estimating nail loads is provided in a concise step-by-step format in Appendix 1. A series of load versus nail length plots for each instrumented nail are included in Appendix 2. On these figures, the steel load, estimated total nail load, and an upper bound nail load estimate are presented. The steel load is plotted not only to provide a lower limit of the nail load, but also to report the strain data in a usable form.

Chapter 2

Historical Review

2.1 Introduction

This chapter summarizes the relevant information gathered from the available literature with regard to soil nail forces. The summary presented herein includes: a discussion of nail force magnitudes and distributions; a brief description of previous case histories involving instrumented the *soil nails*; and methods of estimating the soil nail forces from measured strain data. The discussions of the above topics are presented in an approximate chronological order in order that the history of the developments can be traced.

The summarized information relates to experimental or actual soil nail walls instrumented with strain gauges. Previous researchers have proposed to either of the following procedures to relate the measured strains to the nail loads. These are: a) ignoring the concrete grout and reporting only the steel loads; b) performing laboratory tests by pulling on the ends of an instrumented steel bar encapsulated in grout, and correlating the composite stiffness measured in the laboratory with the measured strain data to estimate composite nail loads. An empirical method of predicting soil nail forces derived from instrumented soil nail results was also advocated.

2.2 First soil nailing application

The first recorded soil nail wall was constructed by Soletanche, a specialty contractor, in 1972 near Versailles, France for a railroad widening. The pullout test results with grout curing time for some of the nails were reported for this

case. The pullout capacity increased from 15 kN, 12 hours after installation, up to 90 kN, 11 days after installation (Bruce and Jewell, 1986).

2.3 Bodenvernagelung

A relatively more thorough research with instrumented soil nail walls was performed by the Bodenvernagelung project in, what was, then West Germany. Initiated in 1975, this was a five year research and development program which included theoretical stability analyses, model tests, and tests with seven full scale walls. These test walls were instrumented and loaded to failure by increasing surcharges (Gassler, 1992).

The results of this project were first presented at the International Conference on Soil Reinforcement in Paris, by Stocker, et al (1979). The major conclusions of this study were (Stocker, 1990):

- The reinforced soil nail zone acts much like a gravity wall;
- Nail lengths are typically 0.5 - 0.8 times the height of the wall;
- Nail spacing is typically 1.5 m;
- Earth pressure on the facing is usually 0.4 to 0.7 times active soil pressures and is distributed uniformly;
- Soil nail walls can withstand dynamic loading.

It was later noted that soil nails within these test walls did not undergo any significant bending (Gassler, 1990b).

The distributions of axial nail forces along the nails were discussed for test wall B. The changes in the nail forces with changes in the surcharge load were reported. The upper nails displayed maximum nail forces at or near the middle of the nail length. The lower nails showed maximum forces located near

the predicted critical slip surface for surcharge loads close to the surcharge load in which the wall failed (Stocker, et al., 1979).

2.4 Research at UC Davis

The first recorded research on soil nailing in the United States was for the Good Samaritan Hospital excavation in Portland, Oregon in 1976. Researchers of the University of California at Davis were involved with instrumenting this wall with inclinometers, and as a follow up of the work, conducted a research program which involved constructing a full scale test wall at the UC Davis campus in 1979 (Shen, et al, 1981). The soil nails in one cross-section were instrumented with four sets of strain gauges distributed along the nail lengths. The reported axial nail forces were compared with the predicted forces based on finite element analyses performed during the research program. The results from this study culminated in the development of the method of limit equilibrium analysis, commonly termed the "Davis method".

2.5 CLOUTERRE

In 1986, the four year French national research project "CLOUTERRE" was initiated. This work led to publication of the French soil nail design manual (Schlosser, et al, 1992). The results of three full-scale experimental soil nail walls were reported in 1990. The test walls investigated three possible failure modes- breakage of the nails, pullout of the nails, and excessive excavation below the reinforcement (Plumelle, et al, 1990). The first wall, CEBTP #1, instrumented the nails in order to measure tensile nail forces. Strain gauges were placed along the nail in pairs attached to the top and bottom of aluminum

tubes which were grouted into the borehole. An aluminum tube encased in concrete grout was tested in the laboratory in axial tension to develop a tensile force-displacement curve. This curve was used to interpret the strain gauge data in order to estimate the nail forces (Plumelle, et al, 1990). This is the first known study which attempted to account for the composite stiffness of the soil nail inclusion. In this case, the grout diameter of the nail was small and strains were large enough for the grout to have much influence on the nail force. Also, since the nails were designed to fail by breaking, the strains exceeded the elastic range of the aluminum tube, thus making accurate nail load estimation difficult.

The CEBTP #1 wall was failed by saturating the ground from a water basin placed above the reinforced soil zone. Fortuitously, the observed failure zone coincided with the measured maximum tensile force line. The tensile force in the nails was mobilized in the following two excavation stages after nail installation. Bending of the nail was not observed until large deformations had occurred, just prior to complete failure. The maximum measured tensile forces were slightly greater than the predictions based on assumed at-rest soil conditions near the top of the wall and slightly less than those based on assumed active soil conditions near the bottom. Although no tensile force was observed on the bottom nail at the end of construction, a small force was measured three months later which was possibly due to soil creep.

The major conclusions from the three experimental walls (Plumelle and Schlosser, 1991) include:

- Reinforcement is provided by axial tensile forces in the nail;
- The maximum tensile force is not located at the face, but tends to be near the failure zone;

- Wall displacements develop during excavation below the competed portion of the wall;
- Horizontal and vertical displacements are of the same magnitude;
- The wall displacements at the top are typically 0.1% to 0.3% of the wall height.

2.6 FHWA sponsored research

A study sponsored by the Federal Highways Administration (FHWA) led to the analysis of four soil nailing case histories: CEBTP #1; the Davis test wall; the Paris wall reported by Cartier and Gigan (1983); and the first Cumberland Gap soil nail wall (1985). The findings were reported by Juran and Elias (1987). The distribution of horizontal displacements and maximum axial nail forces were reported for each case history. The similarity in the loads experienced by soil nails and the bracing systems in braced excavations was reviewed in this study. The authors proposed that the apparent earth pressure diagrams for braced cuts (Terzaghi and Peck, 1967) could be used for preliminary design of soil nail walls provided the wall geometry is similar to the intended geometry of the diagrams.

As shown in Figure 2.1, some modifications to the apparent earth pressure envelope were proposed. The first modification was to account for soils exhibiting both friction and cohesion. However, it was noted that the approach appeared too sensitive to small changes in soil properties to be very useful in design. Secondly, for sands, the empirical diagram shape was modified. The trapezoidal shape of the distribution used for stiff clays by Terzaghi and Peck (1967) was proposed regardless of soil type. In the report,

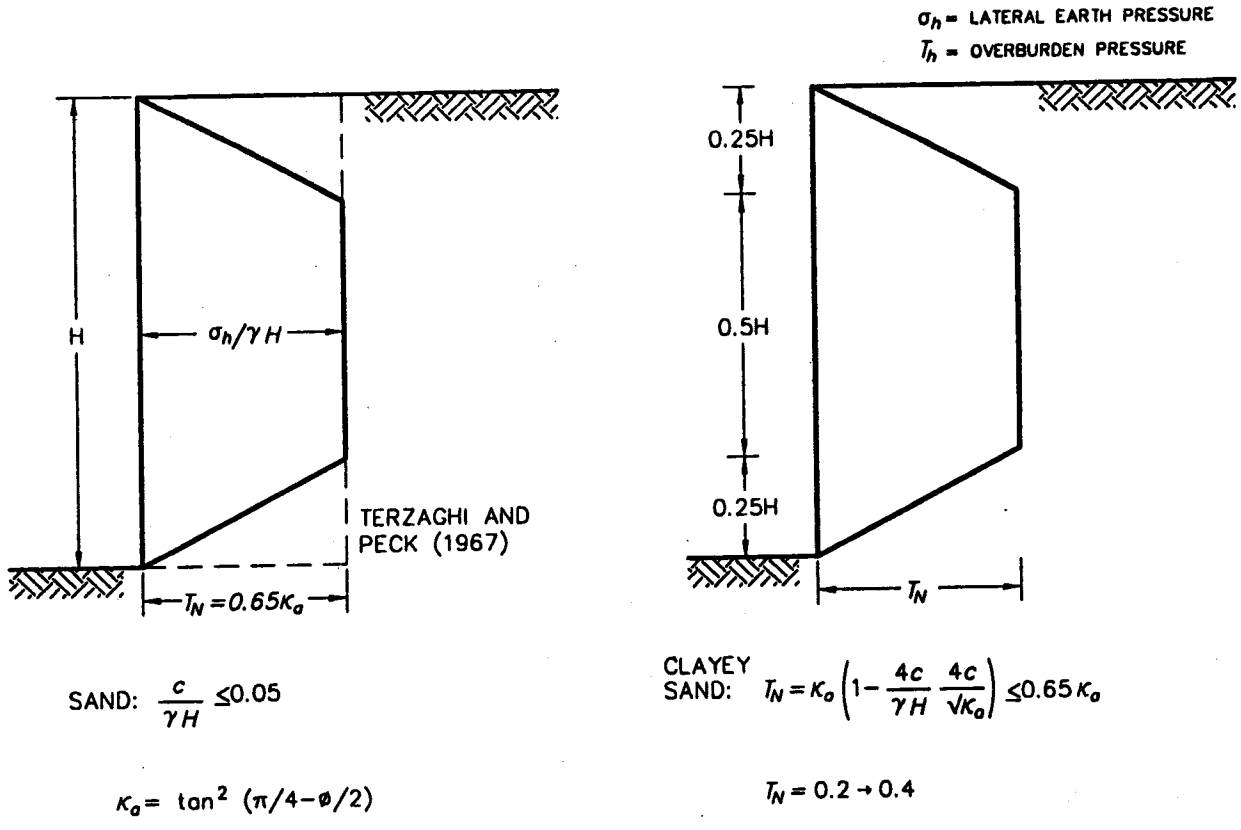

FIGURE 2.1 EMPIRICAL EARTH PRESSURE DIAGRAM (AFTER JURAN AND ELIAS, 1991).

the empirical diagrams were plotted with the non-dimensional nail forces obtained from measured data. The nail force was normalized by the soil unit weight, wall height, vertical nail spacing, and horizontal nail spacing.

Juran and Elias also observed that long-term soil creep has been noted in the strain data. For example, for the Cumberland Gap 1985 project, displacements measured by inclinometers stabilized within two to three months after construction, while tensile forces continued to increase with time. The authors claimed that this was due to creep of residual soils. It should be pointed out that the nail load refers only to the tensile forces in the steel rebar without attempting to account for the surrounding concrete grout.

In 1990, a report for the FHWA (Elias and Juran, 1990) discussed similar research results. Four case histories were presented: CEBTP #1; San Bernadino; I-78 Allentown; and the second instrumented soil nail wall at Cumberland Gap (1988). The maximum nail forces were compared with the empirical diagram. It should be mentioned that the data from the last three walls have been reinterpreted in this thesis.

In the discussion of the San Bernadino wall, the authors attributed the low nail forces (considering only the steel rebar) to the large diameter borehole (203 mm) and noted that the large grout column is capable of carrying significant tensile loads while only the balance would be carried by the steel rebar. They also contended that the composite force could only be analyzed if a crack occurred right at the gauge location. The difference in strain readings before and after cracking could be used to back calculate the composite stiffness. Since the strain data at San Bernadino did not indicate possible cracking, interpretation was not attempted by the authors.

In the chapter written for the Foundation Engineering Handbook (Juran and Elias, 1991), the results of the Davis wall and the CEBTP #1 wall, and the proposed empirical diagram were reiterated.

2.7 Polyclinic soil nail wall

Thompson and Miller (1990) presented a paper describing the performance of the Polyclinic soil nail wall in Seattle, Washington, designed and instrumented by Golder Associates. A description of this wall and instrumentation can be found in Chapter 4. Only the pertinent information of historical interest is discussed in this section. As with the San Bernadino wall, the instrumented nails consisted of strain gauges attached to the rebar and grouted in a 203 mm diameter borehole . A combined influence of the concrete grout and steel was noted.

There were two noteworthy differences in this case. First, some of the strain histories appeared to indicate cracking of the grout, as Elias and Juran had hypothesized. Secondly, the strain history plots showed a pattern of possible soil creep after construction ended However, the nails were constructed in very dense glacial outwash sands and gravels, and no changes in deformation was recorded by the inclinometers after the construction ended. The authors proposed that if wall deformations have not occurred, it is more likely that the increase in strain could be due to the redistribution of the load from the concrete to the steel due to creep of the concrete grout. They suggested that, although concrete has a low modulus compared to steel, the large grout area allows the concrete column to carry a large proportion of the load prior to cracking.

The authors estimated the nail loads from the strain data by two different ways. As an upper bound, the concrete creep effects were ignored and reasonable concrete modulus values were applied based on curing age. By assuming the measured strains were uniform across the nail section a composite nail load was calculated. For a lower bound, they assumed the jumps in the strain histories represented a crack in the grout at the gauge location. The authors assumed that the strains prior to cracking can be related to a composite stiffness and the strains measured after cracking relate only the steel stiffness. The nail loads for the remaining strain data were determined using the back calculated composite stiffness. This was labeled a lower bound because if the crack did not occur right at the gauge, the observed jumps in strain would represent only a partial release of the grout tensile force. Therefore, back calculating would yield too low a composite stiffness. The lower bound did not take into account any concrete creep or curing effects.

The instrumentation data from this wall was applied to a simplified kinematical soil-nail interaction model by Byrne (1992). The input parameters required reasonable estimates of soil modulus, initial soil stress conditions and soil-nail shear stiffness. The nail stiffness was determined by using a composite stiffness based on uniform strain across the nail section. The nail stiffness was modified for interpreting strain data collected long after construction by adjusting the grout modulus. To account for creep of the grout, the grout modulus was calibrated with changes in long-term strain measurements. This simplified soil-nail interaction model was able to reasonably predict maximum nail load distribution and locations of maximum straining immediately after construction, and nine months later. The model showed that nail loads varied little over the

nine months. However, this result was achieved by assuming additional strains after the end of construction were due only to concrete creep. This was the first attempt to include concrete creep in estimating soil nail forces.

2.8 Recent developments

The research conducted for an instrumented soil nail wall in Guernsey, U.K. included laboratory testing to simulate a soil nail in axial tension. A pair of strain gauges were attached to a steel bar encased in grout. The test specimen was constructed with the same materials that were used for soil nail wall construction. The ends of the steel bar were subjected to axial tension while strains were measured from the embedded strain gauges (Farham, 1992). The resulting applied load vs. measured strain plot, not withstanding some testing problems (the chosen initial strain reading probably did not correspond to zero stress), displayed two different slopes. The initial slope was high, representing the behavior of a composite nail. After severe grout cracking, the slope reduced to the stiffness of the steel bar.

As part of an instrumentation program for a soil nail wall built under a bridge abutment, near Portland, OR, the Oregon Department of Transportation (ODOT) performed similar laboratory tests to simulate a soil nail in axial tension (Sakr and Barrows, 1991). A steel reinforcing bar encased in grout was instrumented with a pair of strain gauges and loaded in axial tension by pulling on the bar ends while the strain measurements were recorded. The authors observed four different strain zones characterized by different stiffness slopes. The first zone, from 0 to 134 microstrain, represented a composite nail stiffness. The second and third zones showed softening due to concrete cracking. Finally, the fourth

zone, not reached until 1,000 microstrain, represented the steel bar stiffness alone. The laboratory results were applied to the soil nail strain data in order to estimate nail loads.

2.9 Summary

The main topics of this review included the reinforcing mechanism of soil nails, measured and predicted nail force magnitudes and distribution along the nail, and proposed and applied methods of interpreting strain gauge data. The important points which emerged from this review are:

- Soil nails act primarily in axial tension and bending resistance may be ignored except at failure;
- The nail forces develop by shear between the initially passive inclusion and the deforming soil mass;
- The maximum tensile nail force is not located at the wall face but at some location behind the face where maximum straining of the soil occurs;
- Soil nail walls may be analogous to braced cuts. Somewhat similar deformation patterns and loads have been observed in the two kinds of earth retaining systems;
- A soil nail is a composite reinforcing member and both the grout and steel may contribute to the stiffness of the nail;
- Strain measurements of the steel bar require interpretation of the grout influence to determine the total soil nail forces.

Chapter 3

Method of Estimating In-service Nail Loads

3.1 Introduction

The primary objective of this thesis was to examine the distribution and magnitude of the soil nail forces in several soil nail walls instrumented with strain gauges. To do this, it was necessary to develop a method of interpreting the strain data measured on the steel reinforcing bars. This chapter discusses the method that was developed in this study to estimate the working nail loads for soil nail walls based on the record of their performance.

The method of data interpretation was designed to yield the axial tensile forces which developed in the soil nails. It has been concluded that soil nails act primarily in axial tension and bending resistance is not mobilized until failure is imminent (Chapter 2). The soil nails were instrumented with strain gauges attached to the rebar at various locations along the nail length. Figure 3.1 displays a typical instrumented soil nail cross-section. Commonly, strain gauges were attached in pairs, as shown in the figure, in order that the average axial strains may be determined. If a particular instrumentation program did not install strain gauges in pairs, the measured strains were assumed to represent average axial strains. Whether axial strains were measured or assumed is noted later as the results are presented.

As shown in Figure 3.1, the soil nails can be viewed as composite structural members consisting of steel rebar and concrete grout. The strain gauges measure the strain in the steel rebar at the grout-steel interface. From these data, calculating the axial load in the rebar at the gauge location is

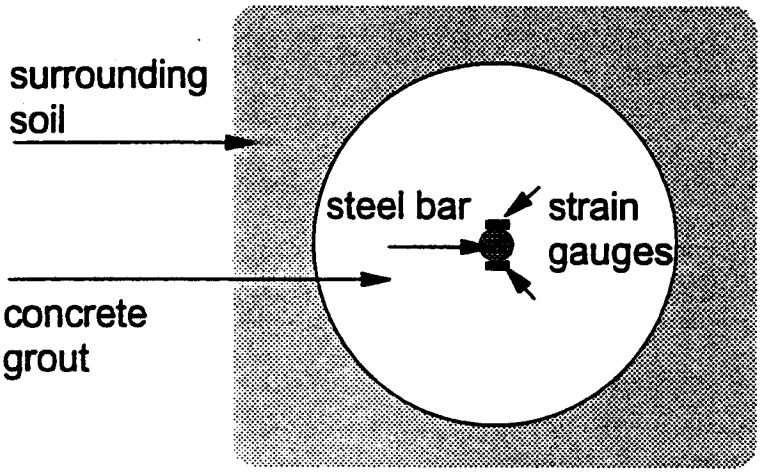

Figure 3.1 Typical soil nail cross-section.

relatively straightforward, since the steel bar can be assumed to behave as a linear elastic material. However, it has been noted that in many cases the steel load alone cannot account for all the axial forces required to maintain stability of the wall (Elias and Juran, 1990, Thompson and Miller, 1990, Sakr and Barrows, 1990). When the soil nails are placed in a large diameter borehole, the surrounding concrete grout may be carrying a significant portion of the total axial nail load. This was evident in the San Bernadino and Polyclinic soil nail walls where 200 mm diameter nails were installed with 25 mm to 32 mm rebar (Elias and Juran, 1990, Thompson and Miller, 1990).

The basic difficulty in estimating the nail loads is to determine how the concrete grout contributes to the axial stiffness of the soil nail. First, the mechanical behavior of concrete is not linear elastic. Secondly, the time-dependent nonlinear effects of curing and creep introduce further complexities. In addition, unlike steel, the material is brittle and undergoes cracking at a relatively smaller load and strain level.

The present method accounts for both curing and creep of concrete to estimate an effective modulus for the grout and to determine the tensile loads in the grout. In the event of cracking, the load carrying capacity of the grout is assumed to be limited by the ultimate tensile strength of the grout. The method derived in this study interprets concrete grout response from the measured strains at the grout-steel interface and estimates the actual force developed in the composite soil nail.

The mechanism of mobilizing the soil nail reinforcing action is reviewed in Section 3.2. This provides the background for understanding soil nail behavior and the assumptions involved in estimating nail loads using the method

developed in this research. The method is explained in Section 3.3, along with the important mechanical characteristics of curing, creep, and cracking of the concrete grout. Section 3.4 explains why the development of such a method was necessary in the context of the other methods described in Chapter 2.

3.2 Development and distribution of nail forces

An idealized distribution of the axial force along the length of a soil nail is shown in Figure 3.2. Since the soil nails are installed passively, relative deformations between the soil nail and the surrounding soil must occur for the nails to act as reinforcements. As the lateral confining pressure on the soil adjacent to the cut is removed by excavation, the soil within the active zone tends to expand and deform towards the excavation. The resistance to this deformation develops at the soil-grout interface in the form of shear forces around the grout circumference. These shear forces are balanced by the axial forces within the soil nail. As explained earlier, this axial force is shared by the steel section and the concrete grout.

Since the shear stresses act along the circumferential area of the nail, the axial force at the ends of the nails must be zero. The force at the wall face may be zero or larger, depending on the characteristics of the facing elements. Presumably, the soil nail may develop its maximum axial force where shear stresses at the soil-grout interface reverse directions. The location of maximum force may coincide with the divide between the active soil wedge and the stationary soil mass. However, the actual magnitude and location of maximum nail force varies with the soil deformation pattern, construction sequence, and required reinforcement.

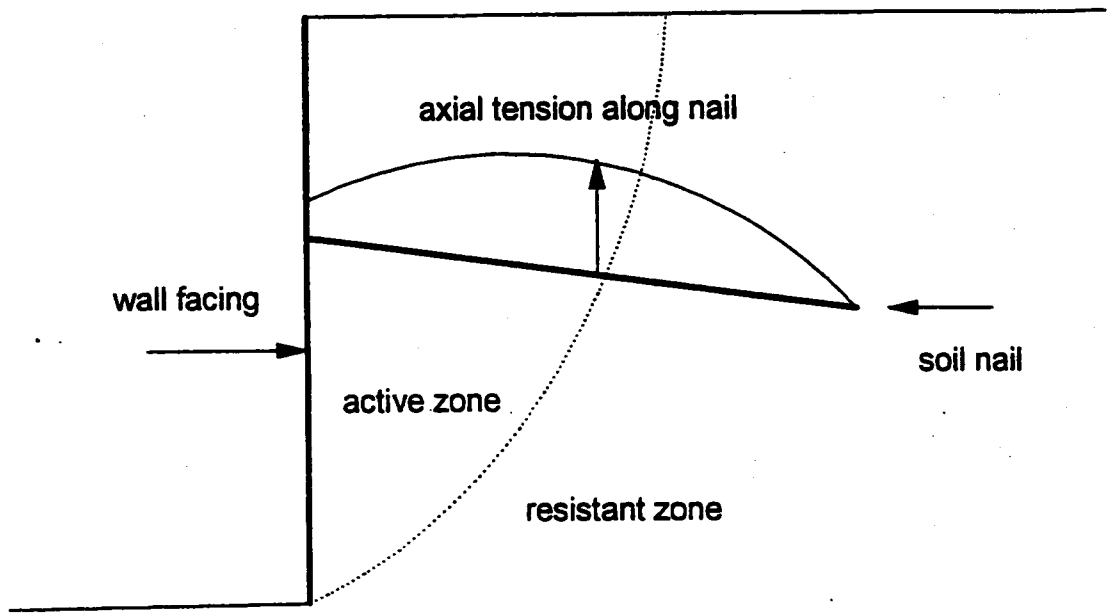

Figure 3.2 Idealized soil nail reinforcment

3.3 Estimating axial nail forces

A hypothetical load-deformation behavior of a composite cross-section in axial tension is shown in Figure 3.3. Phase 1 reflects the composite behavior while the concrete grout remains intact. A gradual reduction of the contribution of the grout occurs throughout Phase 2 as the grout undergoes cracking until the grout is no longer effective in Phase 3. It is clear from Figure 3.3 that the major issues in the development of a method for estimating the total nail forces are: a composite stiffness during Phase 1, the strain level at the initiation of grout cracking, and an ultimate tensile capacity of the grout. Section 3.3.1 and 3.3.2 are devoted to the considerations necessary to define a composite stiffness. The considerations related to cracking are discussed in Section 3.3.3.

It should be pointed out that the following assumptions were necessary: 1) strains measured at the grout-steel interface are uniform across the entire cross-section; 2) strain compatibility exists at the grout-steel interface when the tensile stress is low enough for the grout to remain intact.

3.3.1 Determining elastic concrete grout properties based on curing time

In order to determine the load carried by the concrete grout, the elastic concrete modulus and the direct tensile strength must be known or assumed. However, these properties change with curing time of the concrete. The nails must perform as reinforcements within a short period after installation and before the concrete is fully cured. The loading on the nails continues to accrue until wall construction is completed. Therefore, an appropriate elastic modulus and tensile strength, based on grout age, should be applied to the measured strains.

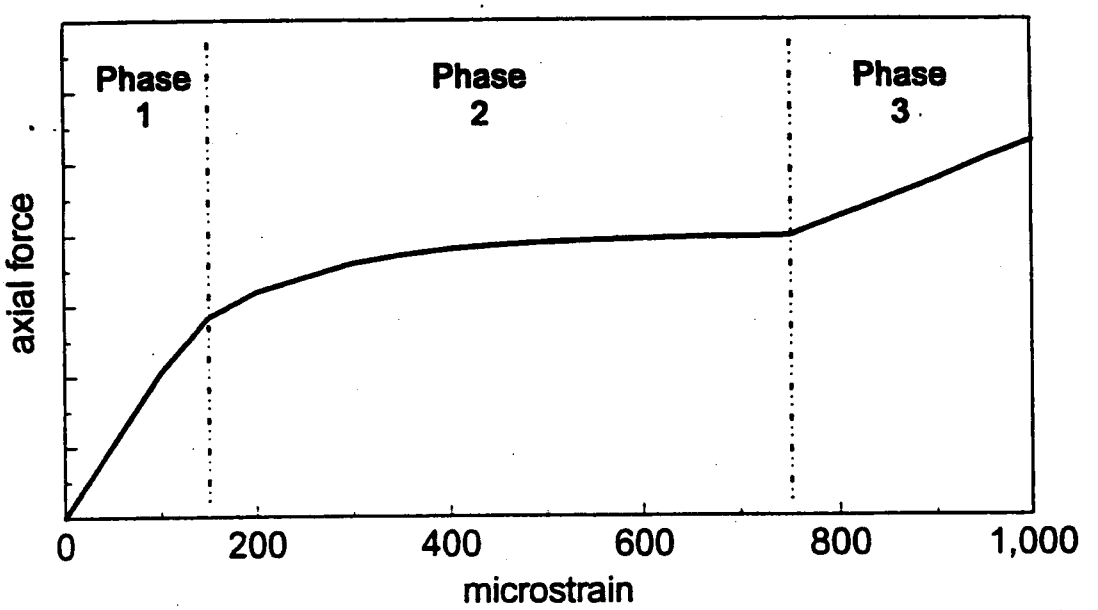

Figure 3.3 A hypothetical laboratory load-deformation plot of a composite soil nail in axial tension.

To account for the variable loading conditions inherent in the sequence of construction, the concrete elastic modulus must be estimated for an average curing age during construction for each nail. Since external loads are applied to the nail throughout the construction period, the tensile strength must be estimated for a curing age corresponding to the end of construction. External load changes after the end of construction can be considered to be insignificant unless specifically noted.

The average concrete grout age was determined between the time of nail installation and the end of construction (EOC) as shown in Figure 3.4. By considering the construction schedule and the strain history of the last instrumented nail installed, the EOC was chosen to be the date that strain changes leveled off, usually two weeks after the last instrumented nail was installed. This allowed time for the facing to be constructed and completion of any other activities that may have influenced external nail loads.

Since the grout properties were not reported for any of the instrumented soil nail walls compiled for this study, the empirical relationships published by the American Concrete Institute (ACI) were adopted for estimating the necessary concrete properties (ACI, 1992a). These relationships are given by Equations 3.1 through 3.3. Equation 3.1 provides the compressive strength of concrete, $(f'_c)_t$, for any time based on a known 28 day strength, $(f'_c)_{28}$, while Equation 3.2 relates the elastic concrete modulus, $(E_c^e)_t$, to the compressive strength, and Equation 3.3 relates the direct tensile strength, $(f'_t)_t$, to the compressive strength (ACI, 1992b).

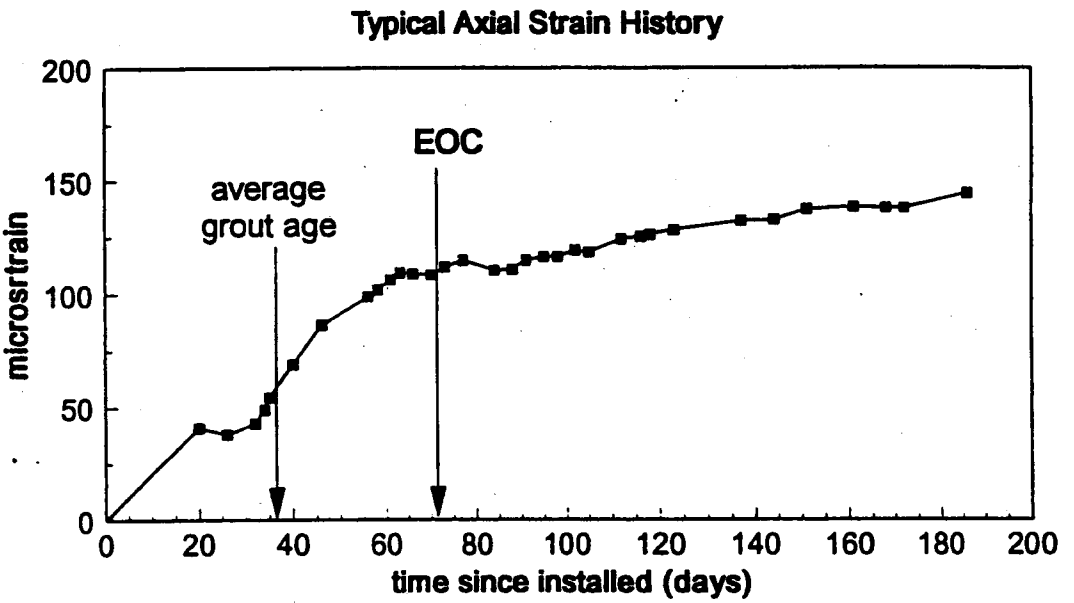

Figure 3.4 Determining average grout age. Data is from Swift - Delta Section 1, Nail 2, strain gauge B5 and B6.

$$(f'_c)_t = (f'_c)_{28} \frac{t}{(4+0.85t)} \quad (3.1)$$

$$(E_c^e)_t = 4800(f'_c)_t^{1/2} \quad (3.2)$$

$$(f'_t)_t = 0.55(f'_c)_t^{1/2} \quad (3.3)$$

where t = age of grout

f'_c, E_c^e, f'_t, in N/mm^2

A typical value of the 28 day compressive strength, $(f'_c)_{28}$ = 20.7 N/mm^2 (3000 psi) was assumed for all the cases; the other properties were determined by the established relationships.

3.3.2 Predicting concrete creep and stress relaxation

Creep and/or stress relaxation phenomena are known to occur in concrete. Creep strain is defined as additional strain that develops over time after a constant load has been applied and maintained. Stress relaxation, on the other hand, is gradual reduction in stress over time when a specimen is held at a constant strain. Despite no apparent external load changes, the measured strains in the nails continued to increase gradually after the end of construction. A typical example of this is shown in Figure 3.5 for the Polyclinic wall. It is likely that the load initially carried by the grout is gradually being transferred to the steel rebar due to creep (Byrne, 1992).

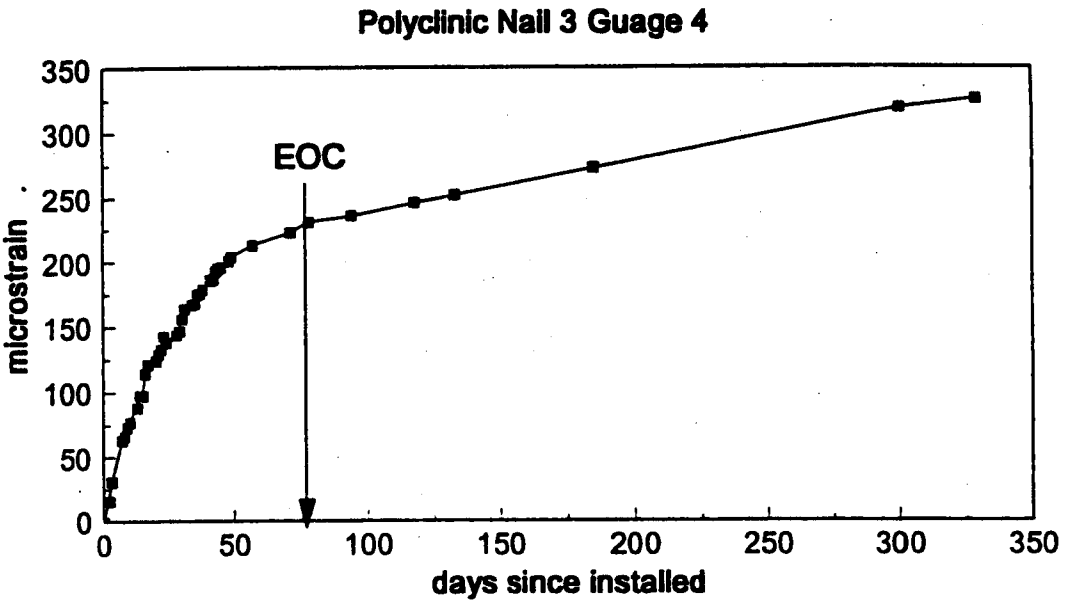

Figure 3.5 Long term strain increases that resemble creep.

The mode of load transfer is presented in Figure 3.6 for a simple loading situation. When an axial tensile load is applied to a soil nail, as shown by position **a**, elastic strain occurs in both the concrete and steel sections as shown by positions **b** and **c**. If the load is maintained, the concrete grout will respond with a combination of creep and stress relaxation, and the final grout load is at position **e**. As the concrete grout creeps, the steel load increases to position **f**, since steel behaves as a linear elastic material. The total load in the soil nail remains constant, as shown between positions **a** and **d**.

In order to estimate the grout load after creep and stress relaxation have occurred, the ACI-209 estimating procedure was adopted (ACI, 1992a). Although the procedure was originally intended for concrete compressive loads up to 40% of the ultimate strength, and soil nails are loaded in tension with loads often near 100% of the ultimate strength, there were no other generally accepted creep prediction methods more suitable to the conditions of a soil nail. The limited research of concrete creep in tension indicates that it is similar to creep in compression, for stresses at the same proportion to the ultimate strength (Neville, 1970). For stresses greater than 40% of the ultimate strength, the creep rate is higher than predicted by the procedure (ACI, 1992, a).

The ACI-209 procedure is given by the relationships presented in Equations 3.4 and 3.5. Equation 3.4 defines a creep ratio, v_d. The creep ratio is calculated from Equation 3.5.

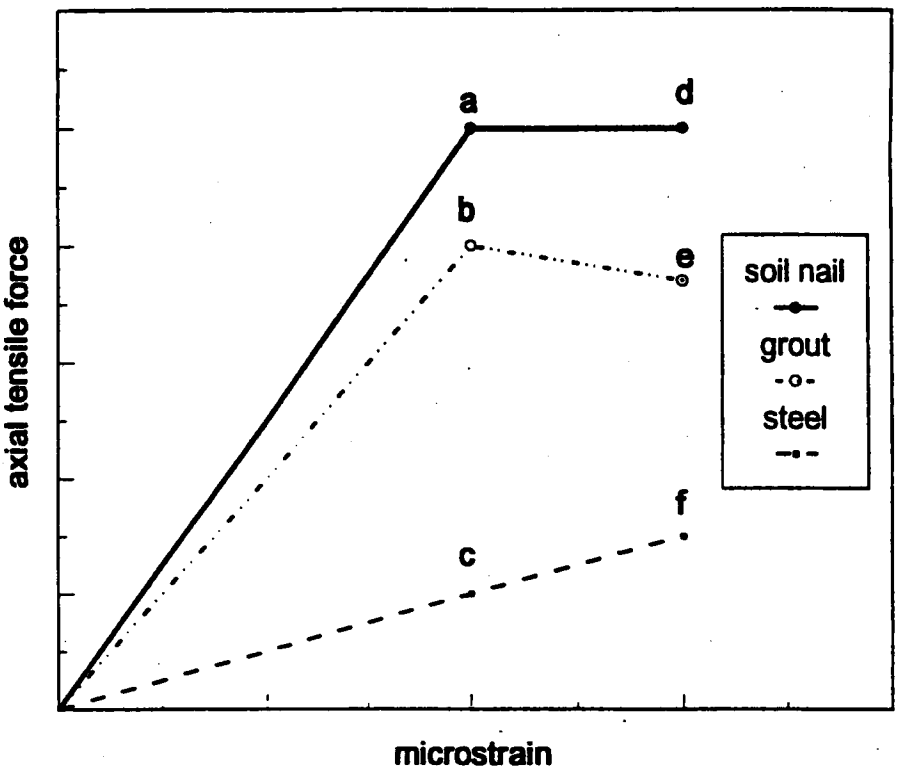

- **a:** initial soil nail force
- **b:** initial grout tensile force
- **c:** initial steel tensile force
- **d:** soil nail force after grout creep and stress relaxation
- **e:** grout tensile force after creep and stress relaxation
- **f:** steel tensile force after grout creep and stress relaxation

Figure 3.6 Response of soil nail, grout, and steel to grout creep and stress relaxation.

$$v_d = \varepsilon_c / \varepsilon_e \tag{3.4}$$

$$v_d = \frac{Cd^{0.6}}{10 + d^{0.6}} \tag{3.5}$$

v_d = creep ratio after d days

ε_c = creep strain

ε_e = elastic strain

d = duration of load in days

C = constant

The constant, C, depends on the moist cured concrete age at the time of loading, the surrounding humidity, and the thickness of the concrete member.

The creep ratio is used to determine an effective concrete modulus, $(E_c^s)_d$, as given by Equation 3.6. Since creep depends on load duration, for each date strains were recorded there is a corresponding effective concrete modulus. The effective modulus was used with the measured strains to determine grout load.

$$(E_c^s)_d = \frac{(E_c^e)_t}{1 + v_d} \tag{3.6}$$

in which t = average grout age in days

d = duration of load in days

The variables, t and d, are displayed in Figure 3.7.

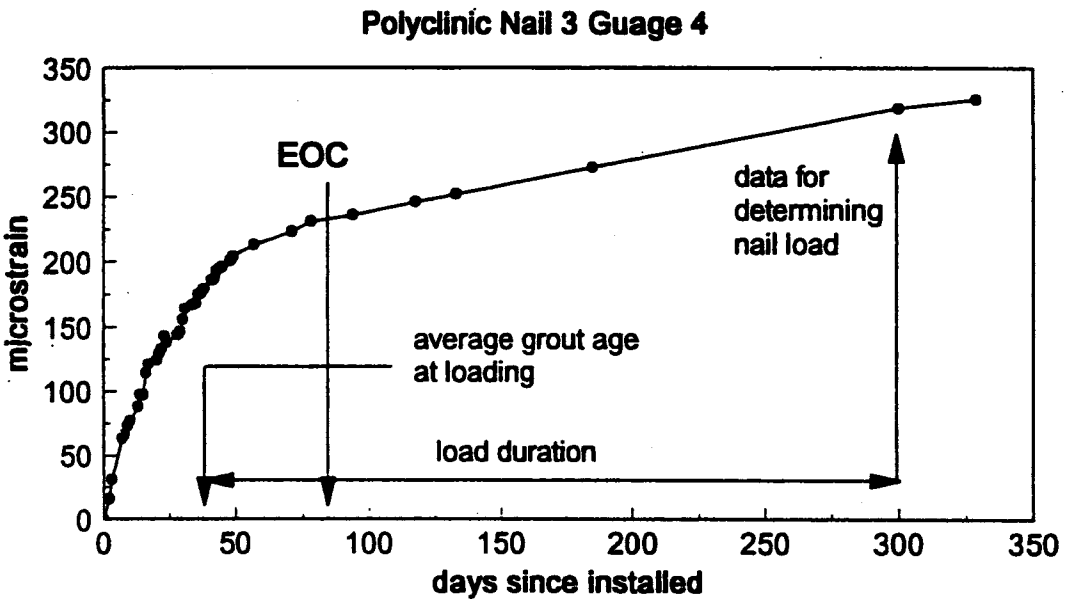

Figure 3.7 Typical stress-strain plot noting required time factors for estimating concrete grout creep.

Figure 3.8 illustrates how the effective concrete modulus is used to determine the concrete grout load. For a given measured strain, the effective modulus is used to determine the final stress. The final stress is multiplied by the grout cross-sectional area to yield the grout load. The soil nail load is the sum of the grout load and steel load.

After estimating nail loads from strain data collected at various times after the end of construction for several instrumented walls, it appears that the ACI-209 method under predicts the creep rate for soil nails. Estimated nail loads using data collected long after construction were larger than estimated nail loads using data collected at the end of construction, even though there was no evidence of external load changes to the nail. This indicates that concrete grout creep and stress relaxation occurred faster than was predicted.

For these reasons, in-service nail loads were estimated by using data collected at the end of construction (EOC). By using data soon after all external loads had been applied to the nail, concrete grout creep had less influence on the estimated nail loads. The larger nail loads, estimated from strain measurements long after the end of construction, may be considered an upper bound nail load. It will be shown in the following section that when the grout cracks, a larger upper bound is necessary.

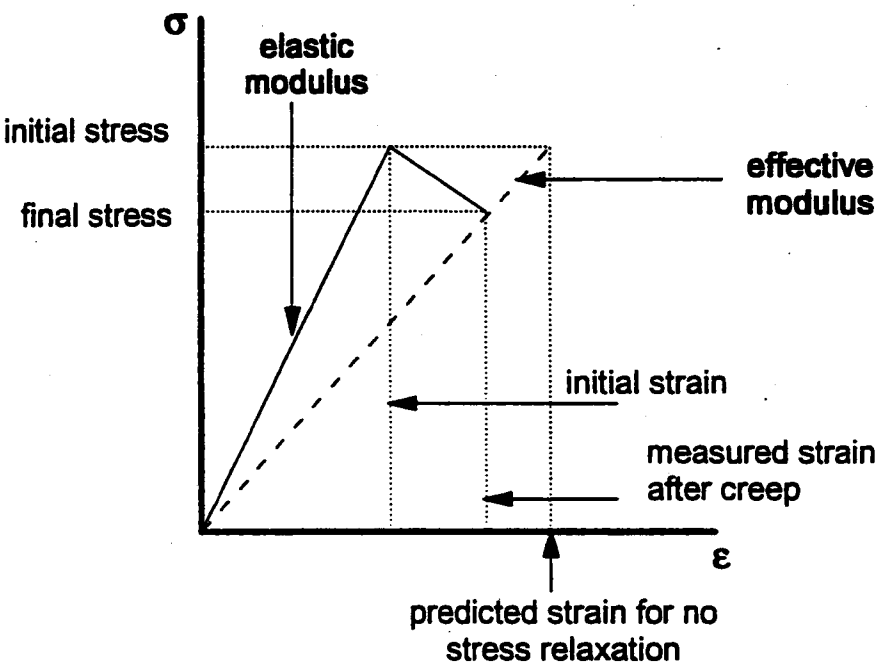

Figure 3.8 Idealized concrete grout stress-strain plot displaying effective modulus method.

3.3.3 Accounting for cracking of the concrete grout

Figure 3.9 displays the stress distribution in a soil nail as the grout cracks. Far from any cracks there is stress in both the steel and concrete. At a crack, there is no stress in the concrete. Near a crack, where bond stress develops between the concrete and steel, there is a transition zone in which there is more stress in the steel and less stress in the concrete. These three possible cases need to be defined in order to properly interpret the strain data.

Figure 3.10 is an example of how these three cases have been defined for this study. The concrete grout stiffness is determined using an appropriate effective modulus for each date that strains were measured after the end of construction. The grout remains intact while the grout load, calculated with the measured strain, is less than the limit grout load defined by Equation 3.7. The limit nail load before cracking is calculated by Equation 3.8.

$$(P_c)_{lim} = f'_t \, A_c \tag{3.7}$$

$$(P_{sn})_{lim} = (P_c)_{lim} + \varepsilon_{lim} \, A_s E_s \tag{3.8}$$

$$\text{in which:} \quad \varepsilon_{lim} = \frac{f'_t}{(E_c^s)_{EOC}}$$

To estimate in-service nail loads, strain data collected at the end of construction were interpreted, as explained in Section 3.3.2. The grout load is calculated using the measured strain by Equation 3.9. The estimated in-service nail load is determined by Equation 3.10.

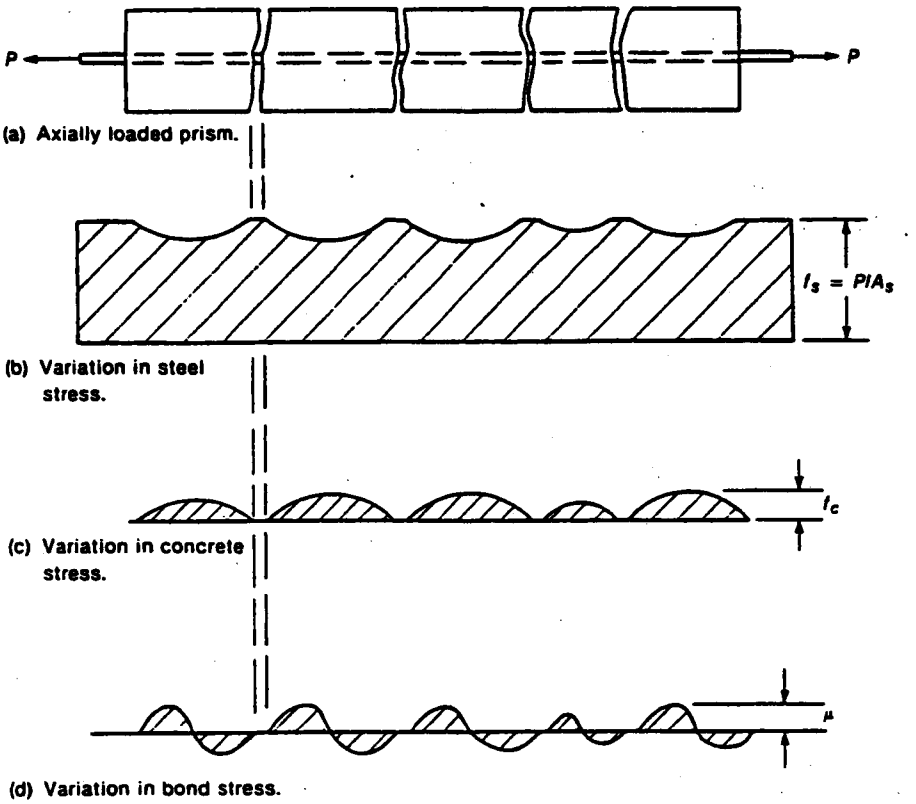

Figure 3.9 Steel, concrete, and bond stress in a cracked prism (after MacGregor, 1988)

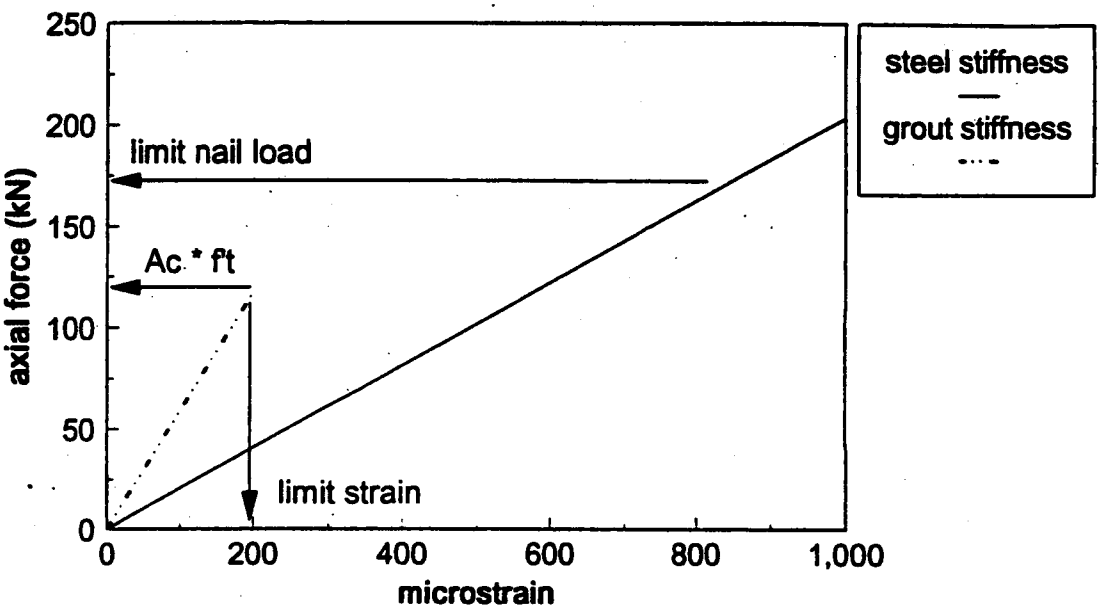

Figure 3.10 Typical stiffness relationship with limit strain and limit composite nail load noted.

$$P_c = \varepsilon E_c^s A_c \tag{3.9}$$

$$\text{If } P_c \leq (P_c)_{lim}, \quad P_{sn} = \varepsilon \left[E_s A_s + E_c^s A_c\right] = P_s + P_c$$

$$\text{If } P_c > (P_c)_{lim}, \quad P_{sn} = (P_{sn})_{lim} \tag{3.10}$$

If P_c is greater than $(P_c)_{lim}$, the assumption of strain compatibility between the grout and steel is no longer valid because the grout load cannot be greater than the limit grout load. A crack has probably formed near the strain gauge and bond stresses have developed between the steel and grout interface. In this case, the estimated nail load is the limit nail load.

The estimated nail load is constrained by lower and upper bounds. Since strain gauges are attached to the steel bar and steel behaves as a linear elastic material, the steel load can always be determined. Therefore, a lower bound is the largest steel load calculated from strain data collected any time after the end of construction. An upper bound is the largest composite nail load using strain data collected any time after construction and calculated by Equation 3.11.

$$(P_{sn})_{max} = (P_s)_{max} + (P_c)_{max} \tag{3.11}$$

$$\text{in which: } (P_c)_{max} \leq (P_c)_{lim}$$

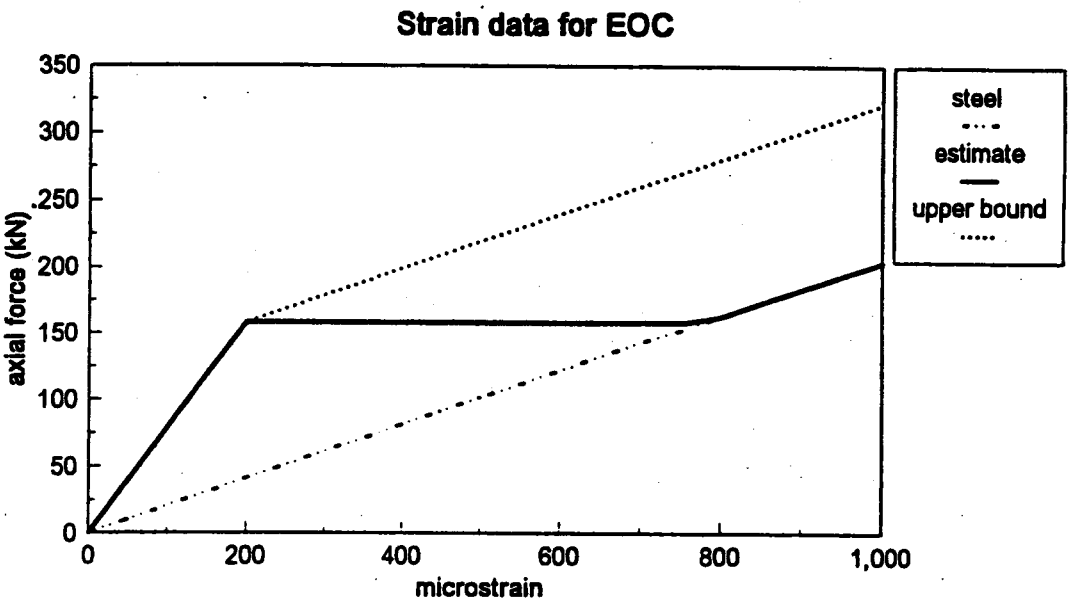

Figure 3.11 Estimated nail load, lower, and upper bounds for a typical nail.

Notice that if the grout has cracked, the upper bound determined by Equation 3.11 assumes the grout continues to carry its limiting load. Figure 3.11 displays the estimated nail load, as well as lower and upper bounds for a typical nail using only strain data collected at the end of construction. The three cases displayed in Figure 3.9 are clearly interpreted by the three slopes of the estimated nail load in Figure 3.11.

3.4 Comparison to other methods of estimating nail loads

In Chapter 2, two other approaches for calculating composite nail loads were discussed; back calculating the composite stiffness from a crack recognized in the strain data, and laboratory testing of a specimen with similar materials and dimensions as the soil nail. The following discussion explains why these other two methods were not used and why the present method was developed.

Only one case history (Polyclinic) was found with strain histories that indicated definite cracking. Many other case histories reported large strains, interpreted as grout cracking, but no jumps in strain were recognized. Therefore, back calculating could not be applied to all case histories. Also there is no way of knowing if a crack occurred right at the gauge location. If the crack did not occur right at the strain gauge, only a partial grout stress release occurs at the gauge and back calculating would under-estimate the composite nail stiffness (Figure 3.9). Additionally, if an external load change occurred during the time interval of cracking, strains before and after cracking cannot be set to an equal composite nail load.

Estimation of nail loads by using a laboratory measured stiffness is a completely different approach from the present method. When strains are correlated with laboratory test information, no assumptions of material properties or response are necessary. A known direct axial tensile load is applied and can be measured with strain gauges attached just as they are in the soil nails. The grout strength and strain relations are tested directly using the same materials used for the in-service soil nails. The changes in stiffness due to grout cracking can be recorded, since a large loading range can be applied.

The first limitation of this method is the fact that the laboratory loading mechanism is different from that of the soil nail. In the laboratory, the free ends of the steel bar are pulled, as opposed to the application of shear stresses to the grout exterior circumferential area. The method of loading and response of actual soil nails are more complex, variable, and difficult to predict than the simple direct tension applied in the laboratory. It would be difficult to simulate the grouting, casting, and curing of a soil nail in the laboratory. The last important limitation is that laboratory testing occurs rapidly at a single concrete age. The laboratory test cannot account for a soil nail loaded in stages at different curing ages, and further, cannot account for creep and stress relaxation of the concrete grout.

The main reason for developing the present method was to allow analysis of an assortment of case histories using a single consistent approach. Back calculating the composite stiffness could not be done for most of the instrumented soil nail walls, because jumps in the strain histories were not observed. Laboratory testing is only a site specific method. Additionally, a

method that accounted for concrete creep was desired in order to interpret long-term strain measurements.

Chapter 4

Estimated In-service Nail Loads

4.1 Introduction

A method of estimating soil nail loads is described in the previous chapter. This method was applied to data sets from several soil nail walls instrumented with strain gauges and the resulting estimated nail loads are reported in this Chapter. For each case history, the soil nail wall and instrumentation program is described, and the estimated axial tensile forces in the nails, after construction was complete, are presented.

Section 4.2 presents some examples of interpreting the strain data using the method described in Chapter 3. These examples illustrate how grout creep and cracking affect the estimated nail loads and the upper bounds of the estimates. Section 4.3 describes each of the instrumented soil nail walls and presents the estimated in-service nail loads. In Appendix 2, the values of the estimated axial nail force, the steel bar force, and the upper bound estimate for each strain gauge location along the instrumented nails are reported.

4.2 Examples of strain data interpretations

Figure 4.1A illustrates the three forms of strain data interpretations that depend on grout cracking. This figure is for the Guernsey soil nail wall which used small diameter (115 mm) soil nails. The strain gauges at the two ends recorded low steel strains, and the grout section was assumed to be intact. Therefore, the estimated nail force at these positions is the calculated composite nail load.

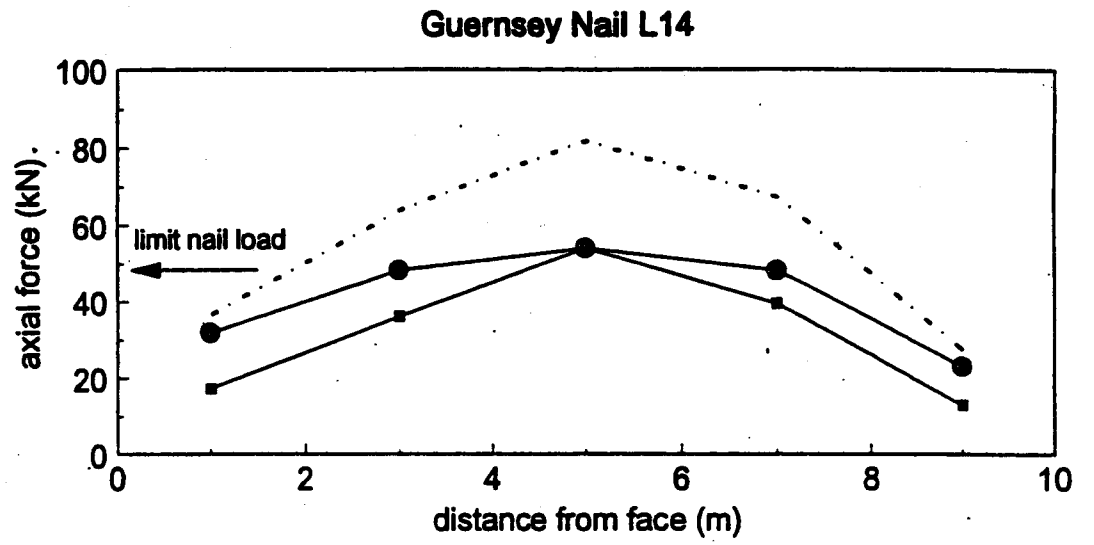

(A)

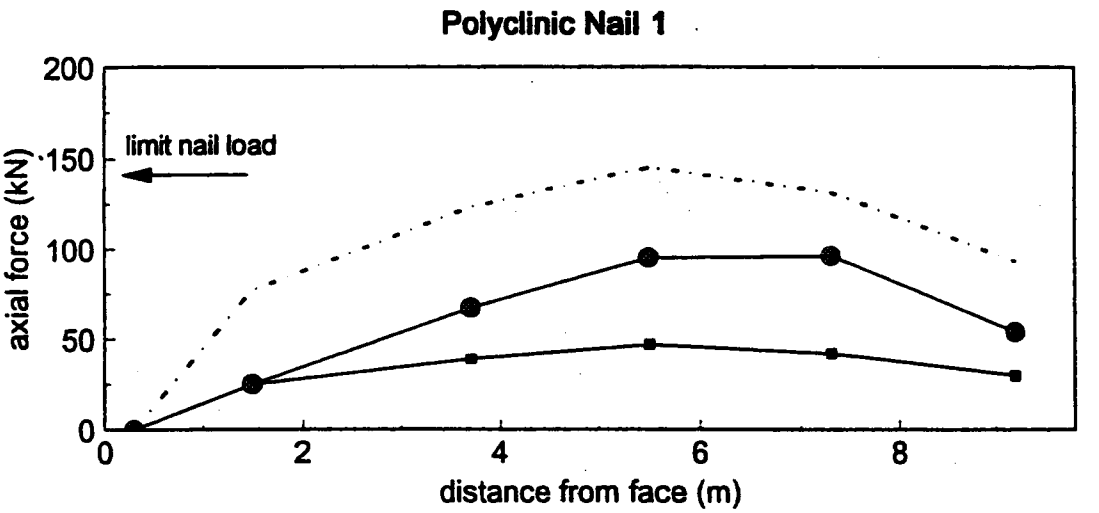

(B)

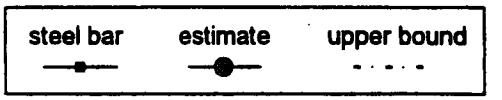

Figure 4.1 Examples of Interpreted Nail Forces.

The strain gauges located 3 m and 7 m from the face recorded high enough strains that the calculated composite load exceeded the assumed limit nail load. This was interpreted to mean that cracking had occurred near the strain gauges, and the limit nail load was considered to be the estimated nail force. The upper bound estimate assumes the grout continues to carry a load equivalent to its ultimate tensile strength. It represents the sum of the measured steel load and the assumed limit grout load.

The strain gauge located at 5 m from the face recorded high steel strains. In this case, the measured steel load exceeded the limit nail load; and hence, the measured steel load was the estimated nail load, which implies that the grout no longer contributed tensile strength to the nail at this location. Again, the upper bound represents the sum of the measured steel load and the limit grout load.

Figure 4.1B illustrates how strain data were interpreted when the grout appeared to creep at a faster rate than the applied creep ratio predicted. This figure is from the Polyclinic Soil Nail Wall where large diameter (229 mm) soil nails were used. The strain gauges along the nail measured relatively low strains. The calculated composite load was less than the limit nail load for the data collected at the end of construction. Since there was no evidence of a change in external loads, the estimated nail forces at these locations were the composite nail loads calculated using data collected at the end of construction. However, when data collected long after completion of construction were used, higher nail forces were calculated, implying that the method of predicting creep underestimated the actual creep rate. Therefore, the upper bound estimate was defined as the largest calculated composite nail load using data from any time.

The largest steel load calculated from data collected at any time was considered to be the lower bound at each gauge location.

4.3 Results of instrumented soil nail walls

The working nail loads were estimated for ten instrumented soil nail walls in which strain gauge data were available. The strain histories allowed the quality of the data to be assessed and provided the necessary time factors to be determined, such as grout age for calculating curing and creep, and an appropriate end of construction (EOC) date. Other researched case histories that did not provide strain time histories, important construction dates, or that only reported estimated nail loads were not used for this study.

Each wall is presented by first discussing important characteristics such as type of structure, soil type and stratigraphy, and the extent of nail instrumentation. This is followed by an assessment of the data quality and the estimated in-service nail forces. The results for each wall are presented in a figure that includes a schematic drawing of the wall cross-section and a plot of the maximum nail load in each nail. The axial nail force distribution is drawn above each instrumented nail in the cross-section. The estimated maximum nail loads for each instrumented nail are graphed vs. the depth of excavation. An empirical diagram based on the work by Juran and Elias (1991) is also plotted to provide a relative measure of the maximum nail loads so that walls with different geometry may be compared qualitatively. This empirical diagram was calculated from the reported design soil parameters. The value of the coefficient of active lateral stress, K_a, was adjusted to account for face slopes and backslopes, and

uniform surcharges were modeled as an equivalent height of soil added to the wall height.

Table 4.1 presents the geometry and structural characteristics of each wall analyzed in this study. When necessary, details of the geometry and/or structure are provided under the discussion of the particular wall.

TABLE 4.1 GEOMETRY AND STRUCTURE CHARACTERISTICS OF ANALYZED SOIL NAIL WALLS

	Swift-Delta Station 1	Swift-Delta Station 2	Polyclinic	Peasmarsh	Guernsey
Height (m)	5.3	5.6	16.8	11	20
Face slope (deg)	0	0	0	20	30
Back slope (deg)	55 kN/m2 surcharge	27	0	0	0
Type of Facing	shotcrete	shotcrete	shotcrete	geogrid	geogrid
Nail Length (m)	6.4	5.2	10.7	6 - 7	10
Nail Inclination (deg)	15	15	15	20	20
Nail Diameter (mm)	127	127	229	127	115
Steel Diameter (mm)	29	29	36	25	25
Spacing, H x V (m)	1.4 x 1	1.4 x 1	1.8 x 1.8	1.5 x 1.5	1.5 x 1.25

TABLE 4.1 continued

	IH-30, Rockwall Section A	IH-30, Rockwall Section B	San Bernadino	Cumberland Gap 1988	I-78, Allentown
Height (m)	5.2	4.3	7.6	7.9	12.2
Face slope (deg)	0	0	6	0	3 m bench
Back slope (deg)	0	75 kN/m2 surcharge	5	33	33
Type of Facing	shotcrete	shotcrete	shotcrete	shotcrete	concrete panels
Nail Length (m)	6.1	6.1	6.7	13.4	6.1 - 9.2
Nail Inclination (deg)	5	5	12	15	10
Nail Diameter (mm)	152	152	203	114	89
Steel Diameter (mm)	19	19	25	29	25 - 32
Spacing, H x V (m)	.75 x .75	.75 x .75	1.5 x 1.5	1.5 x 1.2	1.5 x 1.5

4.3.1 Swift - Delta Station 1

This wall was constructed below an existing bridge abutment. The designers modeled the abutment as 3 m of soil above the wall without nail reinforcement. The bridge was supported by one row of 355 mm steel pipe piles located 0 to 1 m behind the soil nail wall facing and extending below the toe of the wall. The nails were installed between bridge piers which dictated the 1.4 m horizontal spacing. As shown in Figure 4.2, the bottom nail was inclined at 25° below the horizontal. The figures in the paper by Sakr and Barrows (1991) show a slight inclination of the wall face; since no details regarding inclination are provided in the text of the report, a vertical face was assumed for this study.

The soil consisted of a fill characterized as medium dense, damp to moist, poorly graded sand. The groundwater table was located 2 m to 3 m below the base of excavation. The design soil parameters were $\phi = 33°$, $c = 4.8$ kN/m^2, $\gamma = 18$ kN/m^3, and $K = 0.43$ (Sakr and Barrows, 1991).

Each of the five nails were instrumented at five locations. A strain gauge was installed on the top and bottom of the steel bar at each location. After assessing that both gauges were working properly, the average of the top and bottom measurements was used as the axial strain. The strain data were recorded at least weekly during construction and monthly for one and a half years after construction. The pairs of gauges located near the wall indicate bending of the bar. The information received concerning the data did not mention whether the strain readings were adjusted for temperature.

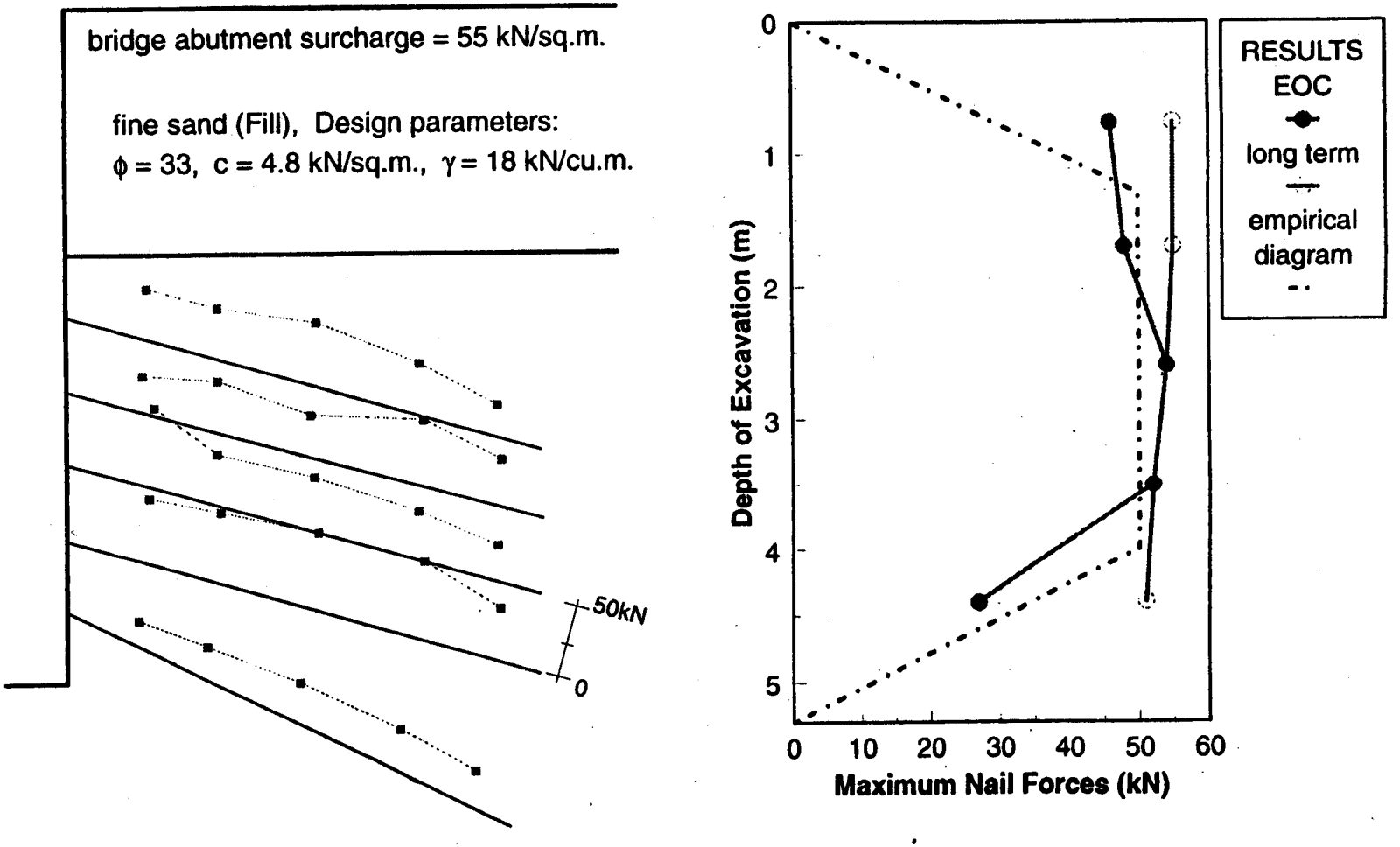

Figure 4.2 Swift-Delta Soil Nail Wall Station1 axial nail force results.

Inclinometers recorded movements for a long time after completion of construction, indicating soil creep. This made estimating in-service nail loads difficult. As explained in Chapter 2, the concrete creep model tends to cause long-term nail forces to be over-predicted. If the soil creeps, actual nail forces in the nails would increase, and long-term nail forces would have to be estimated. Therefore, the results presented in Figure 4.2 include two sets of maximum nail loads-- estimated maximum nail loads at the end of construction, and the largest estimated maximum nail loads using data collected any time after construction.

Estimated maximum nail loads are slightly higher than the empirical diagram predicts. The magnitudes are similar to the loads estimated by the Oregon Department of Transportation using a laboratory stiffness correlation (Sakr and Barrows, 1991). This is notable since the two methods approach the composite stiffness effect in completely different ways. The axial force distributions along the nails are relatively uniform.

4.3.2 Swift - Delta Station 2

This station was not located beneath the bridge abutment, but approximately 15 m to the west. There were no piles or surcharge except for the 27° backslope. The wall was constructed with the same materials.

Explorations in the vicinity of Station 2 encountered fill soils which consisted of silty fine sand with rock and debris to 2 m. Clayey silt was present from 2 m to 3 m. Below 3 m was the same sand fill that was present at Station 1. Groundwater was 2 m to 3 m below the base of excavation. The design soil parameters were the same as reported for Station 1.

Instrumentation was the same as for Station 1, except only four locations on each nail were instrumented because the nails were shorter. The strain data were collected in the same manner as for Station 1.

Inclinometer measurements indicated soil creep at this station also; therefore, estimated maximum nail loads at the end of construction and long-term maximum nail loads are plotted in Figure 4.3. The estimated maximum nail loads are approximately the same as those for Station 1, which means they are higher relative to the empirical diagram. This may be because of the low load carried by the first nail, the different fill materials, and/or the increased depth of excavation below the bottom nail. The axial force distributions along the nails are relatively uniform, except for the peaks in the second and third nails. These peaks appear to be located near the top and bottom contact of the clayey silt layer.

4.3.3 Polyclinic

The geometry and structural parameters listed in Table 4.1 were stated in the data package received from Golder Associates. These were used for the nail load estimations. It should be noted that Thompson and Miller (1990) stated the nail diameter as 203 mm and steel diameter as 32 mm. These values would reduce the loads by the change in grout and steel areas. Nail 1 was installed at an inclination of 20° below the horizontal, as shown on Figure 4.4, to avoid encountering utilities.

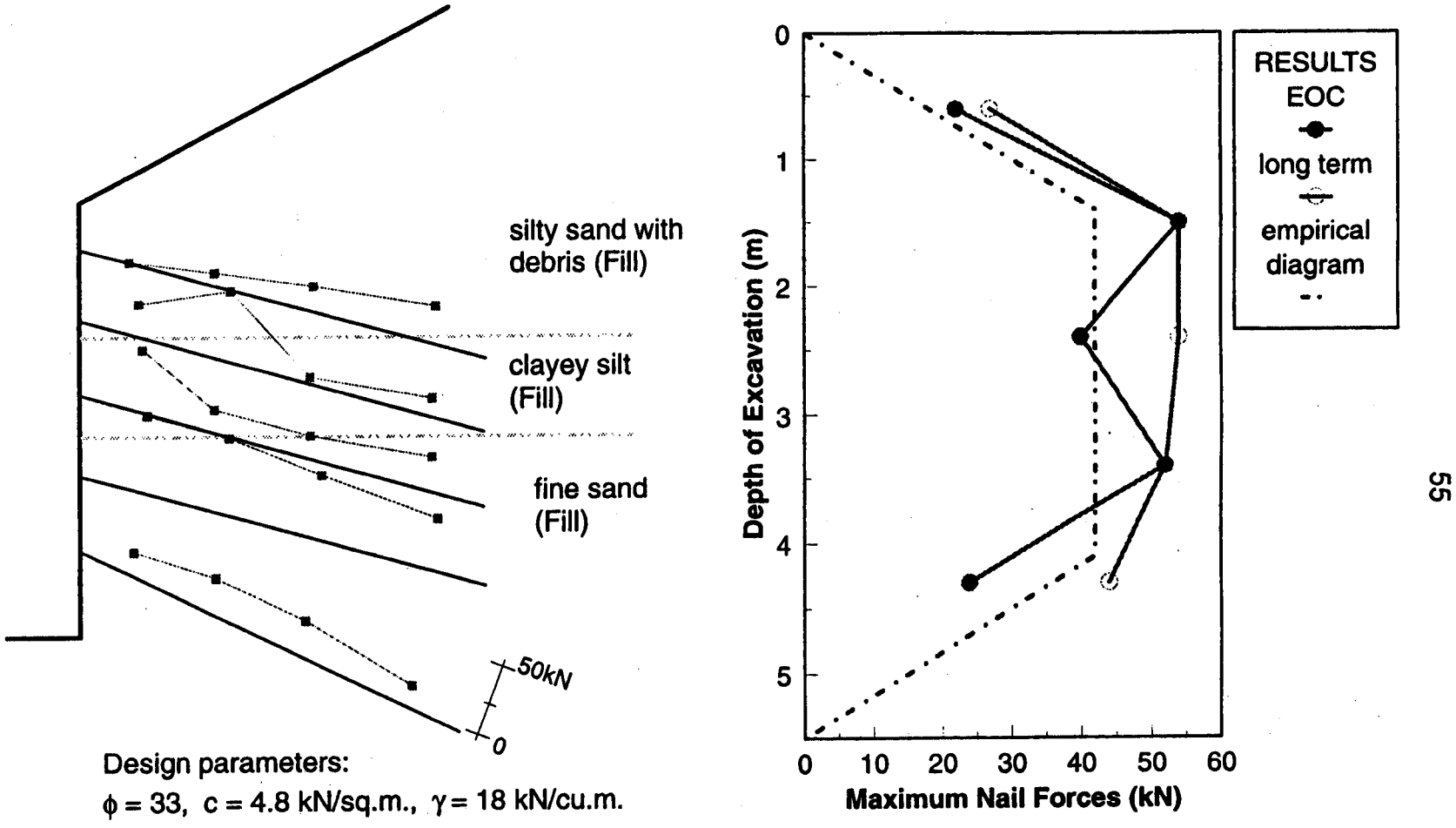

Figure 4.3 Swift-Delta Soil Nail Wall Station 2 axial nail force results.

The soil consisted of a fill for the top 2.4 m, underlain by overconsolidated glacial outwash sand and gravel. Below the bottom of the wall, explorations encountered lacustrine fine sand and silt. The groundwater table was below the depth of excavation. Design soil parameters were $\phi = 40°$, $c = 9.6$ kN/m^2, and $\gamma = 21.2$ kN/m^3 (Thompson and Miller, 1990).

Five of the nine nails were instrumented with four to six strain gauges. The instrumented nails are labeled on the wall cross-section in Figure 4.4. A single strain gauge per nail location was installed at the 3 o'clock position of the rebar. The strain readings were corrected for temperature changes. The data were recorded every workday during construction and six data sets were recorded after construction with the last set recorded nine months after the end of construction.

The measured strains have been assumed to be axial. Possible bending of the nails cannot be accounted for since only one gauge was installed at each location along the nail. In each of the instrumented nails the strain gauges installed nearest the face are most likely to have measured bending effects. Their strain history patterns are inconsistent with other gauges and most showed relatively high loads except for those installed on Nail 1, which indicated compressive strains. The influence of the facing probably caused bending of the rebar in this nail. Most of the gauges measured gradual strain increases with time after construction. The strain increase is most likely due to concrete grout creep since the inclinometer data indicate no movements during this time.

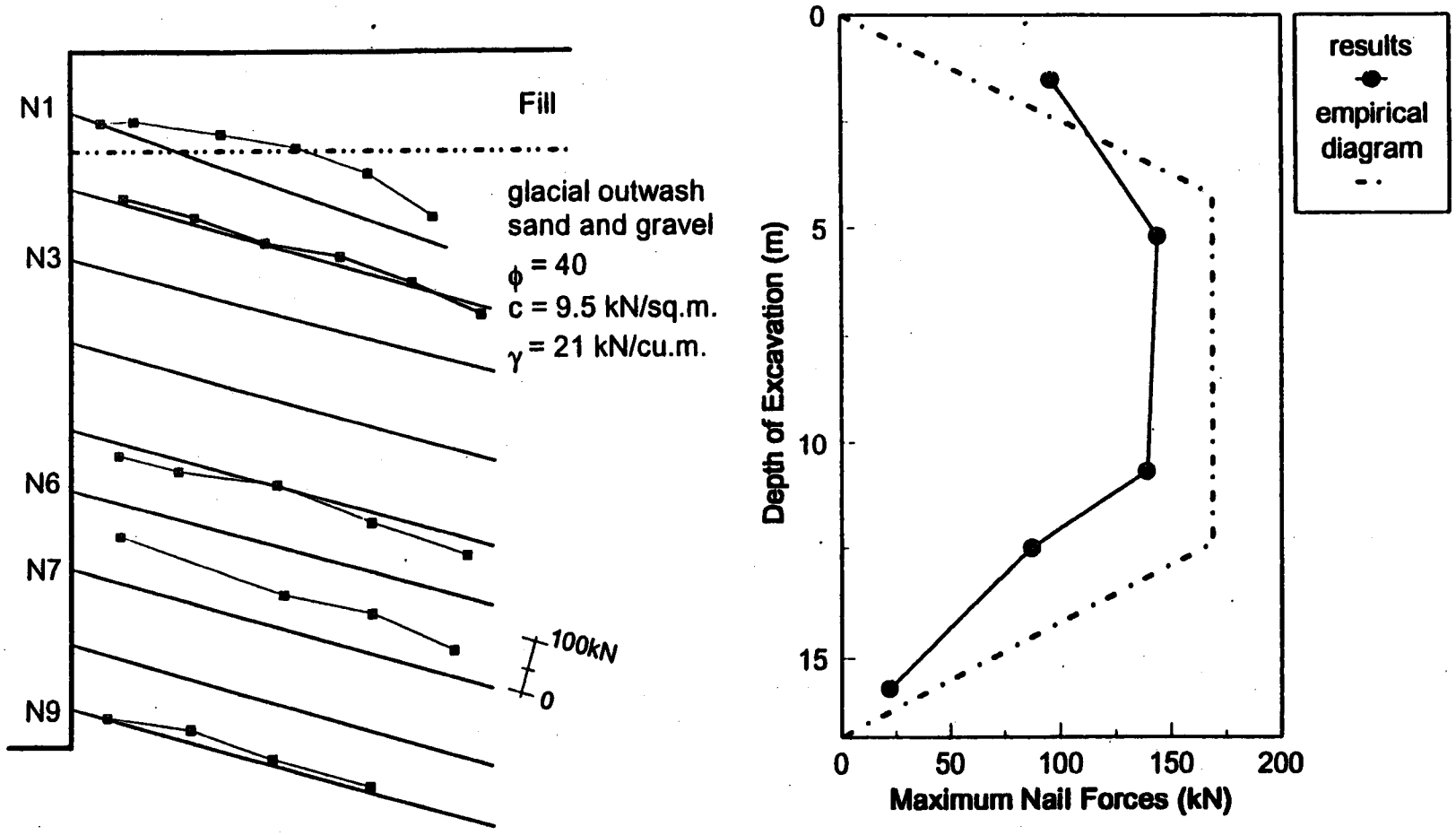

Figure 4.4 Polyclinic Soil Nail Wall axial nail force results.

The results are presented in Figure 4.4. The maximum nail loads are similar to estimates made by Thompson and Miller (1990), and Byrne (1992). Except for the top nail, the estimated maximum nail loads are less than predicted by the empirical diagram. The axial nail force distribution along the nails appears relatively uniform. Implied high forces near the face are probably due to bending which could not be measured.

Gauge 2 in Nail 3 and Gauges 2 and 3 in Nail 6 measured jumps in strain that appear to represent the grout cracking very near the strain gauges. In Nail 6, Gauge 2 cracked 100 days after construction while Gauge 3 cracked during construction. In both cases the estimated composite nail load prior to cracking was comparable to the steel load after cracking. The strain data from these gauges provided an encouraging independent check of the present method of estimating in-service nail forces. Because of the large nail diameter (thus large grout section), estimated nail forces are much larger than steel bar forces except where apparent cracking was observed, as shown in Figure A2.3. In this case history, it was important to consider the composite nail section when interpreting the strain data.

4.3.4 Peasmarsh

The soil nails consisted of the instrumented steel bar grouted within a thin, corrugated PVC sheath which was grouted within the borehole. The top two nails were 6 m long with a 1.5 m horizontal spacing, and the bottom four nails were 7 m long with a 1.75 m horizontal spacing. This is shown on the wall cross-section in Figure 4.5.

The soil consisted of dense, iron cemented silt and fine sand in the top 3.5 m. Stiff, silty clay with bands of claystone was located from 3.5 m to 5 m below the top of the excavation. Below 5 m was interlaminated, very stiff, silty clay with claystone and siltstone. These strata were considered to be horizontal. The groundwater table was not present within the depth of excavation. The design soil parameters were $\phi = 30°$, $c = 0$, and $\gamma = 20$ kN/m^3 (Pedley and Pugh, 1992).

The first, third, and fifth nails were instrumented with strain gauges at five locations along each nail. Data were collected up to one year after construction. The strain histories were received in the form of steel load vs. time, which were easily converted to strain histories. The report of the case history (Pedley and Pugh, 1992) does not mention strain gauges used in pairs but does say only axial tension was observed and no bending. There was no discussion of strain readings corrected for temperature.

The results are presented in Figure 4.5. Except for the top nail, the magnitudes are comparable to those indicated by the empirical diagram. The force distribution shapes reflect the ideal distribution illustrated in Figure 3.2. This is probably due to the sloped face with geogrid protection, which would cause less disturbance to the facing end of the nails than construction of a vertical shotcrete face.

4.3.5 Guernsey

The soil nails were installed to reinforce a 20 m slope, in which excavation steepened the bottom 14 m to 70° from the existing 52° slope. At a later time, excavation continued below the toe and a mini-pile wall was constructed. The

nail loads were estimated prior to the additional excavation in order to analyze a structure comparable to the other soil nail walls.

The soil was described as a clayey, silty sand, residual soil underlain by granitic gneiss. The contact was variable and approximately sub-parallel to the original slope. The approximate contact is shown on the wall cross-section in Figure 4.6. The groundwater table was not present within the depth of excavation. The soil properties, based on the above information, were assumed to be $\phi = 34°$, $c = 5$ kN/m^2, and $\gamma = 20$ kN/m^3.

The bottom five nails were instrumented with strain gauges installed in pairs at five locations along each nail. The strain readings were collected daily during construction until two weeks after construction. The last set of strain data used in this study was collected one month after the end of construction. The strain data from the two gauges at each location were adjusted for temperature and then averaged to obtain axial strains. The data did not indicate significant bending of the nails.

The results are presented in Figure 4.6. The estimated maximum nail loads were less than predicted by the empirical diagram. This may be because the residual soil was stronger than the assumed soil parameters suggested. The distributions of axial nail force along each nail reflects the idealized shape illustrated in Figure 3.2. This may be due to the sloped, geogrid facing which would cause less disturbance to the nail in contrast to shotcrete facings on vertical walls. The bottom nail force distribution peaks close to the face, as would be expected, but this may also indicate that the majority of the nail length penetrated the underlying rock.

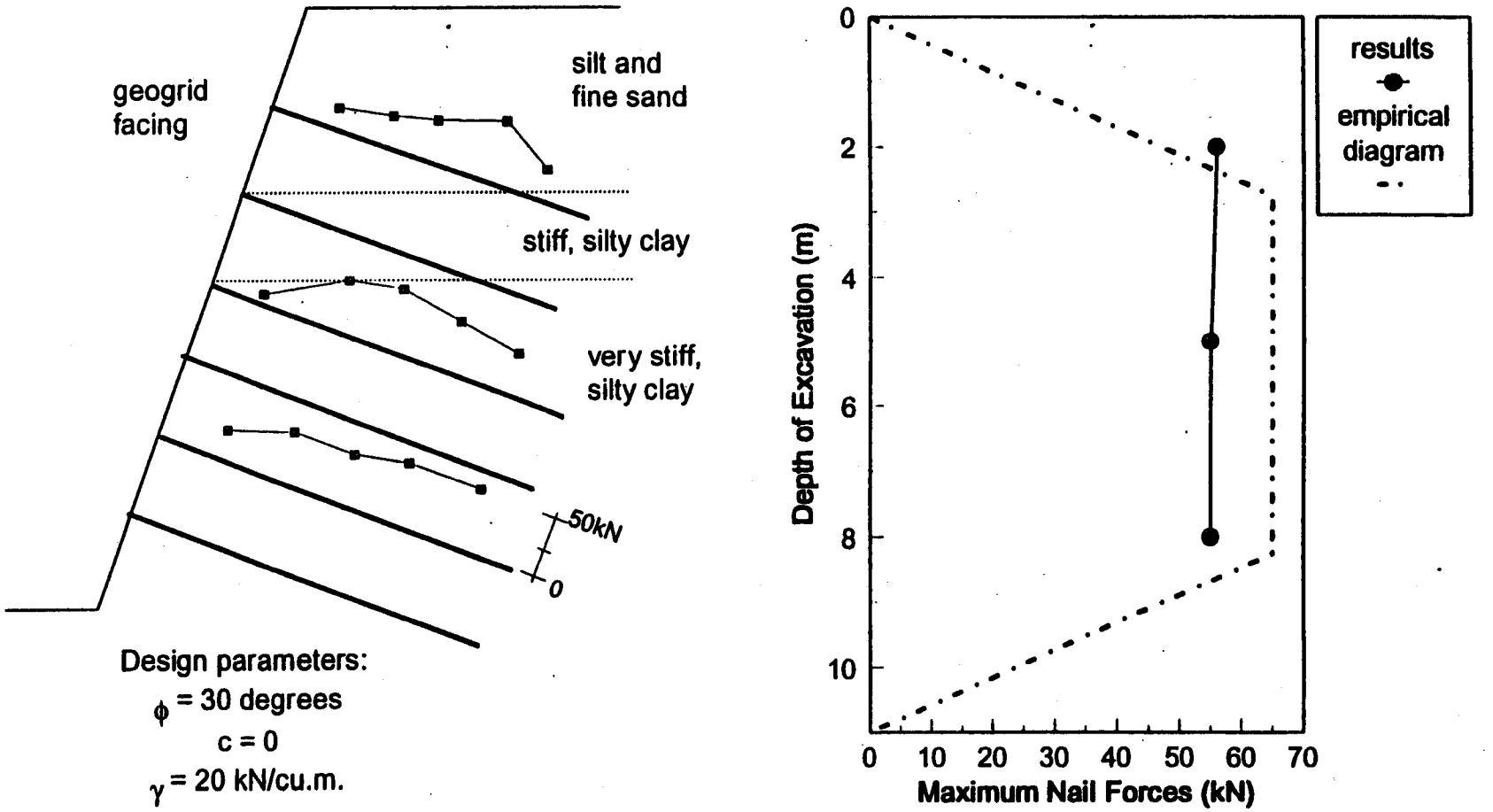

Figure 4.5 Peasmarsh Soil Nail Wall axial nail force results.

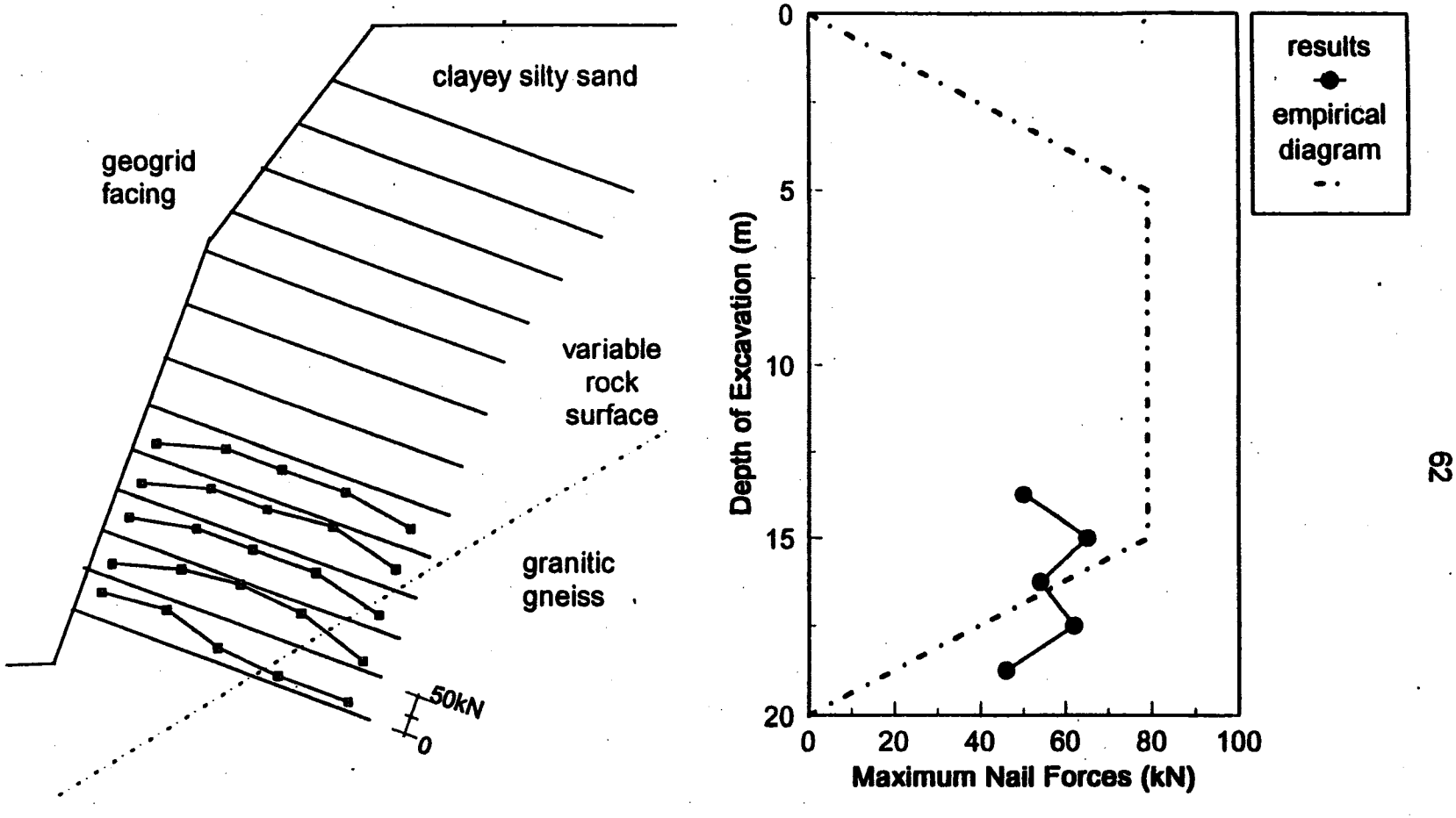

Figure 4.6 Guernsey Soil Nail Wall axial nail force results.

4.3.6 IH-30 Rockwall, Texas Section A

The soil was characterized as very soft to soft, moist, clay (CH). The groundwater table was not present within the depth of excavation. The design soil parameters were c = 13.4 kN/m^2, γ = 18.9 kN/m^3, and K_a = 0.5.

The strain gauges were installed at 2 to 4 locations along each nail. The strain gauges were not used in pairs so bending could not be detected, and the data are assumed to represent axial strains. Corrections for temperature were not mentioned in any of the information received. The strain readings were recorded every 1 to 4 days during construction and weekly after construction for 3 months.

The data from gauges located one foot from the wall face were difficult to interpret because the strain histories had an inconsistent pattern, and there were some large changes after the end of construction. These may have been due to bending and/or temperature change effects. Due to construction problems, the instrumented nail in the second row (Nail 2) was installed after excavation for the third row of nails. This caused the low maximum nail load evident in Figure 4.7.

The estimated maximum nail loads, presented in Figure 4.7, are slightly higher than loads estimated during design (maximum of 40 kN) and much higher than predicted by the empirical diagram. The empirical diagram was calculated based on a purely frictional soil, using the design K_a. Calculating the diagram for a cohesive soil yields much smaller values. The force distributions along the nails are relatively uniform, however the forces near the face may have been influenced by bending, temperature changes, or facing loads.

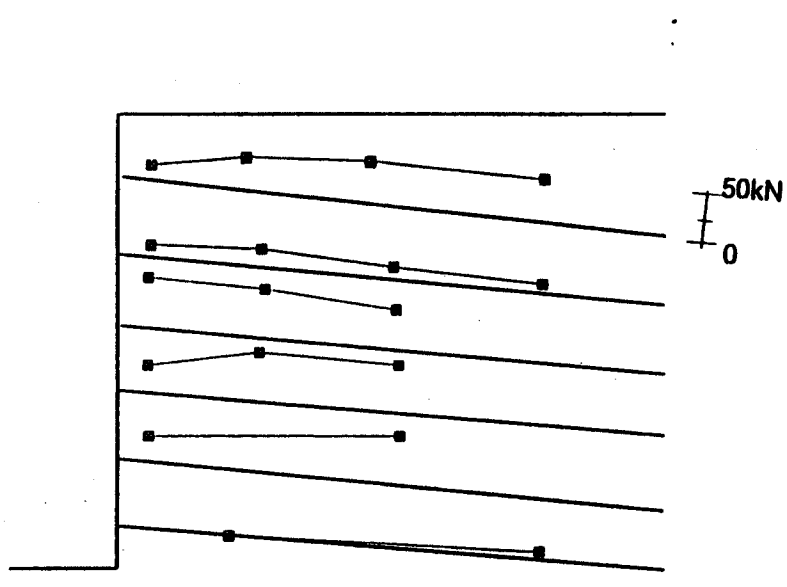

Soft to very soft clay, CH
c = 13.4 kN/sq.m.
γ = 18.9 kNcu.m.
design Ka = 0.50

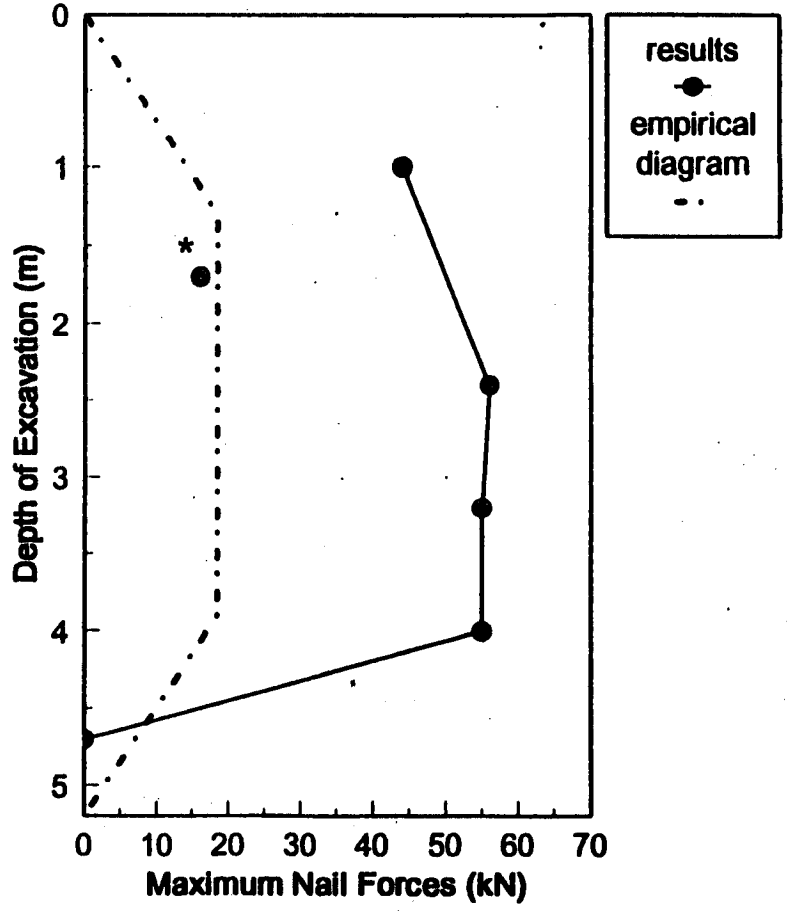

* Nail 2 installed after Nail 3.

Figure 4.7 IH-30 Rockwall, Texas Soil Nail Wall A axial nail force results.

4.3.7 IH-30 Rockwall, Texas Section B

This cross-section was constructed under a 2.7 m bridge abutment located 1.22 m back from the top of the wall. The bridge abutment was modeled as a 75 kN/m^2 surcharge. The soil, instrumentation, and assessment of the data were the same as for Section A. Nail 2 in this section was also installed after excavation for the third nail row.

The estimated nail force results, presented in Figure 4.8, were also similar. The estimated maximum nail loads are larger than those the empirical diagram predicts. The distributions of axial force along each nail are relatively uniform.

4.3.8 San Bernadino

Two cross-sections with the same geometry, materials, and soil were identically instrumented. The estimated axial nail force results are presented for both sections (Figures 4.9 and 4.10); for discussion, both sections are considered to be the same soil nail wall.

The soil consisted of a highly variable silty, gravelly sand with cobbles and boulders. The groundwater table was not present within the depth of excavation. Laboratory testing results indicated ϕ = 34° to 42° and c $\cong$ 7.2 kN/m^2 (Elias and Juran, 1990). The empirical diagram was calculated using the assumed soil parameters ϕ = 38°, c = 7.2 kN/m^2, and γ = 17.3 kN/m^2.

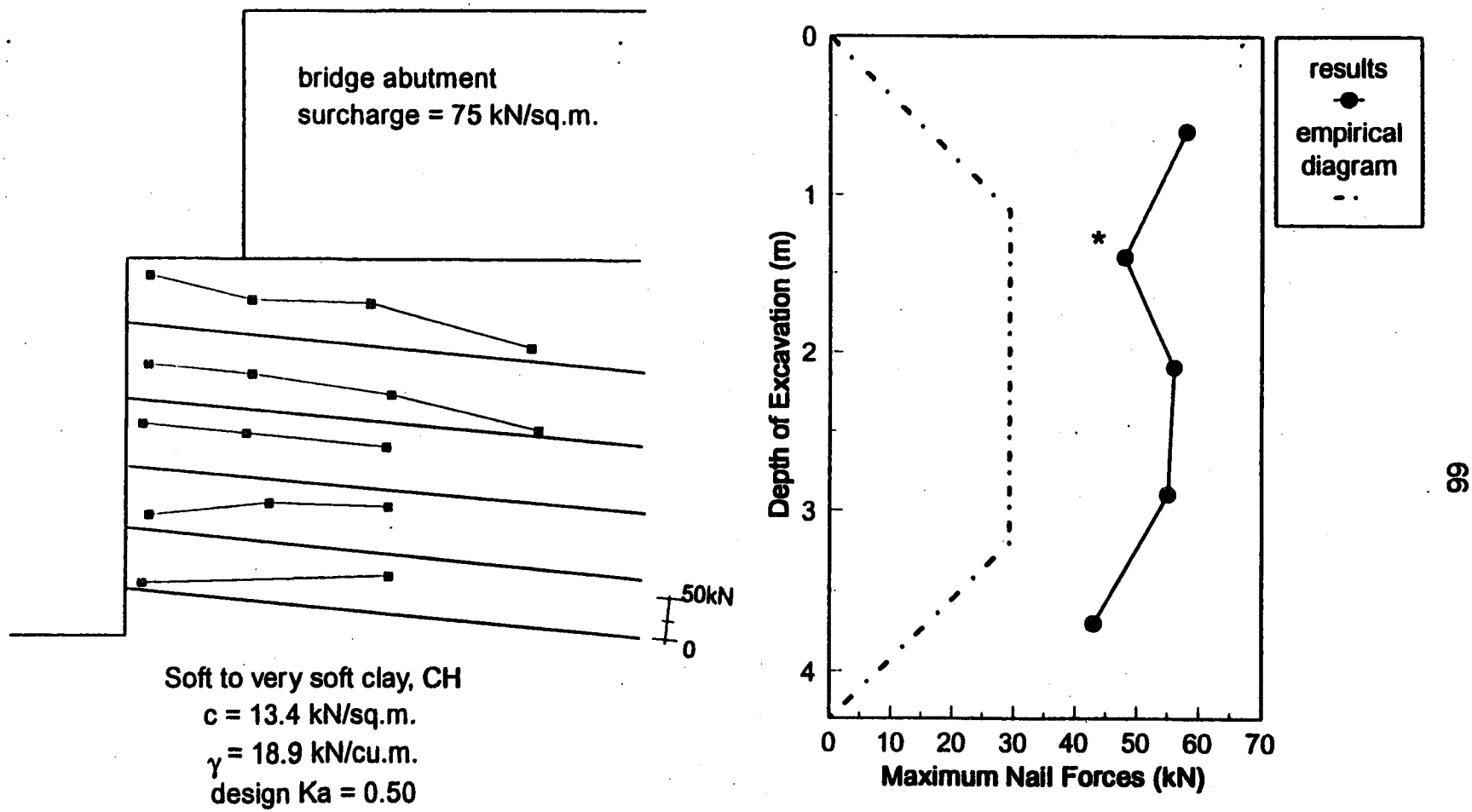

Figure 4.8 IH-30 Rockwall, Texas Soil Nail Wall B axial nail force results.

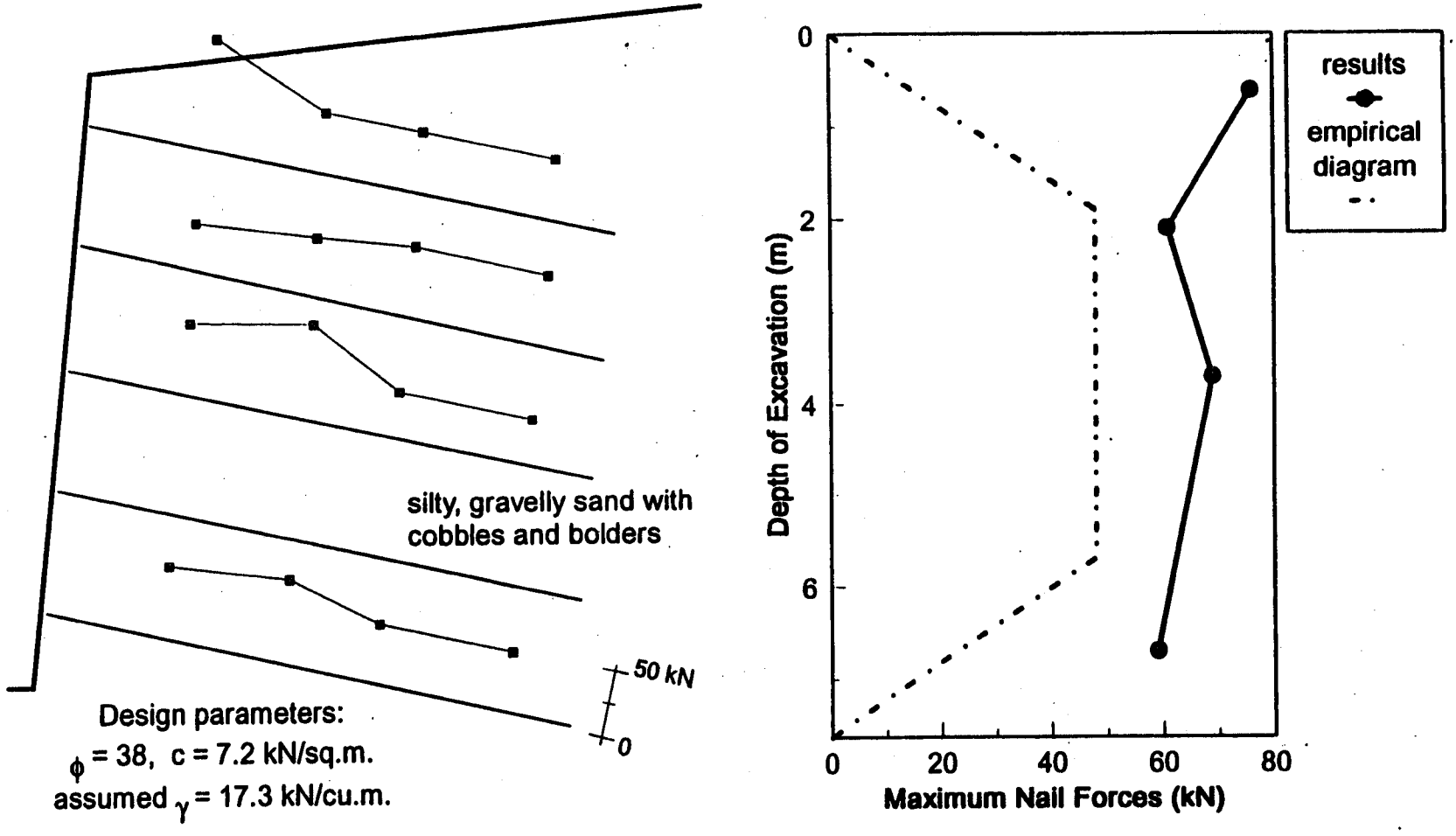

Figure 4.9 San Bernadino, Left Station axial nail force results.

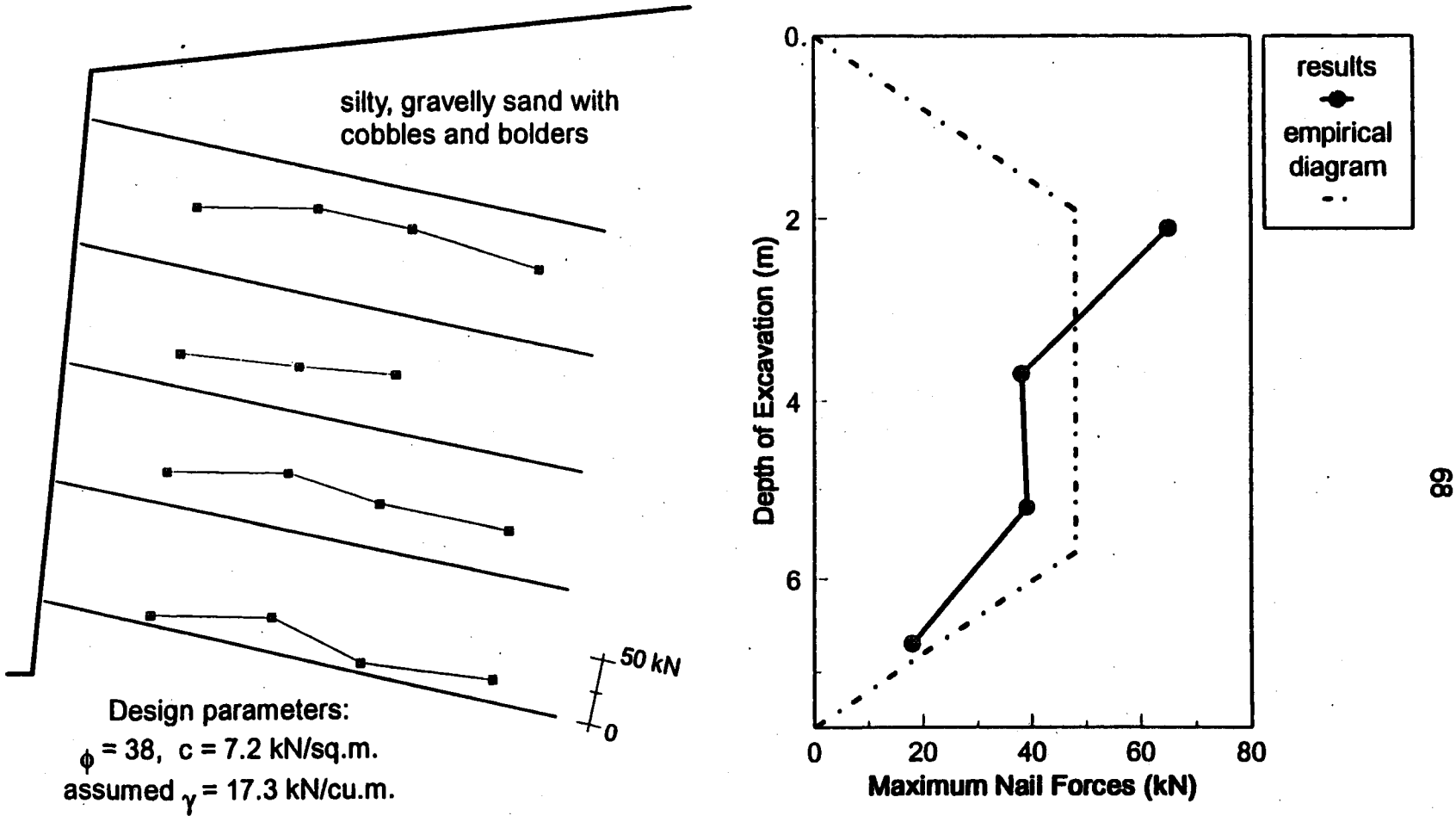

Figure 4.10 San Bernadino, Right Station axial nail force results.

The nails were instrumented with strain gauges placed at four locations on four of five nails in each cross-section. The two gauge locations nearest the face each had four strain gauges installed on the rebar at the top, bottom, left, and right positions. The other two locations had strain gauges placed on the top and bottom of the rebar. The strain readings were adjusted for temperature changes. The data were collected only five times during construction. After the end of construction, the strain data were collected on five additional dates, with the last readings collected approximately two years after construction.

It was beneficial to have 2 to 4 gauges per nail location for assessing bending and averaging the readings to obtain axial strains, because there was a large range of strain readings for gauges at one location. It was not uncommon to have a 30 microstrain difference between the four gauges. This was not always due to bending. For instance, in one case the right and left gauges read high and the top and bottom gauges read low for data collected long after the end of construction. Recording the strain measurements more frequently would have been useful as some strain histories appeared erratic, probably because of the large time gaps between data points. The poor data precision observed in this instrumentation program seems to be relatively unique. There was not a large range in data analyzed from the other walls that installed the strain gauges in pairs.

Results from this wall, presented in Figures 4.9 and 4.10, are interesting because of the low measured strains and large grout section. Based on the present method of determining composite nail forces, no cracking of the grout should have occurred, and the estimated maximum nail loads represent composite nail loads. Although the results seem relatively high compared with

those predicted by the empirical diagrams, they are more realistic than those based on only the steel loads. The uncertainty of the soil properties may be why the estimated maximum loads appear relatively high. The distributions of axial force are relatively uniform along most of the nails. High forces measured near the face were probably due to facing loads.

4.3.9 Cumberland Gap, 1988

This soil nail wall reinforced soil above a rock excavation. Four months after the soil nail wall was completed, rock excavation continued below the toe of the wall. The strain data were analyzed up until the time of rock excavation in order to characterize the structure as a soil nail wall comparable to the other walls in this study.

The only soil information received was a "heterogeneous mixture of residual soil and weathered rock" with $\phi = 38°$ and $c \geq 7.2$ kN/m^2 (Elias and Juran, 1990). The Cumberland Gap, 1985 soil nail wall, constructed adjacent to this wall, reported a soil unit weight of $\gamma = 18.9$ kN/m^3 (Juran and Elias, 1987). This value was assumed for the 1988 wall. The contact between soil and rock is not known. The empirical diagram was calculated using $K_a = 0.35$ to account for the backslope.

The strain gauges were located at four locations along each of the six nails: The strain gauges were installed on the top and bottom of the rebar at 0.3 m and 3 m from the face, while one gauge was installed on the top of the rebar at 6 m and 9 m from the face. The available information did not indicate if the strain data were adjusted for temperature changes. Data were collected every 2

to 4 days during construction and weekly thereafter until the rock excavation began.

The strain gauges 0.3 m from the face measured some bending. After averaging the top and bottom gauge readings to obtain axial strain, the axial force at 0.3 m from the face was the maximum estimated nail force for three of the six nails. It is unfortunate that gauges were only positioned at 3 m intervals along the nails, since the actual maximum nail forces may not have been recorded. The bottom nail was installed 24 days after wall excavation was complete, which accounts for the lack of reinforcement mobilized in this nail.

The results are presented in Figure 4.11. Except for the top nail, the estimated maximum nail loads are less than those predicted by the empirical diagram. The distributions of axial force along the nails are relatively uniform for the first, second, and last nails. The distributions along the third and fourth nails are characterized by low forces measured at both ends of the nails. Significant nail force was only measured near the face in the fifth nail.

4.3.10 I-78 Allentown

Two cross-sections with the same geometry, materials, and soil were identically instrumented. The estimated axial nail load results are presented for both sections (Figures 4.12 and 4.13); results are combined for discussion.

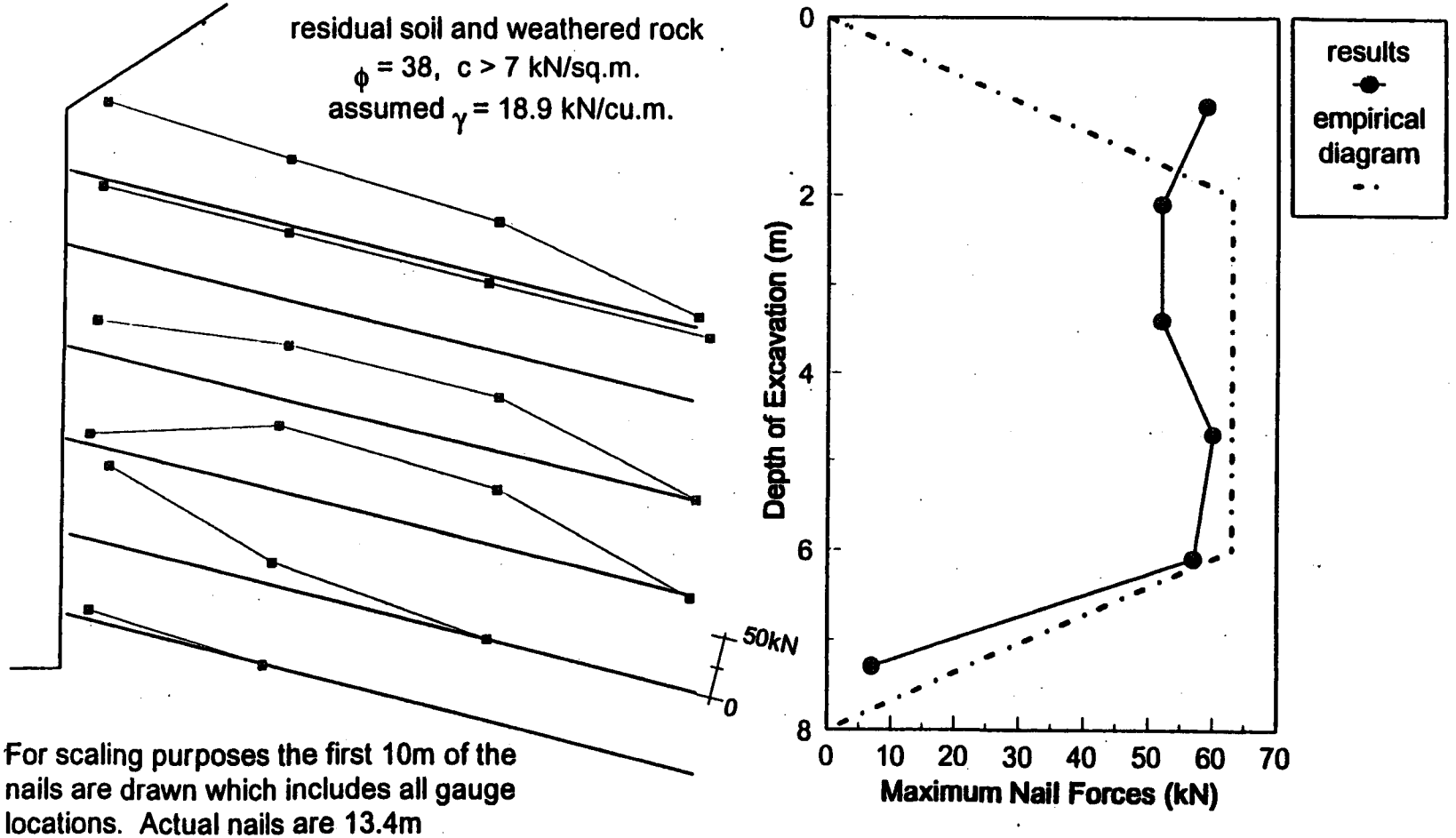

Figure 4.11 Cumberland Gap, 1988 Soil Nail Wall axial nail force results.

The soil nail wall actually consists of two 6.1 m vertical tiers with a 3 m bench separating them. The 33° backslope begins 3 m back from the top of the wall. The top tier was reinforced with 6.1 m nails using 25 mm diameter steel reinforcing bars. The bottom tier consists of 9.2 m nails using 32 mm diameter bars. The wall cross-sections are displayed in Figures 4.12 and 4.13. After excavation of each row, a coat of shotcrete reinforced with wire mesh was applied to the face. After the wall excavation was complete, precast concrete panels, 2 m^2 by 0.165 m thick were attached to the nails. Drain rock filled the space between the shotcrete and concrete panels where the face had been excavated unevenly.

The soil was characterized as colluvium and highly weathered rock. The wall was constructed in an area originally intended to be a competent rock excavation. The colluvium and highly weathered rock appeared to be due to a natural drainage swale at this location (Leichner, 1989). Laboratory testing resulted in ϕ = 39° and c = 86 kN/m^2. Design soil parameters were ϕ = 37°, c = 0, and γ = 19.6 kN/m^3. The empirical diagram was calculated using K_a = 0.35, which includes the backslope but ignores the bench. During nail installation, rock was encountered 1.8 m to 2.4 m from the face in the top tier and 0.3 m to 1 m in the bottom tier.

Four of the eight nails in each section were instrumented with three strain gauges. The gauges were located at 0.3 m, one third the nail length, and two thirds the nail length from the face. Only one strain gauge was installed at each location so bending effects could not be assessed. The available information did not indicate if the strain data were adjusted for temperature changes.

Since concrete panels were attached to the nails, facing construction most likely influenced strains measured close to the face, and bending of the steel bar near the face was likely. Due to the type of facing construction, it is not known if the soil nails were surrounded by soil at the location of the first strain gauge (0.3 m from the face). The gauges further along the nail recorded small strains and were probably located within rock.

The results are presented in Figures 4.12 and 4.13. Except for the top nail in each section, the maximum nail load was measured 0.3 *m from* the face. In Grid 33, the steel load measured near the face in the middle two instrumented nails exceeded the steel yield strength for the rebar. The large measured strains were probably due to bending. The distributions of axial force along each nail are characterized by high forces close to the face and low forces at the other gauge locations. The low nail forces observed further along the nails were probably because the nails were imbedded in competent rock.

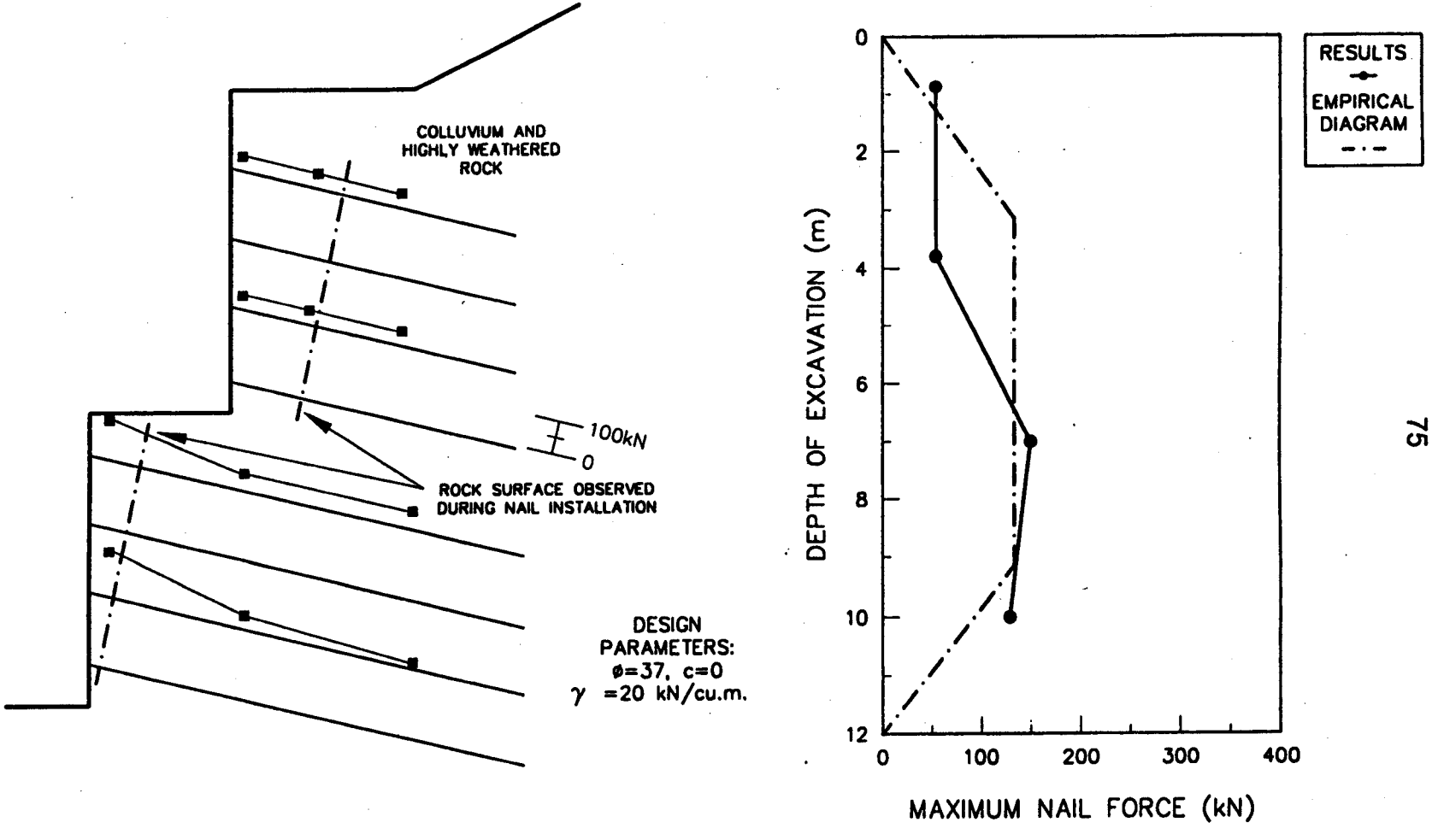

FIGURE 4.12 I–78 ALLENTOWN GRID 24 AXIAL NAIL FORCE RESULTS.

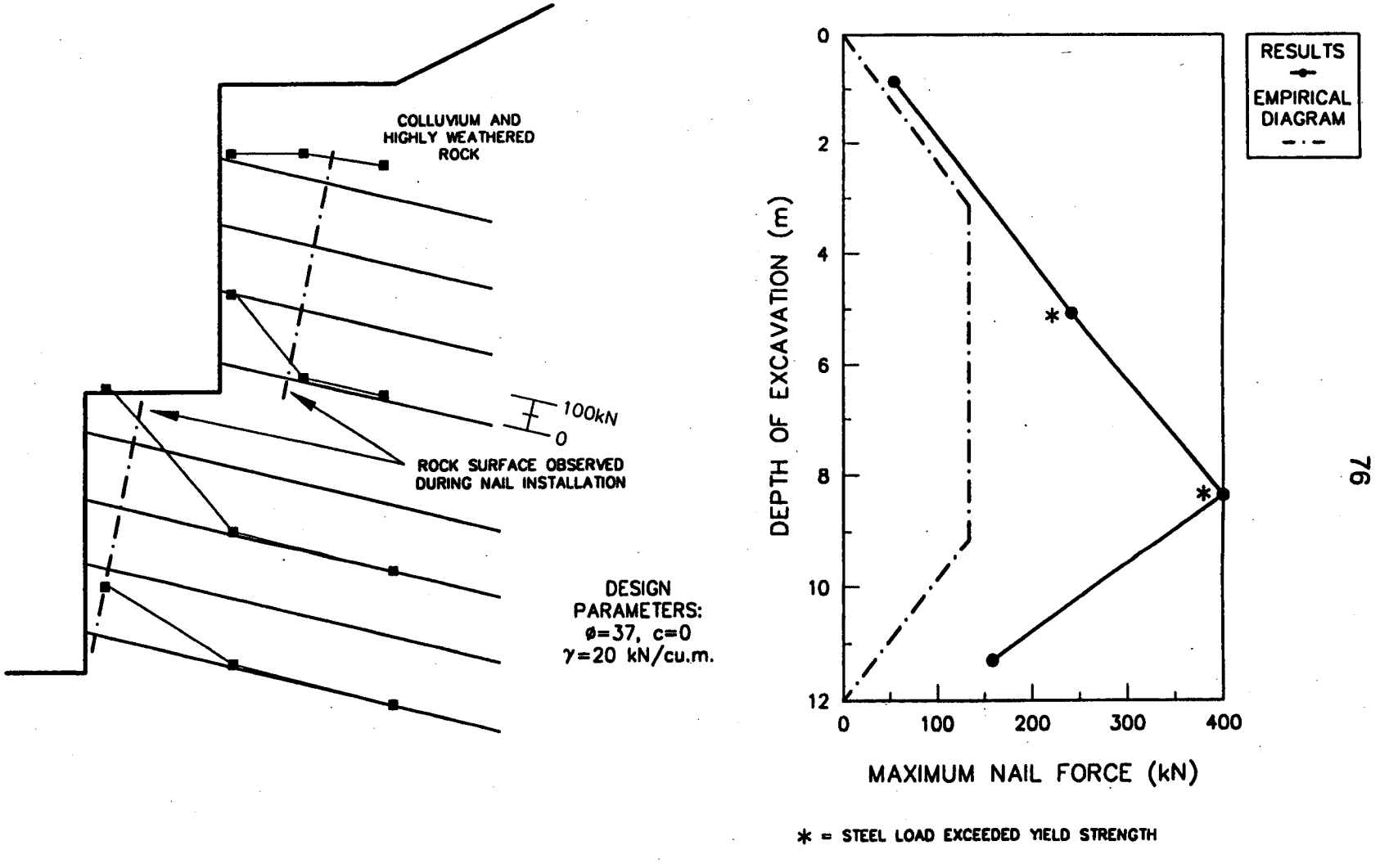

FIGURE 4.13 I–78 ALLENTOWN GRID 33 AXIAL NAIL FORCE RESULTS.

Chapter 5

Conclusions

5.1 Summary

Soil nailing is being successfully employed as the primary support system for construction excavations, walls and slopes. In spite of these successes with soil nailing systems, there is a growing realization that the current design approaches are not sufficiently evolved to predict the performance of the nails under working stress conditions.

The goal of this thesis was to obtain a better understanding of the magnitude and distribution of the loads experienced by the nails under normal working conditions. For that purpose, the observed response of soil nails for a number of walls instrumented with strain gages was reviewed, and a set of general algorithm for estimating nail loads from the strain history data was developed in this thesis.

The proposed approach accounts for the contribution of the concrete grout to the total axial stiffness of the soil nail. Furthermore, the effects of curing, creep and cracking of the concrete grout in the development of the composite nail loads are incorporated in the proposed approach for estimating the nail load from measured strains at the steel-grout interface.

These procedures were applied to the strain data obtained from ten instrumented walls. The estimated distributions of the nail loads along the length of the nails and the maximum loads against depth are presented and discussed for each case history. The estimated maximum loads are compared with the empirical apparent pressure diagram proposed by Juran and Elias (1991).

5.2 Conclusions

In the past, the results of instrumented soil nailing projects have generally reported the tensile force in the steel bar as the nail load without considering the load carried by the surrounding concrete grout. For many soil nail walls, including the walls analyzed for this study, the surrounding grout supports a significant portion of the total load carried by a typical soil nail, and as such, reporting only the steel force as the nail load is misleading. The composite nail stiffness must be considered to improve the estimate of the total nail forces. Some previous works have attempted to account for the composite action of the nail by correlating the strain measurements to the laboratory-determined nail stiffness.

The proposed method for estimating the total nail forces by considering the composite nail section may be applied to any instrumented soil nail, requiring only the measured strain history and the cross-sectional areas of the steel bar and surrounding concrete grout. Thus, it is possible to estimate the development of the axial force in a soil nail with time.

The resulting nail forces, estimated for the analyzed case histories, compared reasonably well with the required reinforcement for active soil conditions predicted by classical soil mechanics. Additionally, the results compare well with reported nail forces estimated by site specific methods that considered the composite action of the nail (Sakr and Barrows, 1991, Thompson and Miller, 1990, Byrne, 1992).

In some of the case histories analyzed in this study, strain measurements were high enough so that the concrete grout had little influence on the total nail

force. Although the load carried by the grout depends on the magnitude of strain and the area of the grout section, it was observed that for small diameter nails the steel force represented the nail load reasonably well. Based on the instrumented nails analyzed in this study, in which the diameters ranged from 89 mm to 229 mm, estimation of nail forces must incorporate the composite action of the nail for soil nails with diameters larger than 100 mm.

A number of trends became evident when comparing the nail forces in the soil nail walls analyzed for this study. The distribution of axial tensile force along the lengths of the nails was relatively uniform, with slight decrease near the far ends of the nails. In most cases, the strains measured near the face were not very reliable due to the affects of bending, facing loads, temperature changes, and/or freezing. Consequently, conclusions regarding face pressure are not very meaningful.

The distribution of maximum nail force down the wall depth was also relatively uniform, except that the estimated maximum nail forces were usually lesser in the bottom row or bottom two rows of nails. This is expected since the nails are tensioned as excavation continues below the nail level, and usually there is no further excavation after installing the bottom row of nails.

The magnitude of the working nail loads for the walls analyzed in this study are compared relative to their respective empirical diagram. In this manner, the nail loads estimated from strain measurements are compared relative to the predicted nail loads based on the design soil properties and wall geometry. The soil nail walls constructed in residual soils and overconsolidated soils generally required less reinforcement than predicted by the empirical diagram. Relatively low reinforcement was required for Polyclinic, Peasmarsh,

Guernsey, and Cumberland Gap. Results from I-78, also constructed in residual soils, are questionable because of probable bending and facing loads, and therefore are not considered in this comparison. The soil nail walls constructed in normally consolidated soils and fill generally required more reinforcement than predicted by the empirical diagram. In particular, the IH-30 walls, constructed in soft clay, required nearly twice the reinforcement predicted by the empirical diagram.

The empirical diagram (Juran and Elias, 1991) evolved from the apparent earth pressure envelope for braced cuts (Terzaghi and Peck, 1967) which was adequately conservative for design of possible strut loads. However, in all of the walls analyzed for this study, at least one estimated maximum nail load exceeded the empirical diagram prediction. Also, the total estimated reinforcement in a wall cross-section exceeded the total reinforcement predicted by the empirical diagram in 6 of the 10 walls analyzed in this study. Additionally, due to the inclination of the soil nails and the method of loading, soil nails are less efficient at reinforcing in situ soil than horizontal struts bracing sheet piles. Thus, the empirical diagram does not appear to be a conservative design for soil nail walls.

5.3 Suggestions for further research

After analyzing soil nail forces from several different instrumentation programs and reviewing several other case histories not included in this study, some suggestions are offered for future research programs.

A minimum of two strain gauges should be attached to the reinforcing bar at each location along a soil nail. The bar should be inserted into the borehole

so that gauges are positioned on the top and bottom of the bar in order to measure potential bending. The spacing of the gauges along the nail should be about 1 to 2 meters. Instruments located within one meter from the wall face should be chosen and monitored carefully. In this study, the strain data from gauges within one meter of the facing were difficult to interpret, due to suspected bending and temperature effects.

Strain measurements should be collected often in order to correlate the strains with the construction sequence. During construction, strain data should be collected daily. After construction, strain data may be collected each time wall and/or soil deformations are measured. To insure a proper initial strain reading representing zero stress, strain readings should be recorded prior to nail installation, immediately after grouting and one day after grouting. All the strain readings need to be corrected for temperature, as these effects have been noticed near the wall face.

In order to improve estimates of the load carried by the concrete grout, specimens of the grout should be collected for laboratory testing. At a minimum, the compressive strength should be determined for a few different curing ages. Determination of the elastic modulus and tensile strength would be an added improvement.

Another suggested research project would be to study the concrete grout tensile creep / stress relaxation relationship for a soil nail. It was noticed during this study that ACI-209 appeared to underestimate the creep rate of the grout in soil nails. This was evident because after the end of construction, nail loads continued to increase when interpreting strain data collected at later times, even

though no external load changes were noticed. Research that could improve the estimation of creep rate would be beneficial.

List of References

ACI 209R-82 (Re-approved 1986), "Prediction of Creep, Shrinkage, and Temperature Effects in Concrete Structures," ACI Manual of Concrete Practice 1992, Part 1.

ACI 207.2R-73 (Re-approved 1986), "Materials and General Properties of Concrete," ACI Manual of Concrete Practice 1992, Part 1, pp. 207.2R-7-11.

Bang, S., Shen, C. K. and Romstad, K. M., "Analysis of an Earth-Reinforcing System for Deep Excavation," Transportation Research Record, No. 749, 1980.

Bang, S., Shen, C. K., Kim, J. and Kroetch, P., "Investigation of Soil Nailing Systems." Prepared for publication in Transportation Research Record, Nov., 1991, 40 pages.

Baska, D. A., "Design and Construction of a Permanent Soil Nailed Wall in Everett, Washington," ASCE Spring Seminar, March, 1992, ASCE Seattle Section, Univ. of Washington, Seattle, WA.

Bastick, M. J., "Soil Nailing and Reinforced Earth," Performance of Reinforced Soil Structures, Proceedings. of the International Reinforced Soil Conference in Glasgow, U.K., Sept. 10-12, 1990, Paper 12.

Bazant, Z. P. and Panula, L., "Practical prediction of time dependent deformations of concrete," RILEM Vol. II No. 65, Sep - Oct, 1978, pp. 307-328.

Bridle, R. J., "The Analysis and Design of Soil Nails," Performance of Reinforced Soil Structures, Proceedings of the International Reinforced Soil Conference in Glasgow, U.K., Sept. 10-12, 1990, Paper 9.

Bruce, D. and Jewell, R. A., "Soil Nailing: Application and Practice, Part 1," Ground Engineering, Nov., 1986, pp. 10-15.

Bruce, D. and Jewell, R. A., "Soil Nailing: Application and Practice, Part 2," Ground Engineering, Jan., 1987, pp. 21-33.

Byrne, R. J., "Soil Nailing: A Simplified Kinematic Analysis," Proceedings of the 1992 ASCE Specialty Conference on Grouting, Soil Improvement and Geosynthetics, Feb. 25-28, 1992, Geotechnical Special Publication No. 30, Vol. 2.

Byrne, R. J., "Soil Nailing: Kinematical Considerations and a Limiting Equilibrium Design Approach," ASCE Specialty Conference, New Orleans, 1992.

Cardoso, A. S. and Carreto, A. P., "Performance and Analysis of a Nailed Excavation," Proceedings of the Twelfth International Conference on Soil Mechanics and Foundation Engineering, Rio de Janeiro, Brazil, Aug. 13-18, 1989, Vol. 2, pp. 1233-1236.

Cartier, G. and Gigan, J. P., "Experiments and Observations on Soil Nailing Structures," Proceedings of the Eighth European Conference on Soil Mechanics and Foundation Engineering: Improvement of Ground, Helsinki, May 23-26, 1983, Vol. 2, pp. 473-476.

Chassie, R. G., "Soil Nailing Overview," ASCE Spring Seminar, Mar. 28, 1992, ASCE Seattle Section, Univ. of Washington, Seattle, WA.

Cotton, D. M., "Soil Nailing: The development of the top down method of permanent wall construction, and local stability problems and resolutions in fill materials, glacial till, outwash, and lacustrine deposits," ASCE Spring Seminar, March, 1992, ASCE Seattle Section, Univ. of Washington, Seattle, WA.

Denby, G., "Two Soil Nailing Case Histories, First Use in Seattle," Proceedings of the 24th Symposium on Engineering Geology and Soils Engineering, Feb. 25th, 1988, Boise, Idaho, pp. 409-423.

Denby, G., Argo, D. and Campbell, D., "Soil Nail Design and Construction of the Swedish Hospital Parking Garage Seattle, Washington," ASCE Spring Seminar, March, 1992, ASCE Seattle Section, Univ. of Washington, Seattle, WA.

Elias, V. and Juran, I., "Summary of Soil Nailing Research Results," U.S. Department of Transportation, Federal Highway Administration, FHWA/RD-90/104, 1990.

England, G. L. and Illston, J. M., "Method of Computing Stress in Concrete from a History of Measured Strain," Civil Engineering and Public Works Review, April 1965, pp. 513-517, 692-694,846-847.

FHWA, Summary of Design Methods Comparison For Nailed Retaining Walls, Preliminary Draft, FHWA demonstration project No. 82, 1991.

Farnham, D. J., "Guernsey: Soil Nail Instrumentation," Trafalgar House Technology, TR. 465, September 1992.

Farnham, D. J., "Guernsey- Soil Nail Monitoring Part 2: Laboratory Testing of Soil Nail," Trafalgar House Technology, TR. 466, September 1992.

Finney, A., "An Evaluation of Soil Nail Analysis Packages," M.S.C.E. Thesis, University of Washington, Seattle, WA, October 1993.

Gässler, G., "Full Scale Test on a Nailed Wall in Consolidated Clay," Proceedings of the International Symposium on Earth Reinforcement Practice, Fukuoka, Japan, November 1988.

Gässler, G., "In-Situ Techniques of Reinforced Soil," Performance of Reinforced Soil Structures, Proceedings of the International Reinforced Soil Conference in Glasgow, U.K., Sept. 10-12, 1990.

Gässler, G., "Soil-Nailing--Theoretical Basis and Practical Design," Proceedings of the International Geotechnical Symposium on Theory and Practice of Earth Reinforcement, Fukuoka, Kyushu, Japan, Oct. 5-7, 1988, pp. 283-288.

Gässler, G., "Vernagelta Geländesprunge - Tragverhalten und Standsicherheit," Doctor Thesis, Publication of the Institute for Soil Mechanics and Rock Mechanics, University of Karlsruhe, FRG, Vol. 108.

Gässler, G. and Gudehus, G., "Soil Nailing--Some Aspects of a New Technique," Proceedings of the Tenth International Conference on Soil Mechanics and Foundation Engineering, Stockholm, June 15-19, 1981, Vol. 3, pp. 665-670.

Gässler, G. and Gudehus, G., "Soil Nailing: Statistical Design," Improvement of Ground: Proceedings of the Eighth European Conference on Soil Mechanics and Foundation Engineering, Helsinki, Finland, May, 1983, Vol. 2, pp. 491-494.

Goldnail User's Manual, Golder Associates, Redmond, WA, Jan., 1993, 20 pages.

Gudehus, G. and Schwing, E., "Soil-Nailing--Design and application to modern and ancient retaining walls," International Geotechnical Symposium on Theory and Practice of Earth Reinforcement, Fukuoka, Japan, 1988, pp. 605-610.

Guilloux, A., Notte, G. and Gonin, H., "Experiences on a Retaining Structure by Nailing in Moraine Soils," Improvement of Ground: Proceedings of the Eighth European Conference on Soil Mechanics and Foundation Engineering, Helsinki, Finland, May 23-26, 1983, Vol. 2, pp. 499-502.

Hettler, A. and Schwing, E., "Scatter of Nail Forces in Soil Nailing," Proceedings of the Twelfth International Conference on Soil Mechanics and Foundation Engineering, Rio de Janeiro, Brazil, Aug. 13-18, 1989, Vol. 2, pp. 1253-1255.

Ho, C.L., Ludwig, H. P., Fragaszy, R. J., & Chapman, K. R., "Field Performance of a Soil Nail System in Loess," Foundation Engineering Proceedings, ASCE, CO Division, Evanstan, IL June 25-29, 1989.

Houghton, D. L., "Determining Tensile Strain Capacity of Mass Concrete," ACI Journal Proceedings V. 73, No. 12, Title No. 84-M29, Dec. 1976, pp. 691-700.

Jewell, R. A., "Soil Nailing," Performance of Reinforced Soil Structures, Proceedings. of the International Reinforced Soil Conference in Glasgow, U.K., Sept. 10-12, 1990.

Jewell, R. A.. "Review of theoretical models for soil nailing," Performance of Reinforced Soil Structures, Proceedings of the International Reinforced Soil Conference, British Geotechnical Society, Glasgow, Sept., 1990.

Jones, C. J. F. P. and O'Rourke, T. D., "Overview of Earth Retention Systems: 1970-1990," Design and Performance of Earth Retaining Structures, ASCE Special Publication No. 25, 1990, pp. 22-49.

Juran, I., Baudrand, G., Farrag, K. and Elias, V., "Design of Soil-Nailed Retaining Structures," Design and Performance of Earth Retaining Structures, ASCE Special Publication No. 25, 1990, pp. 644-659.

Juran, I. and Elias, V., "Behavior and Working Stress Design of Soil Nailed Retaining Structures," Performance of Reinforced Soil Structures, Proceedings. of the International Reinforced Soil Conference in Glasgow, U.K., Sept. 10-12, 1990, Paper 2.

Juran, I. and Elias, V., "Ground Anchors and Soil Nails in Retaining Structures," Chap. 26 in Foundation Engineering Handbook, 2nd ed., Ed. H. Fang, Van Nostrand Reinhold, New York, 1991.

Juran, I. and Elias, V., "Soil Nailed Retaining Structures: Analysis of Case Histories," ASCE Geotechnical Special Publication No. 12, 1987, pp. 232 - 244.

Kakurai, M. and Hori, J., "Soil--Reinforcement with Steel Bars on a Cut Slope," Takenaka Technical Research Report No. 46, Takenaka Corporation, Tokyo, pp. 101-108.

Kosmatka, S. H. and Panerese, W. C., Design and Control of Concrete Mixtures, 13th ed., Portland Cement Association, 1990.

Leichner, C. H., "Case History of a Soil Nailed Wall, in Northhampton County, PA.," Transportation Research Board, 68th Annual Meeting, Meeting Preprint, 1989.

MacGregor, J., Reinforced Concrete, Mechanics and Design, Prentice Hall, 1988, pp. 259-260.

Metha, P. K. and Monteiro, P. J., 2nd Edition, Concrete, Structure, Properties and Materials, 1993, pp. 66, 70, 89-111, 456.

Munfakh, G. A., "Soil Reinforcement: A Tale of Three Walls," Proceedings of the Twelfth International Conference on Soil Mechanics and Foundation Engineering, Rio de Janeiro, Brazil, Aug. 13-18, 1989, Vol. 2, pp. 1285-1288.

Neville, A. M., Creep of Concrete: Plain, Reinforced and Prestressed, North Holland Publishing Co., Amsterdam, (Elsevier), 1970, pp. 91-92, 220-225, 317, 387-392.

Pedley, M. J. and Jewell, R. A., "Analysis For Soil Reinforcement With Bending Stiffness," Journal of Geotechnical Engineering, ASCE, Oct., 1992, Vol. 118, pp. 1505-1528.

Pedley, M. J. and Jewell, R. A., "Soil Nailing Design: The Role of Bending Stiffness," Ground Engineering, Vol. 23, No. 2, March 1990, pp. 30-36.

Pedley, M. J. and Pugh, R.S., "Soil Nailing in the Hastings Beds," 28th Conference of the Engineering Group of the Geological Society, Manchester, England, Sept., 1992.

Pedley, M. J., Jewell, R. A. and Milligan, G. W. E., "A Large Scale Experimental Study of Soil Reinforcement Interaction. Part 1," Ground Engineering, Vol. 23, No. 6, July/August, 1990, pp. 44-50.

Pedley, M. J., Jewell, R. A. and Milligan, G. W. E., "A Large Scale Experimental Study of Soil Reinforcement Interaction. Part 2," Ground Engineering, Vol. 23, No. 7, Sept., 1990, pp. 45-49.

Pfister, P., "Permanent Ground Anchors - Soletanche Design Criteria," FHWA., Report No. RD-81/150.

Plumelle, C. and Schlosser, F., "Three full scale experiments of the french project on soil nailing: CLOUTERRE," Proceedings of the 70th Annual Meeting, Transportation Research Board, Washington, D.C., 1991.

Plumelle, C., Schlosser, F., Delage, P. and Knochenmus, G., "French National Research Project on Soil Nailing: CLOUTERRE," Design and Performance of Earth Retaining Structures, ASCE Special Publication No. 25, 1990, pp. 660-675.

Raphael, J. M., "Tensile Strength of Concrete," ACI Journal NO. 81-17, Mar-Apr, 1984.

Ross, A. D., "Creep of Concrete under Variable Stress," Journal of the American Concrete Institute, March 1958, Title No. 54-41, pp. 739-758.

Sakr, C., "Soil Nailing of a Bridge Fill Embankment," Construction Report, Federal Highway Administration Experimental Features, Oregon Dept. of Transportation, August, 1991.

Sakr, C. and Barrows, R., "Soil Nailing: Its Applicability to Bridge Embankment Retention," Western Bridge Engineer's Seminar, Seattle, WA, Sept. 23-25, 1991.

Salama, M. E., "Analysis of Soil Nail Retaining Walls," Ph. D. Thesis, University of Illinois at Urbana - Champaign, 1992.

Sawicki, A., Lesniewska, D. and Kulezykowski, M., "Measured and Predicted Stresses and Bearing Capacity of a Full Scale Slope Reinforced with Nails," Soils and Foundations, Vol. 28, No. 4, 1988, pp. 47-56.

Schlosser, F., "Behavior and Design of Soil Nailing," Proceedings of the International Symposium on Recent Developments in Ground Improvement, Bangkok, Nov. 29 - Dec. 3, 1982, pp. 399-413.

Schlosser, F. and Unterreiner, P., "French Design Practice," ASCE Specialty Conference on Grouting, Soil Improvement and Geosynthetics, New Orleans, Feb 25, 1992.

Schlosser, F., Unterreiner, P. and Plumelle, C., "French Research Program CLOUTERRE on Soil Nailing," Proceedings of the 1992 ASCE Specialty Conference on Grouting, Soil Improvement and Geosynthetics, Feb. 25-28, 1992, Geotechnical Special Publication No. 30, Vol. 2, pp. 739-751.

Schlosser, F. and Unterreiner, P., "Soil Nailing in France: Research and Practice," Transportation Research Board, 70th Annual Meeting, Washington, D.C., Jan., 1991.

Shen, C. K., Bang, S. and Herrman, L. R., "Ground Movement Analysis of Earth Support System," ASCE Journal of Geotechnical Engineering, Vol. 107, No. 12, Dec. 1981, pp. 1610-1624.

Shen, C. K., Bang, S., Herrman, L. R. and Romstad, K. M., "A Reinforced Lateral Earth Support System," Proceedings of a Symposium on Earth Reinforcement, ASCE, Pittsburg, PA, 1978.

Shen, C. K., Bang, S., Romstad, K. M., Kulchin, L. and DeNatale, J. S., "Field Measurements of an Earth Support System," ASCE Journal of Geotechnical Engineering, Vol. 107, No. 12, Dec., 1981, pp. 1625-1642.

Shen C. K., Herrman, L. R., Romstad, K. L., Bang, S., Kim, J., & DeNatale, J. S., "An In Situ Earth Reinforcement Lateral Support System," Department of Civil Engineering, University of California at Davis, Report No. 81-03, 1981.

Snail User's Manual, Version 2.05, Caltrans, Sept., 1992.

Steel Sheet Piling Design Manual, Pile Buck, Inc., 1987.

Stocker, M. F., Korber, G. W., Gässler, G. and Gudehus, G., "Soil Nailing," C.R. Coll. Int. Reinforcement des sols, Paris, 1979, pp. 469-474.

Stocker, M. and Riedinger, G., "The Bearing Behavior of Nailed Retaining Structures," Design and Performance of Earth Retaining Structures (G. S. P. 25), edited by Lambe, P. C. and Hansen, L. A., ASCE, New York, 1990, pp. 612-628.

Terzaghi, K. and Peck, Soil Mechanics in Engineering Practice, Wiley, 1967.

Thompson, S. R. and Miller, I. R., "Design, Construction, and Performance of a Soil Nailed Wall in Seattle, Washington," Design and Performance of Earth Retaining Structures, ASCE Special Publication No. 25, 1990, pp. 629-643.

U. S. Department of the Navy, Facilities Engineering Command (NAVFAC), Design Manual DM-7.01, U. S. Government Printing Office, Washington, D. C., 1986.

U. S. Department of the Navy, Facilities Engineering Command (NAVFAC), Design Manual DM-7.02, U. S. Government Printing Office, Washington, D. C., 1986.

Wood, S. L., "Evaluation of Long-term Properties of Concrete," ACI Materials Journal, Vol. 88, No. 6, 1991.

Appendix 1

Procedure for Estimating and Presenting Soil Nail Load Results

To summarize and clarify details on how the soil nail load results were obtained, the procedure is presented below in a step by step format.

1) Assemble strain histories for all gauges. Calculate strains from gauge readings (adjusted for temperature if possible).

2) Judge the quality of the data. Make a plot of strain history for all gauges at one location and mark significant construction dates on the plot. Average strains for working gauges at each location to get axial strains. Throw out bad data and document what was discarded and why.

3) Choose an end of construction (EOC) date. This will usually be when the strains in the bottom nail "level" off. Assume no significant load changes after this date unless otherwise noted.

4) Obtain steel material properties, E_S and A_S.

5) Choose grout elastic material properties vs. time. If none are provided with case history, assume $(f'_c)_{28}$ = 20.7 N/mm^2 (3000 psi). Use empirical relations recommended by ACI-209.

$$(f'_c)_t = (f'_c)_{28} \frac{t}{(4+0.85t)} \qquad (3.1)$$

$$(E^e_c)_t = 4800(f'_c)_t^{1/2} \qquad (3.2)$$

$$(f'_t)_t = 0.55(f'_c)_t^{1/2} \qquad (3.3)$$

where t = age of grout

f'_c, E^e_c, f'_t, in N/mm^2

6) Choose creep ratio equation, based on ACI - 209.

$$v_d = 2.94 \cdot C_h \cdot C_w \left[\frac{d^{0.6}}{\left(10 + d^{0.6}\right)} \right] t^{-0.118}$$

d= duration of load in days

t = age of grout upon loading in days

C_h= humidity constant

C_w= thickness constant

7) Calculate time variables. Determine average times during loading.

During construction:

t = d = (days since installed) / 2

for tensile strength of grout, $(f'_t)_t$ use t = days since installed.

After construction:

t = (EOC date - install date) / 2

d = (days since installed) - t

for tensile strength of grout, $(f'_t)_t$ use t = EOC date - install date.

8) Calculate effective grout modulus and grout tensile strength, vs. time.

$$(E_c^s)_d = \frac{(E_c)_t}{1 + v_d}$$

$$(f'_t)_t = 0.55(f'_c)_t^{1/2}$$

9) Calculate grout load, $P_C = \varepsilon * A_C * E_c^s$ (based on strain compatibility).

10) Calculate steel load, $P_S = \varepsilon * A_S * E_S$.

11) Calculate possible nail load for all dates.

a) Calculate the limit grout load, $(P_c)_{lim} = f'_t \, A_c$.

b) Calculate limit nail load,

$$(P_{sn})_{lim} = (P_c)_{lim} + \varepsilon_{lim} \, A_s E_s$$

in which: $\varepsilon_{lim} = \frac{f'_t}{E_c^s}$

c) **Calculate nail load, P_{sn}, for each date.**

If $P_c \leq (P_c)_{lim}$, $P_{sn} = P_s + P_c$

If $P_c > (P_c)_{lim}$, P_{sn} = greater of: $(P_{sn})_{lim}$ or P_s.

12) Estimate Nail Load since EOC.

If for all dates $P_c \leq (P_c)_{lim}$, $P_{sn} = P_{sn(EOC)}$,

upper bound is maxP_{sn}.

If for any dates $P_c > (P_c)_{lim}$, P_{sn} = greater of: $(P_{sn})_{lim(EOC)}$ or P_s ,

upper bound is maxP_s + $(P_c)_{lim}$.

13) Plot Nail Loads and upper bounds along each instrumented nail.

14) On wall cross-section plot maximum estimated nail load for each nail.

15) Compare with empirical earth pressure diagram (Juran and Elias, 1991).

Appendix 2

Axial Tensile Forces along the Instrumented Soil Nail Lengths

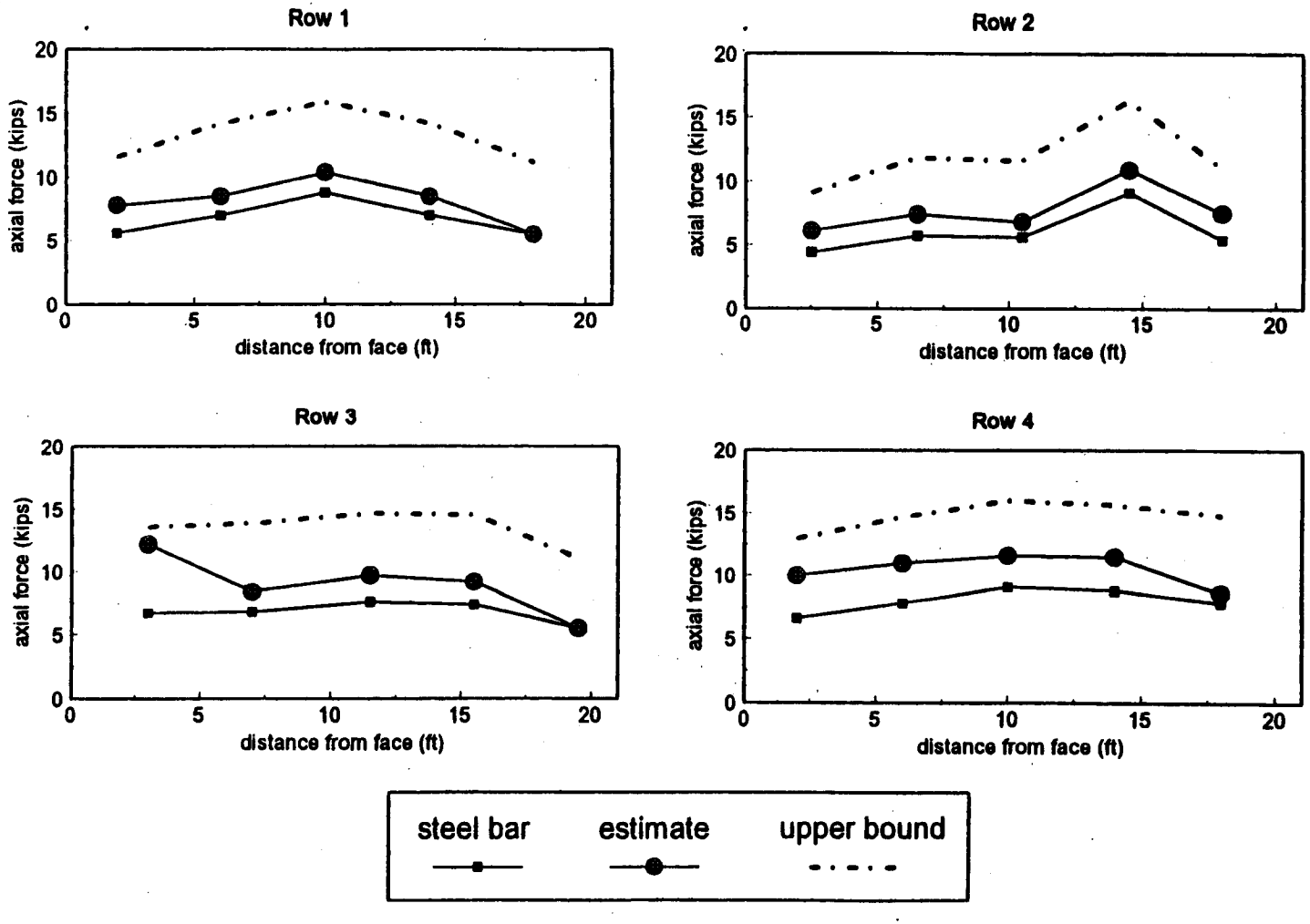

Figure A2.1 Swift - Delta Station 1 axial force vs. nail length plots.

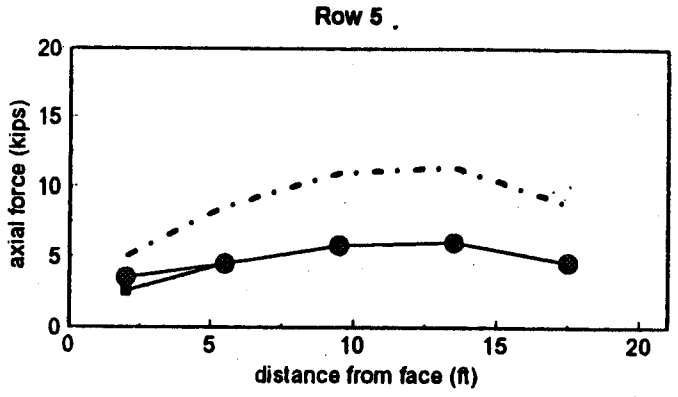

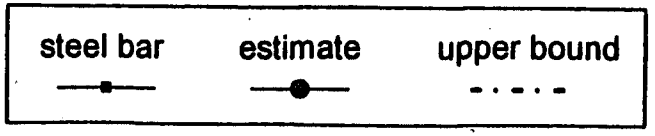

Figure A2.1 continued Swift - Delta Station 1 axial force vs. nail length plots.

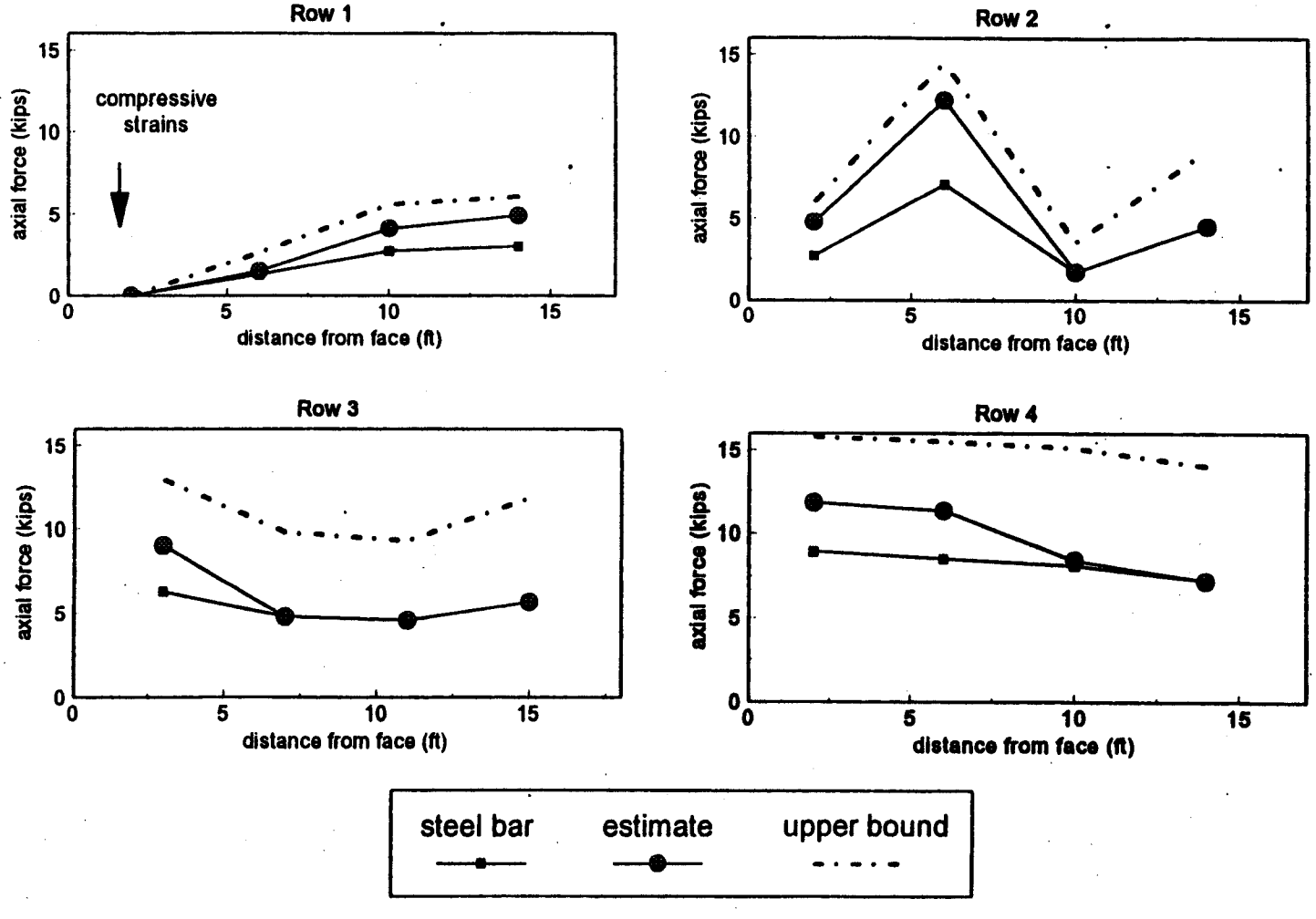

Figure A2.2 Swift - Delta Station 2 axial force vs. nail length plots.

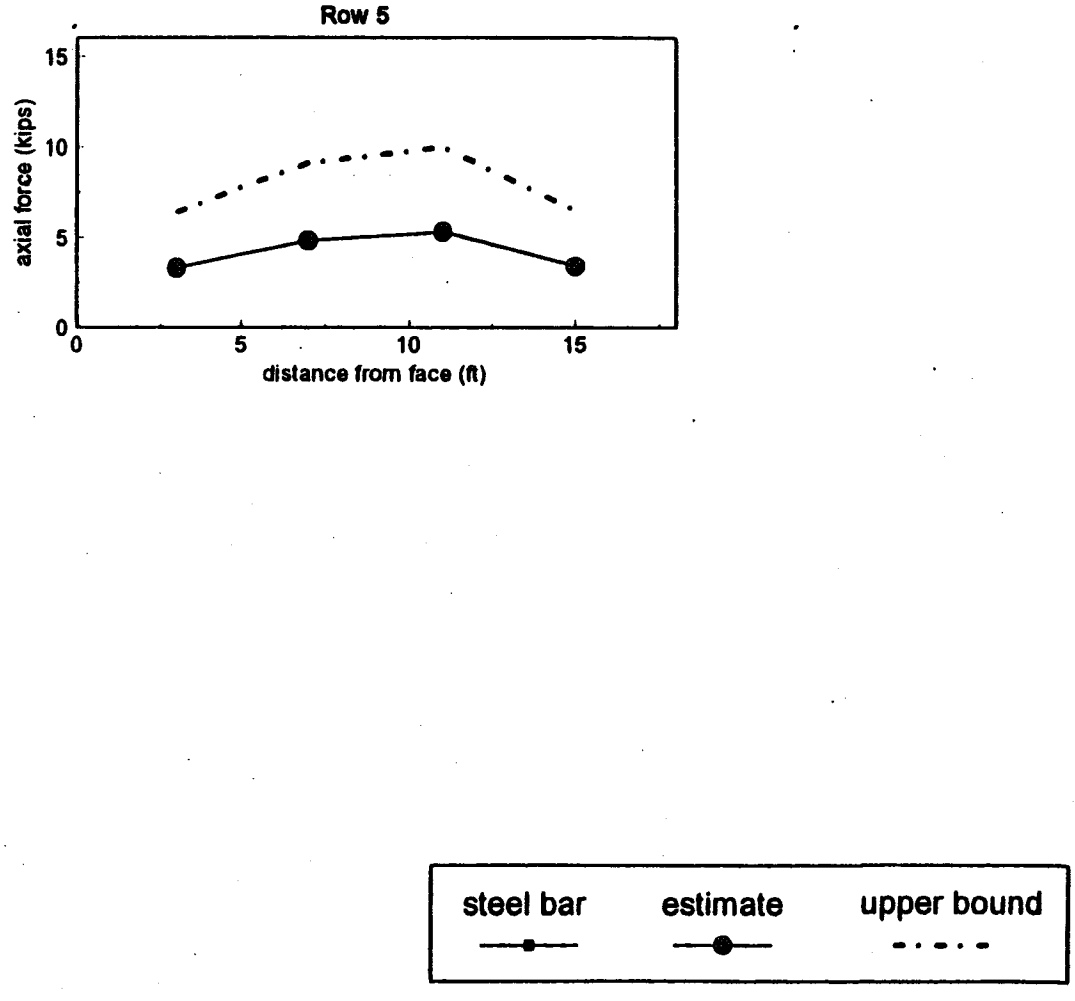

Figure A2.2 continued Swift - Delta Station 2 axial force vs. nail length plots.

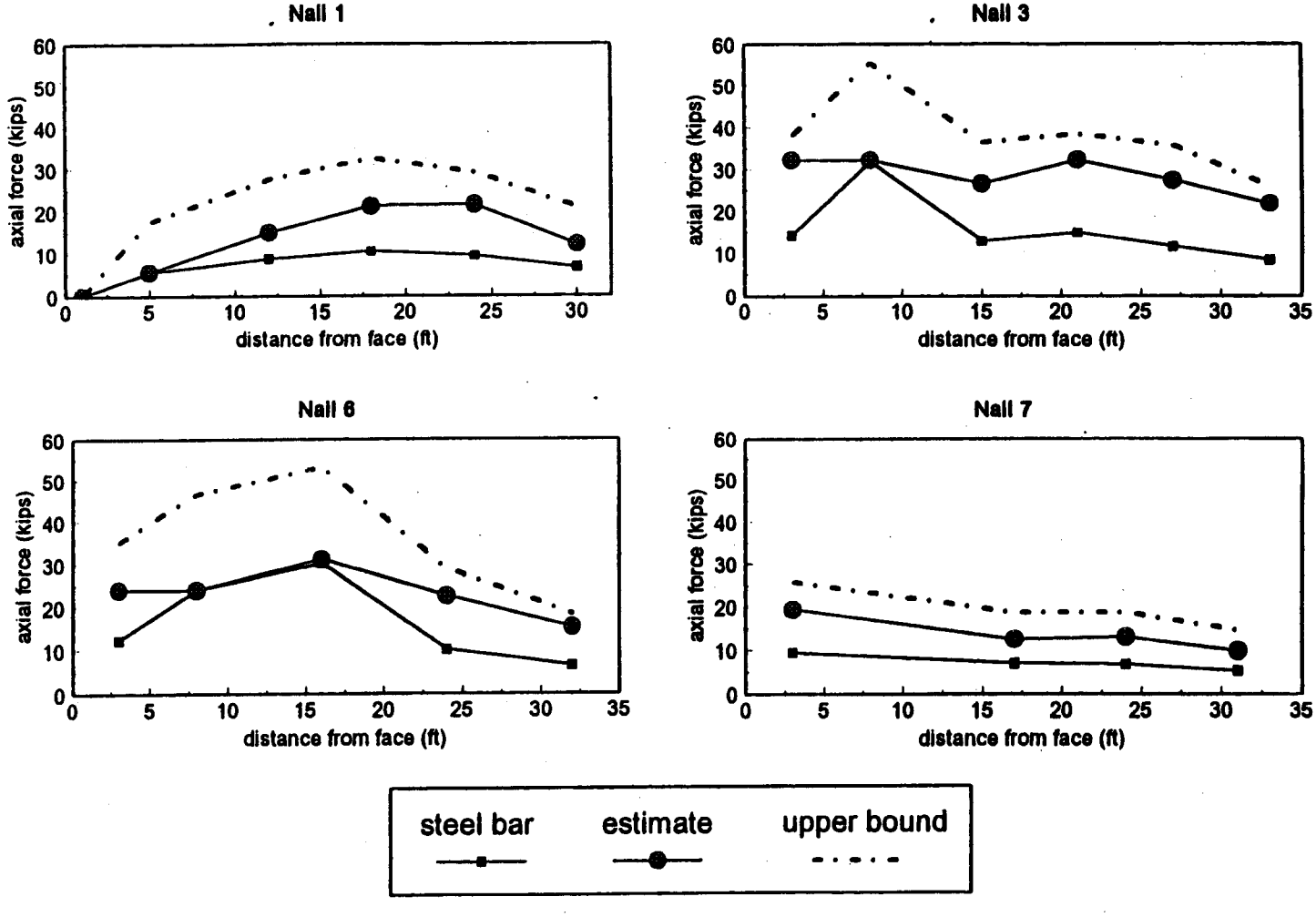

Figure A2.3 Polyclinic axial force vs. nail length plots.

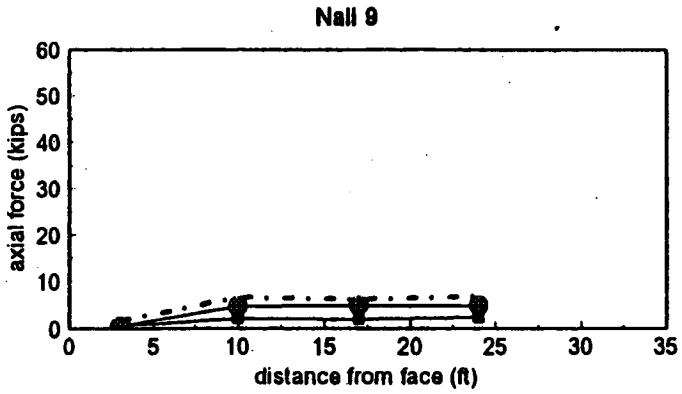

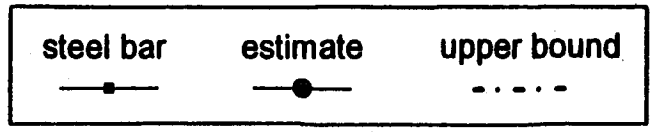

Figure A2.3 continued Polyclinic axial force vs. nail length plots.

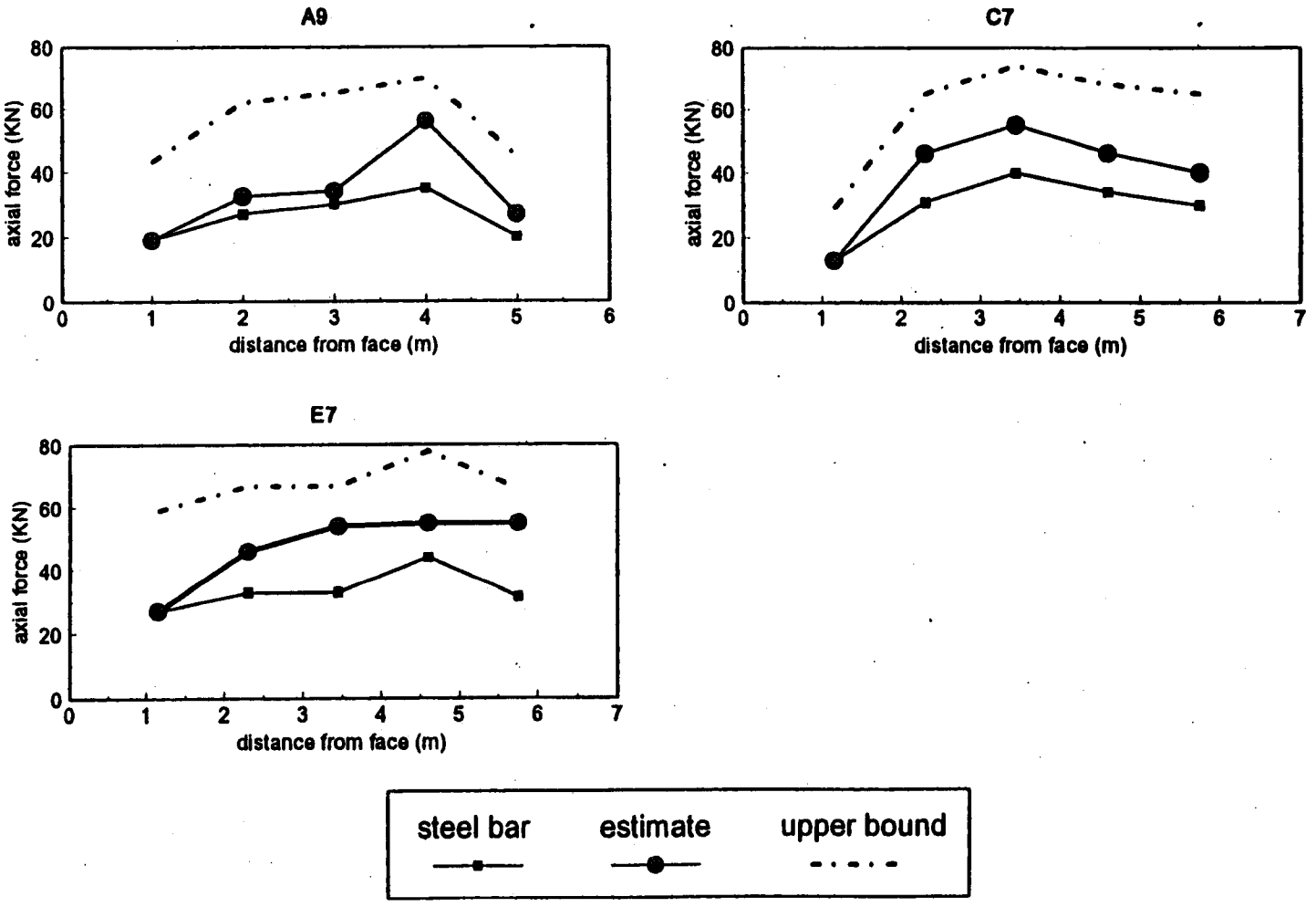

Figure A2.4 Peasmarsh axial force vs. nail length plots.

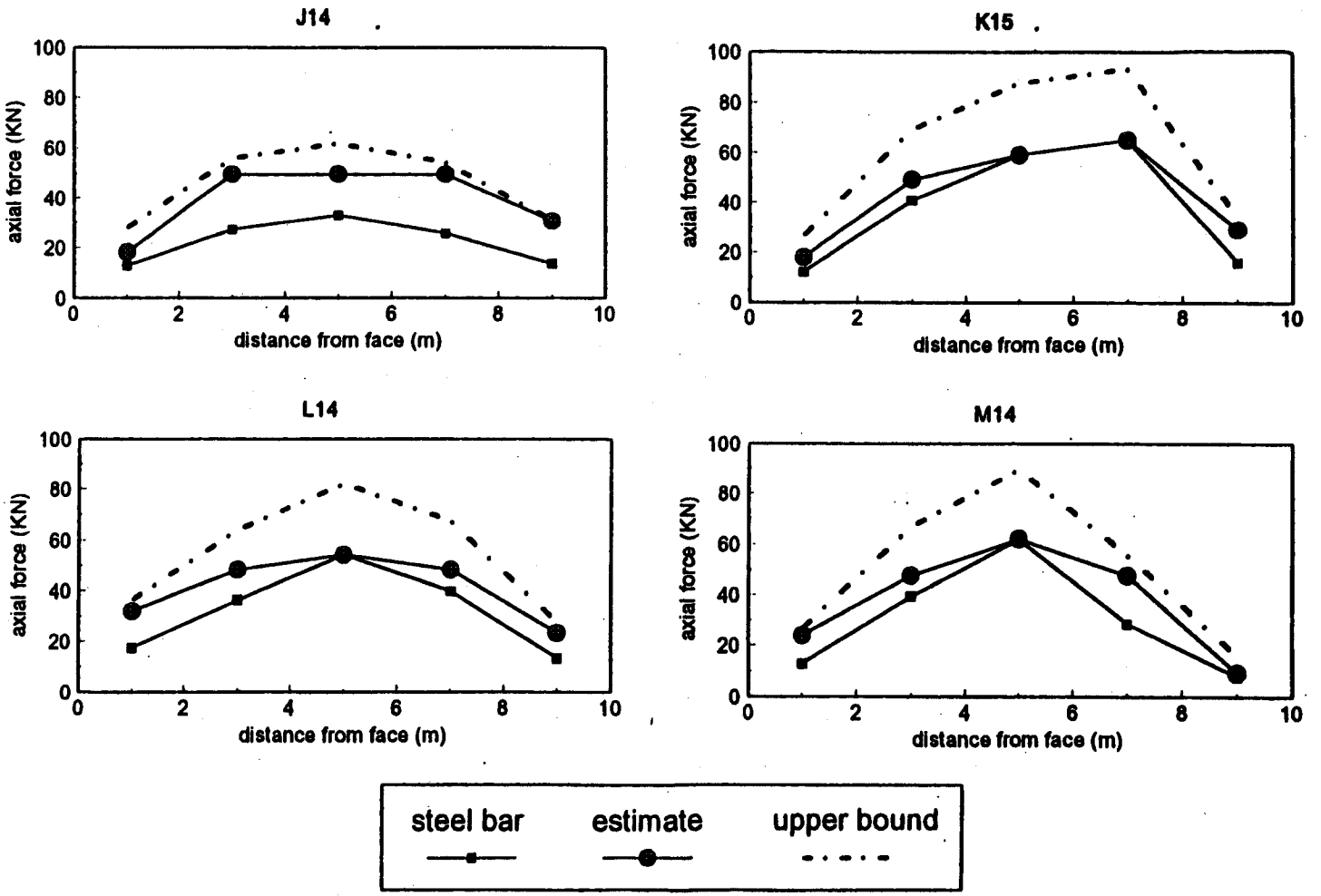

Figure A2.5 Guernsey axial force vs. nail length plots.

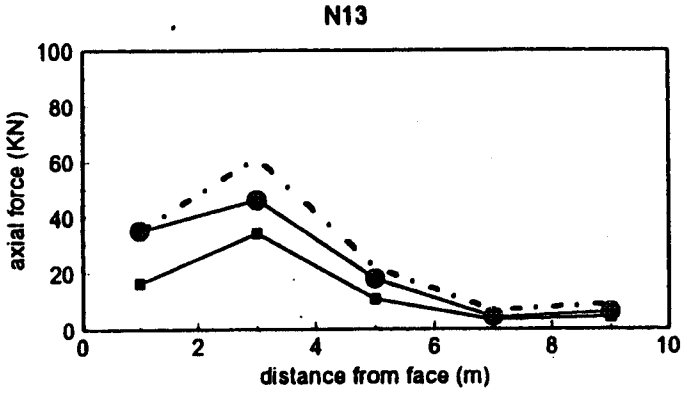

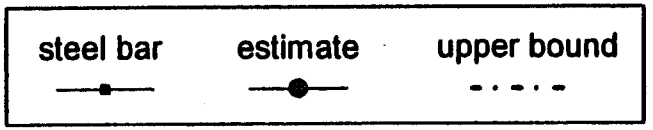

Figure A2.5 continued Guernsey axial force vs. nail length plots.

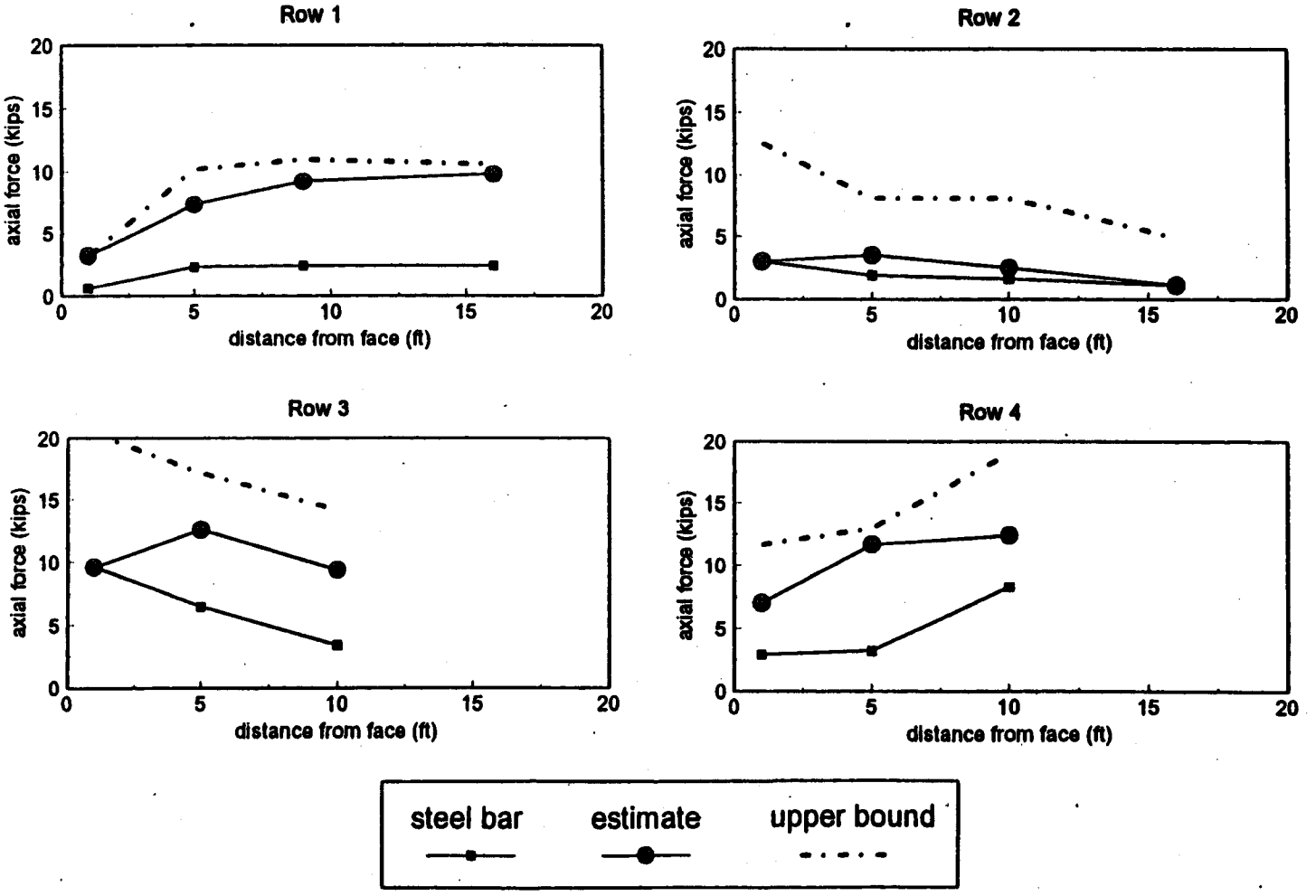

Figure A2.6 IH-30 Rockwall, Texas Range A axial force vs. nail length plots.

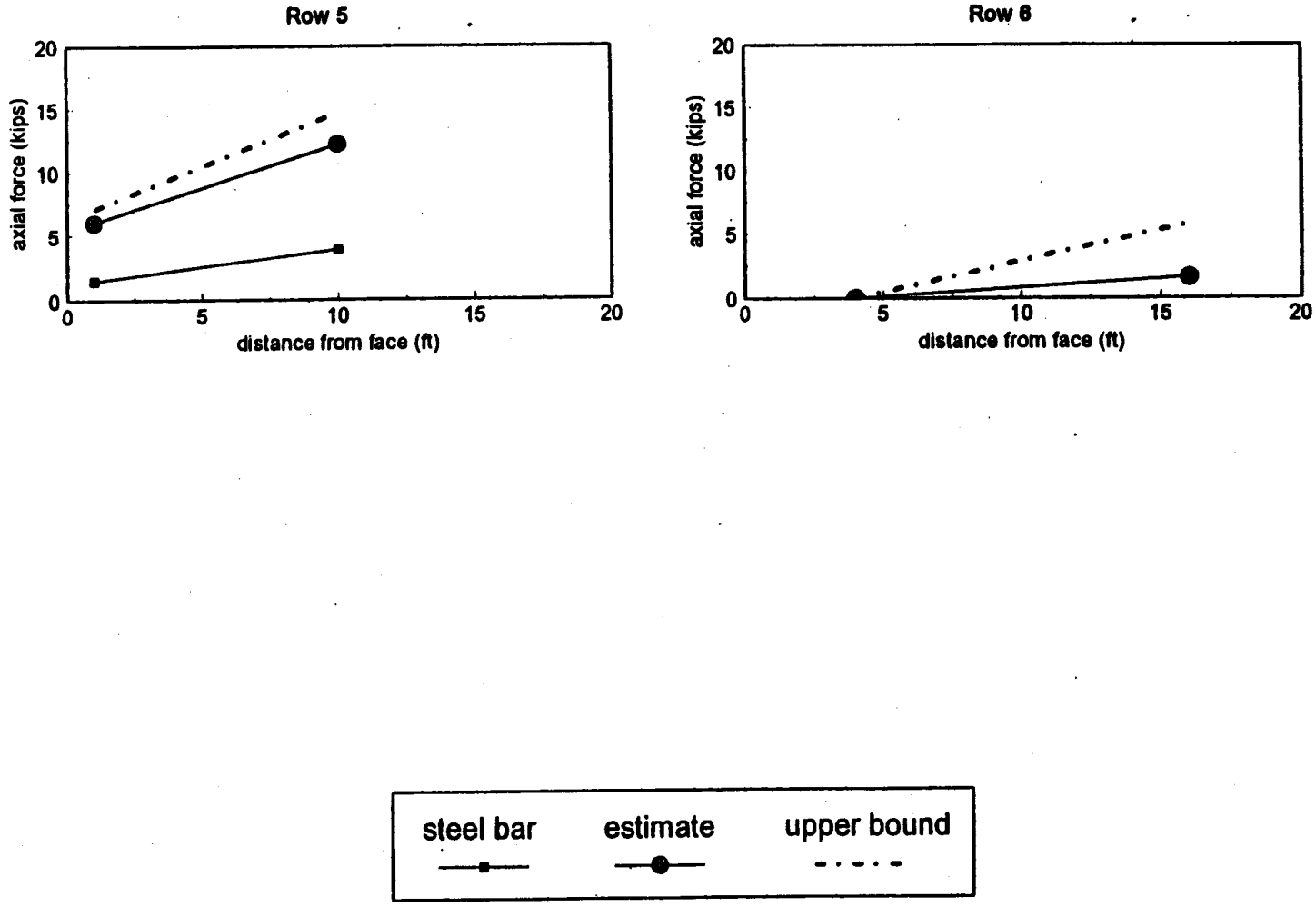

Figure A2.6 continued IH-30 Rockwall, Texas Range A axial force vs. nail length plots.

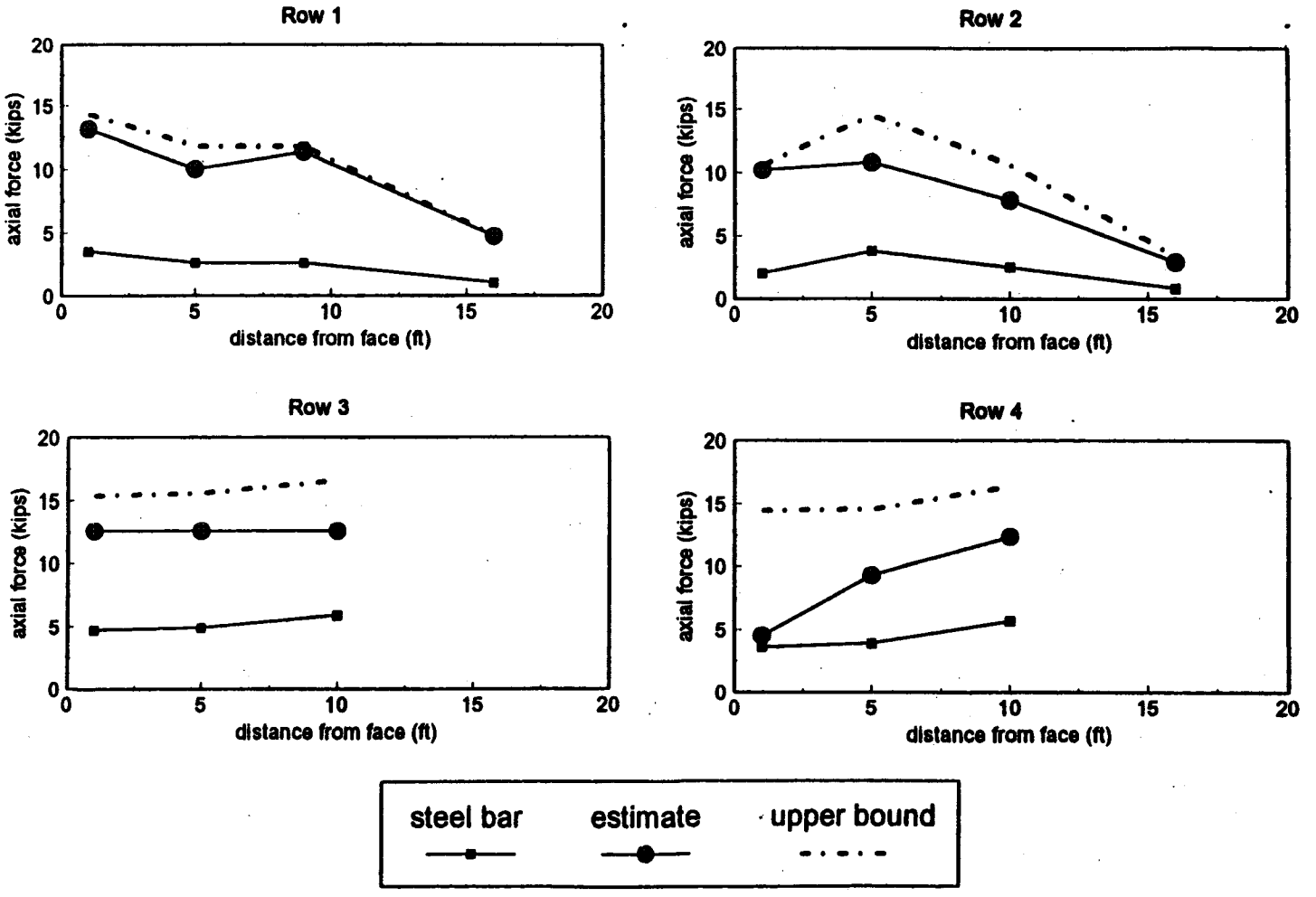

Figure A2.7 IH-30 Rockwall, Texas Range B axial force vs. nail length plots.

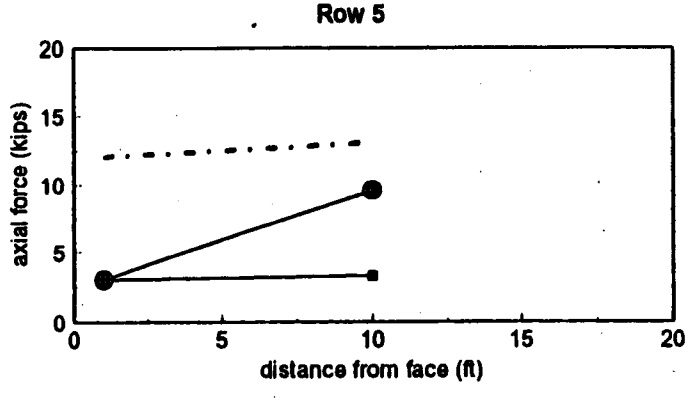

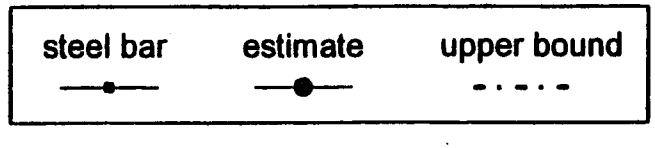

Figure A2.7 continued IH-30 Rockwall, Texas Range B axial force vs. nail length plots.

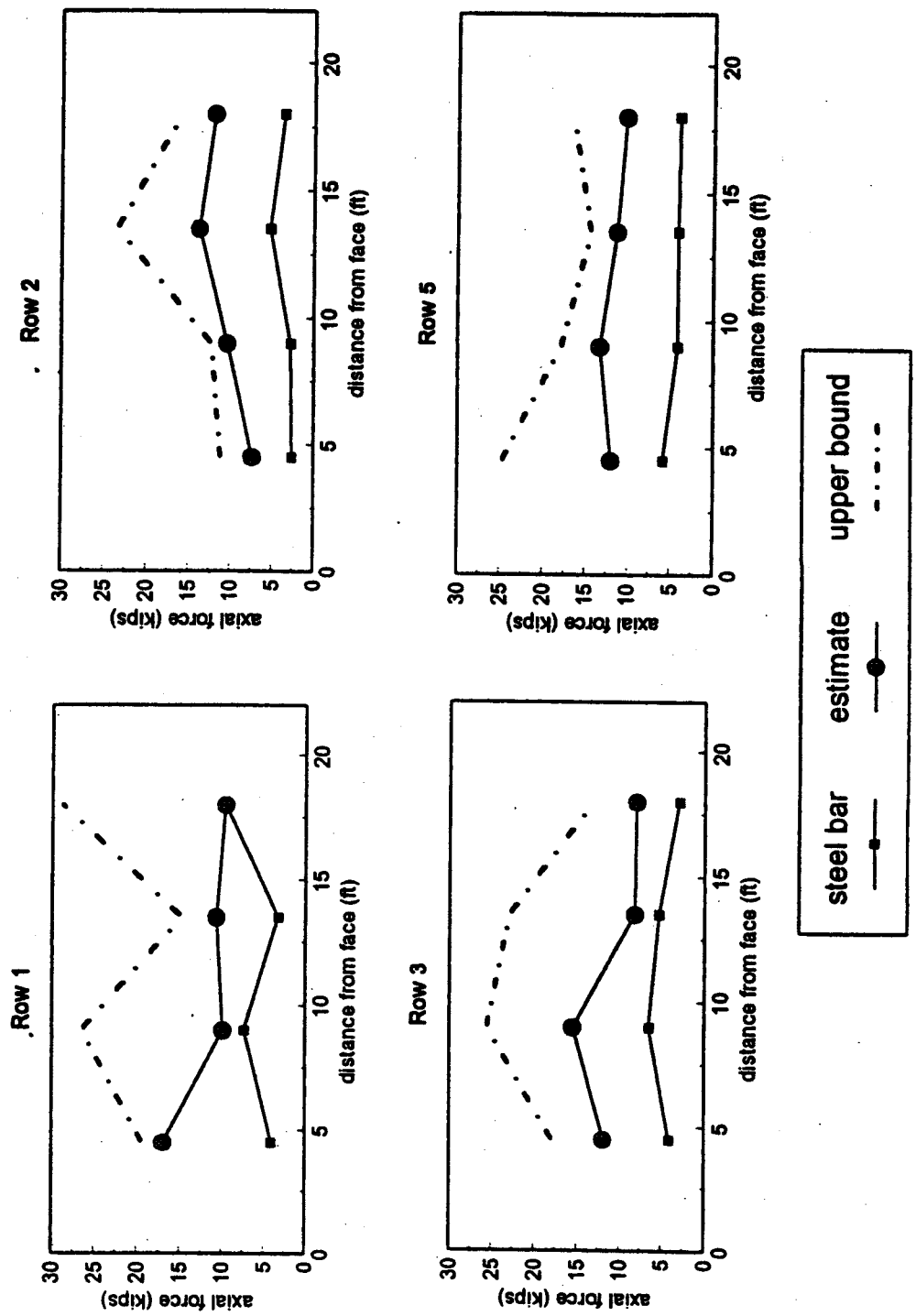

Figure A2.8 San Bernadino Left Station axial force vs. nail length plots.

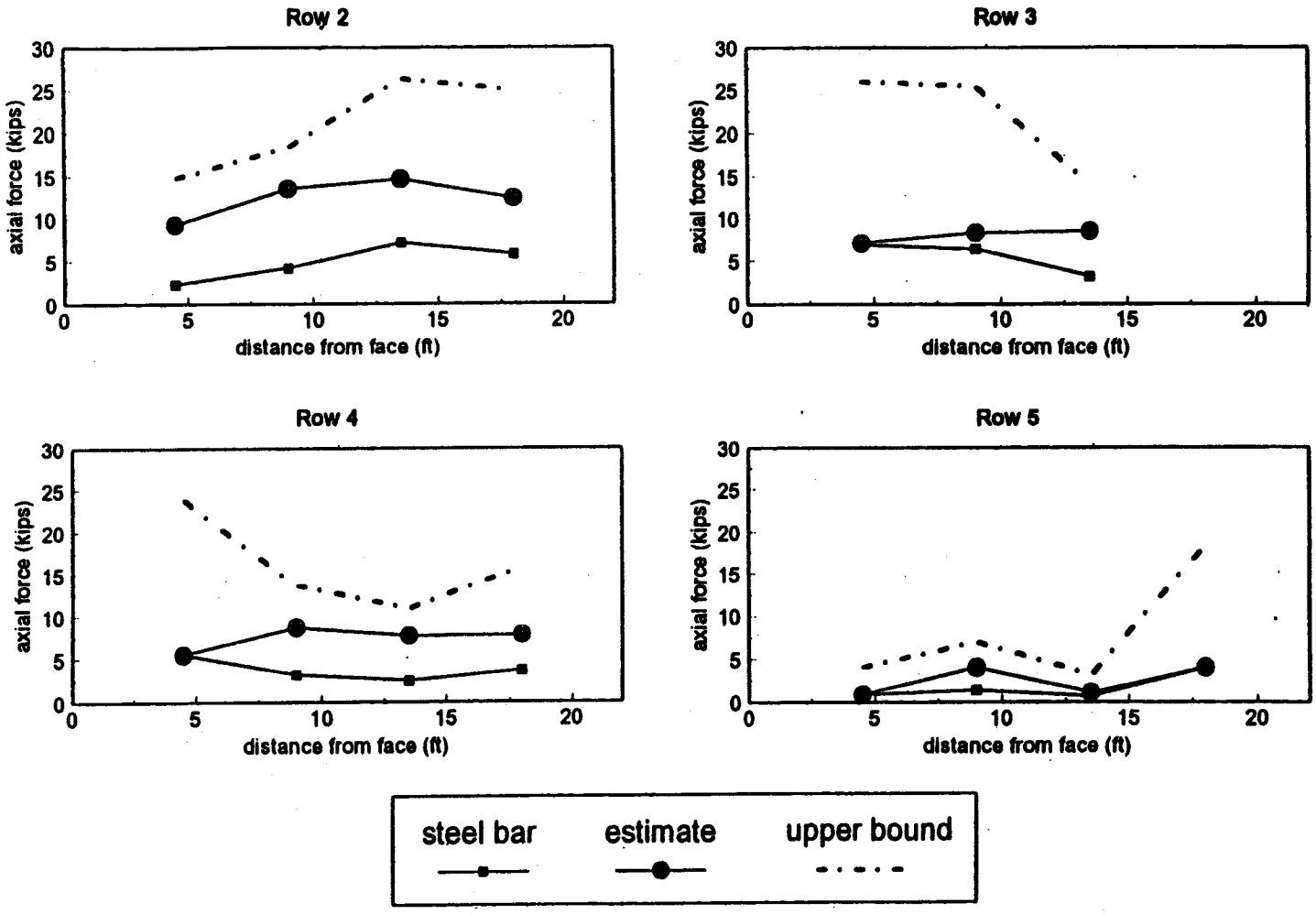

Figure A2.9 San Bernadino Right Station axial force vs. nail length plots.

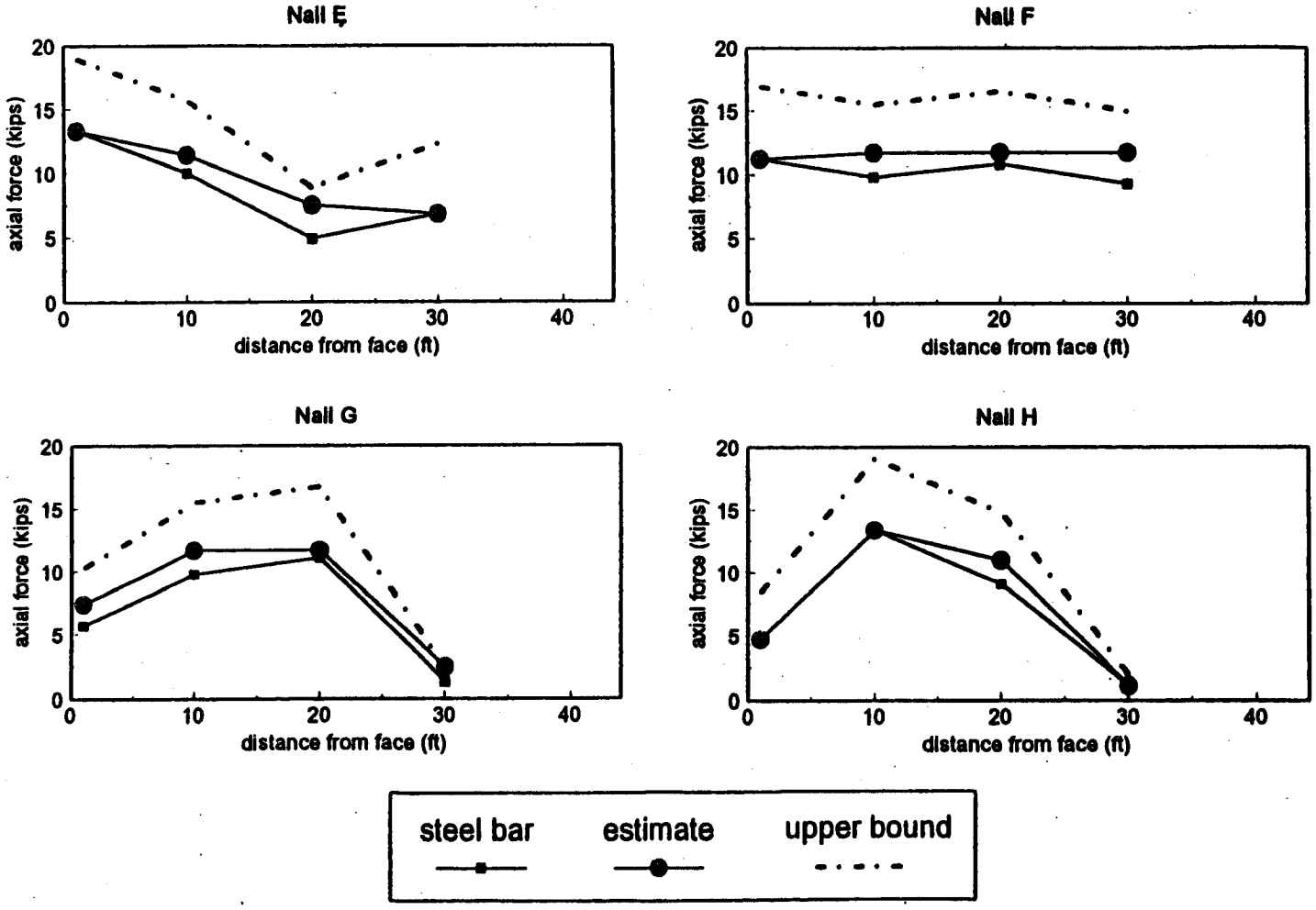

Figure A2.10 Cumberland Gap, 1988 axial force vs. nail length plots.

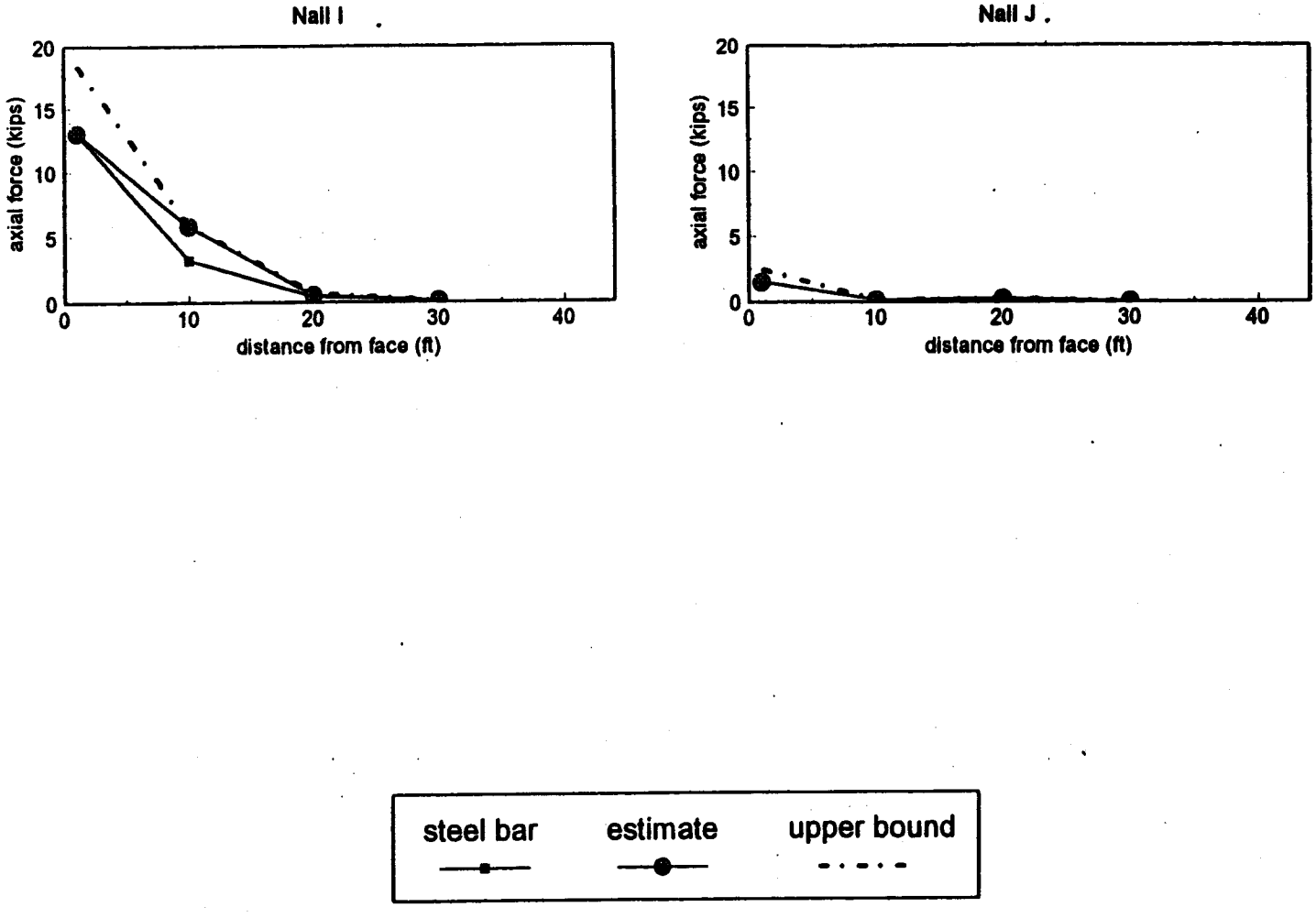

Figure A2.10 continued Cumberland Gap, 1988 axial force vs. nail length plots.

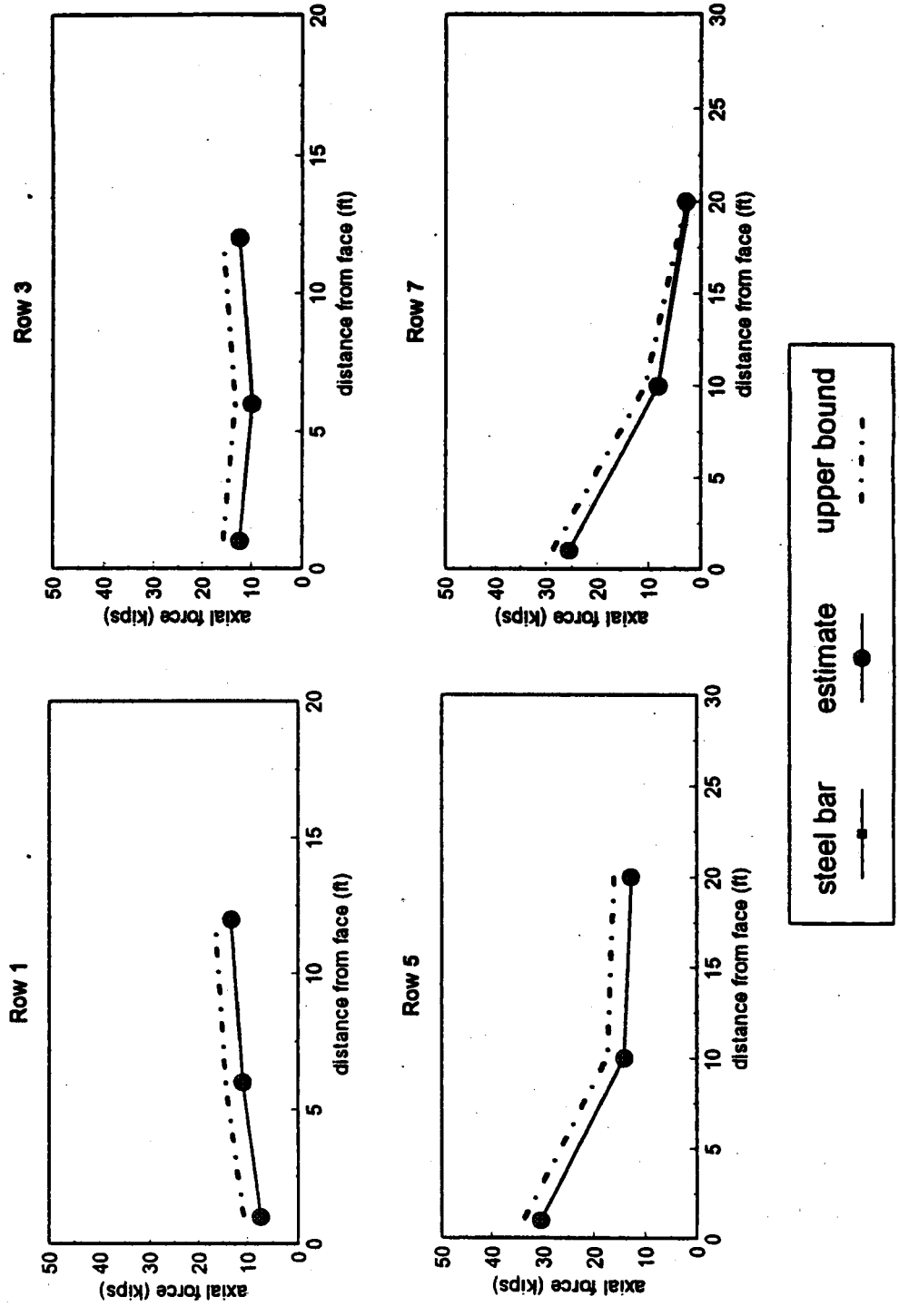

Figure A2.11 I-78 Allentown Grid 24 axial force vs. nail length plots.

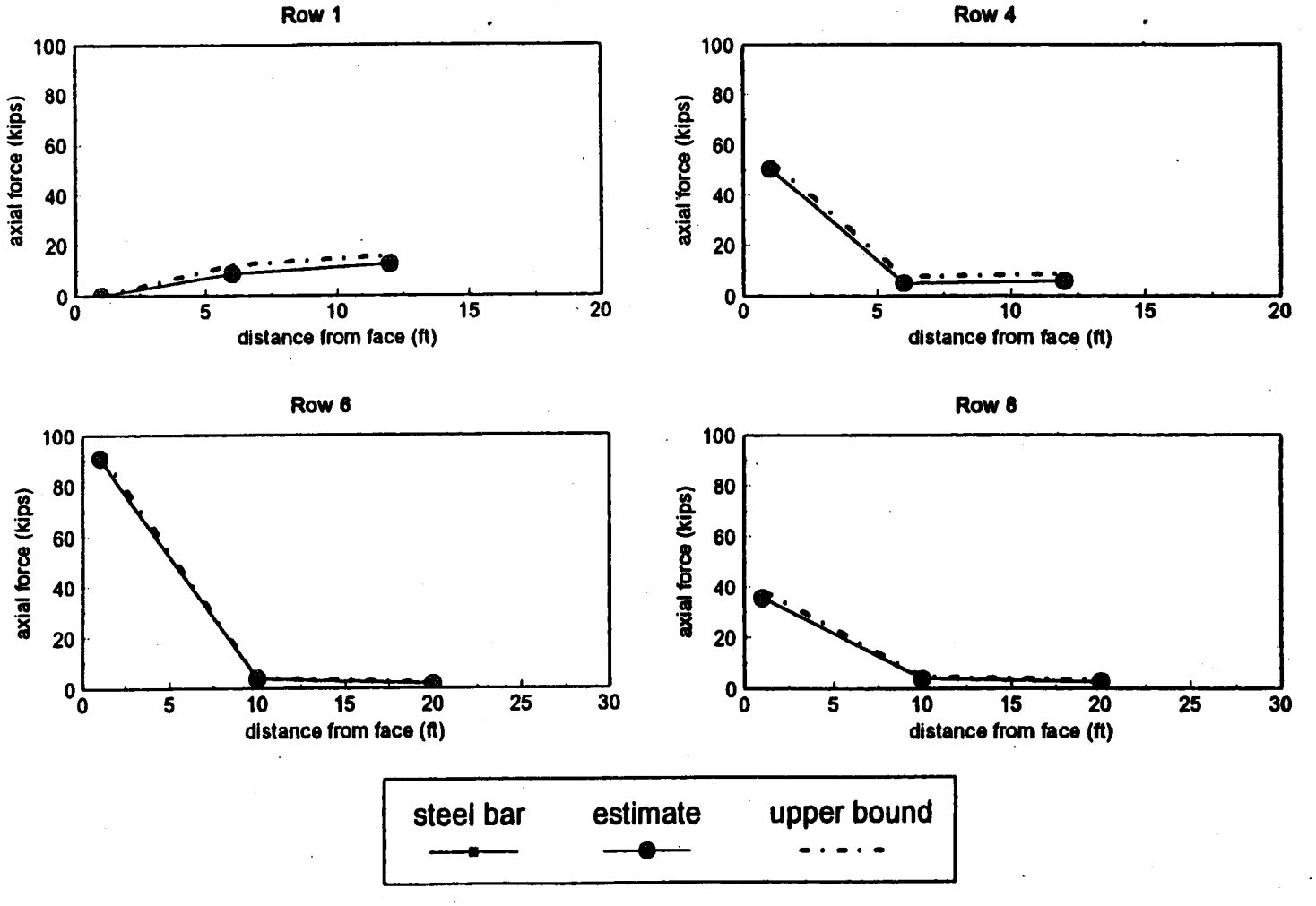

Figure A2.12 I-78 Allentown Grid 33 axial force vs. nail length plots.